

1984

A Study Of Blue Mould Of Tobacco Caused By Peronospora Hyoscyami Fsp Tabacina

Antonet Maria Svircev

Follow this and additional works at: <https://ir.lib.uwo.ca/digitizedtheses>

Recommended Citation

Svircev, Antonet Maria, "A Study Of Blue Mould Of Tobacco Caused By Peronospora Hyoscyami Fsp Tabacina" (1984). *Digitized Theses*. 1336.

<https://ir.lib.uwo.ca/digitizedtheses/1336>

This Dissertation is brought to you for free and open access by the Digitized Special Collections at Scholarship@Western. It has been accepted for inclusion in Digitized Theses by an authorized administrator of Scholarship@Western. For more information, please contact tadam@uwo.ca, wlsadmin@uwo.ca.

The author of this thesis has granted The University of Western Ontario a non-exclusive license to reproduce and distribute copies of this thesis to users of Western Libraries. Copyright remains with the author.

Electronic theses and dissertations available in The University of Western Ontario's institutional repository (Scholarship@Western) are solely for the purpose of private study and research. They may not be copied or reproduced, except as permitted by copyright laws, without written authority of the copyright owner. Any commercial use or publication is strictly prohibited.

The original copyright license attesting to these terms and signed by the author of this thesis may be found in the original print version of the thesis, held by Western Libraries.

The thesis approval page signed by the examining committee may also be found in the original print version of the thesis held in Western Libraries.

Please contact Western Libraries for further information:

E-mail: libadmin@uwo.ca

Telephone: (519) 661-2111 Ext. 84796

Web site: <http://www.lib.uwo.ca/>

CANADIAN THESES ON MICROFICHE

I.S.B.N.

THESES CANADIENNES SUR MICROFICHE



National Library of Canada
Collections Development Branch

Canadian Theses on
Microfiche Service

Ottawa, Canada
K1A 0N4

Bibliothèque nationale du Canada
Direction du développement des collections

Service des thèses canadiennes
sur microfiche

NOTICE

The quality of this microfiche is heavily dependent upon the quality of the original thesis submitted for microfilming. Every effort has been made to ensure the highest quality of reproduction possible.

If pages are missing, contact the university which granted the degree.

Some pages may have indistinct print especially if the original pages were typed with a poor typewriter ribbon or if the university sent us a poor photocopy.

Previously copyrighted materials (journal articles, published tests, etc.) are not filmed.

Reproduction in full or in part of this film is governed by the Canadian Copyright Act, R.S.C. 1970, c. C-30. Please read the authorization forms which accompany this thesis.

**THIS DISSERTATION
HAS BEEN MICROFILMED
EXACTLY AS RECEIVED**

AVIS

La qualité de cette microfiche dépend grandement de la qualité de la thèse soumise au microfilmage. Nous avons tout fait pour assurer une qualité supérieure de reproduction.

S'il manque des pages, veuillez communiquer avec l'université qui a conféré le grade.

La qualité d'impression de certaines pages peut laisser à désirer, surtout si les pages originales ont été dactylographiées à l'aide d'un ruban usé ou si l'université nous a fait parvenir une photocopie de mauvaise qualité.

Les documents qui font déjà l'objet d'un droit d'auteur (articles de revue, examens publiés, etc.) ne sont pas microfilmés.

La reproduction, même partielle, de ce microfilm est soumise à la Loi canadienne sur le droit d'auteur, SRC 1970, c. C-30. Veuillez prendre connaissance des formules d'autorisation qui accompagnent cette thèse.

**LA THÈSE A ÉTÉ
MICROFILMÉE TELLE QUE
NOUS L'AVONS REÇUE**

A STUDY OF BLUE MOULD OF
TOBACCO CAUSED BY
PERONOSPORA HYOSCYAMI F.SP. TABACINA.

by

Antoneta Maria Svircev
Department of Plant Sciences

Submitted in partial fulfillment of
the requirements for the degree of
Doctor of Philosophy

Faculty of Graduate Studies
The University of Western Ontario

London, Canada

August 1983

ABSTRACT

Temperature, humidity and light play a key role in the development of P. hyoscyami f.sp. tabacina in the tobacco plant. The conidia of this obligate parasite germinate at temperatures between 0 and 30°C. The optimum temperature for germination is between 15 and 20°C. Varying intensities of artificial light have no effect on percentage germination. However conidia are markedly affected by ultraviolet irradiation. The thin walled conidia can withstand prolonged storage at low temperatures. Conidial germination is inhibited by low concentrations of carbon dioxide.

P. hyoscyami f.sp. tabacina conidia lodge in the depressions between the epidermal cells above the anticlinal walls, and commence to produce short germ tubes within 60 min. in an optimal environment. An appressorium forms immediately at the tip of the germ tube above or near an anticlinal wall separating adjacent epidermal cells. The cuticle and epidermis are usually penetrated between 1.5 and 3.5 h. after inoculation near an anticlinal wall. A flange forms around the infection tube, between the appressorium and host wall. After penetration the multinucleated protoplasm surges through the penetration tube from the appressorium into a spherical vesicle, about 12 μm in diameter. An electron-transparent plug is formed in the inner end of the penetration tube. A 'nipple', about 1-2 μm in width, begins to form on the vesicle and

develops, into a lobulate, carrot-shaped hypha, which may branch, prior to passing through the lower epidermal wall, into a palisade cell or an intercellular space. In the epidermal cell the vesicle and hypha are always surrounded by host cytoplasm, and a sheath, or extrahaustorial matrix is not present. Dictyosomes are always present alongside nuclei and tubular vesicles, numerous in the cytoplasm, often project through the fungal plasmalemma into the fungal wall.

Once the intracellular hypha leaves the epidermal cell it develops in the intercellular spaces of the host tissue. The intercellular hyphae grow between the host cells, follow their contour and send haustoria of various shapes and sizes into adjoining cells. As the intercellular hyphae age, they become increasingly vacuolated. At 15-20°C, in low light and high relative humidity the fungus develops extensively in the leaf tissue. Between 5 and 6 days after inoculation, knots of intercellular hypha occupy the stomatal chamber. Juvenile conidiophores are evident emerging from the hyphal knots. Under high relative humidity and darkness the conidiophore matures. Five to 6 dichotomies occur prior to the initiation of conidial formation. The maturation on conidia occurs within 5 to 15 minutes. Sexual structures were present in tobacco leaves during the first year following collection. The 1979 Ontario isolate of P. hyoscayami f.sp. tabacina lost its ability

to produce antheridia and oogonia.

Haustorial formation in P. hyoscyami f.sp. tabacina passes through three stages, bulb, cane and coil, during development. After host wall penetration, the haustorium becomes bulb-shaped and grows into a straight hypha about 7-10 μm in length that bends at its tip to produce a cane-like handle. The tip of the handle grows into a torulose coiled structure up to 50 μm in length. A papilla or collar is never formed. The young haustorium is surrounded by extrahaustorial matrix composed of a thin inner electron-opaque layer on the haustorial wall and a much thicker electron-transparent layer, which extends to the extra-haustorial membrane. The electron-transparent layer frequently does not extend to the end of the haustorium. Haustoria occur in the mesophyll, palisade, lower and upper epidermis. Normally the haustoria are filled with organelles, occasionally they are vacuolated or shrunken.

Starch accumulation/formation in infected tissue is different from that in the healthy controls. Starch degradation was retarded as early as 2 h after infection and this retardation continued throughout the latent and sporulation period. Starch formation was retarded 31 h after inoculation and thereafter. The iodine test served well for indicating gross fluctuations in starch levels during the course of infection. The total starch assay determined specific quantities of starch per gram of dry tissue. After 5 days of infection a considerable increase in total

proteins was apparent. Semi-purified tobacco leaf extracts had higher starch degrading activity at 5 or more days after infection than at earlier periods of infection.

ACKNOWLEDGEMENTS

In the summer of 1979 Ontario tobacco growers and plant pathologists were confronted with a virulent plant pathogen in a susceptible cash crop. Dr. W. E. McKeen was directly involved with this problem from its origin. It was an honor and privilege to observe, work and learn from a truly 'non partisan plant pathologist'.

My thanks and gratitude to R. J. Smith for his technical, practical and friendly guidance.

To Dr. A. W. Day and his laboratory thank you for your advice and generosity.

I extend appreciation to Dr. P. Cavers for his helpful criticisms and assistance during the course of my studies.

Thanks to A. M. Lutz for the accuracy and efficiency in the final preparation of the manuscript.

Thank you Jim Coveart, my husband, for your continuing encouragement and support during this endeavor.

This thesis is dedicated to my parents for all the love and support throughout the years.

TABLE OF CONTENTS

CERTIFICATE OF EXAMINATION	ii
ABSTRACT	iii
ACKNOWLEDGEMENTS	vii
TABLE OF CONTENTS	viii
LIST OF DIAGRAMS	xii
LIST OF PHOTOGRAPHIC PLATES	xiii
LIST OF GRAPHS	xvi
LIST OF TABLES	xvii
ABBREVIATIONS	xviii
CHAPTER 1. INTRODUCTION	1
1.1. The History of Tobacco Downy Mildew	1
1.1.1. Taxonomy	1
1.1.2. Early History	2
1.1.3. Tobacco Downy Mildew in the United States	3
1.1.4. Tobacco Downy Mildew in Canada prior to 1979	5
1.1.5. Tobacco Downy Mildew in Europe, Australia and Cuba	6
1.1.6. Recent History of Downy Mildew of Tobacco in Canada	7
1.2. Effects of the Physical Environment on the Disease Cycle	8
1.2.1. Germination, Penetration and Development in the Host	8
1.2.2. Sporulation	10
1.3. Morphological Aspects of Host-Pathogen Interaction	12
1.3.1. Structural Changes in Host Tissue	12

1.3.2. Structure of the Host-Pathogen Interface	14
1.4. Objectives	18
CHAPTER 2. MATERIALS AND METHODS	20
2.1. Conidial Inoculation	20
2.2. Temperature Experiments	21
2.2.1. Optimum Germination Temperatures	21
2.2.2. Determination of the Rate of Germination	21
2.2.3. Exposure of Conidia to High Temperatures	22
2.3. Control of Water Potential by Sucrose Solutions	22
2.4. Humidity Experiments	22
2.5. Light Experiments	23
2.5.1. Fluorescent Light	23
2.5.2. Ultraviolet Light	23
2.6. Exposure of Conidia to Carbon Dioxide	24
2.7. Light Microscopy	25
2.7.1. Leaf Clearing Solutions	25
2.7.2. Staining Procedures	26
2.8. Electron Microscopy	26
2.8.1. Transmission Electron Microscopy	26
2.8.2. Scanning Electron Microscopy	28
2.8.3. Critical Point Drying	28
2.9. Starch Analysis in Infected Tobacco Leaves and Healthy Controls	30
2.9.1. Plant Pre-conditioning and Inoculation	30
2.9.2. Macroscopic Detection of Starch	30

2.9.3.	Total Starch Assay	31
2.10.	Enzyme Assay	31
CHAPTER 3.	RESULTS	33
3.1.	<u>In vivo</u> Development	33
3.1.1.	Disease Development in the Field and in Growth Chambers	33
3.1.2.	Host Cells of <u>N. tabacum</u>	34
3.1.3.	Conidiophore and Conidial Formation ...	34
3.1.4.	Sexual Structures	35
3.2.	<u>In vitro</u> Conidial Germination	36
3.3.	Germination, Penetration and Early Development	39
3.4.	Haustorial Formation	44
3.4.1.	Light Microscopy	44
3.4.2.	Electron Microscopy	45
3.5.	Starch Accumulation and Degradation in Infected and Healthy Host Tissue	48
CHAPTER 4.	DISCUSSION	51
4.1.	<u>In vivo</u> Development	51
4.2.	<u>In vitro</u> Conidial Germination	52
4.3.	Germination, Penetration and Early Development	55
4.4.	Haustorial Ultrastructure	62
4.4.1.	Penetration of the Host Wall	62
4.4.2.	Terminology	63
4.4.3.	Haustorial Electron-Opaque Layer	66
4.4.4.	Haustorial Electron-Transparent Layer	67
4.4.5.	The Extrahaustorial Membrane	69
4.4.6.	Host Response to Fungal Invasion	70

4.4.7.	Ultrastructural Changes in Aging Haustorial and Intercellular Hyphae ...	71
4.5.	Starch Accumulation and Degradation in Infected and Healthy Tissue	72
4.6.	Effects of Fungus on Host Chloroplast Ultrastructure	76
	PHOTOMICROGRAPHS	77
	APPENDICES	189
	REFERENCES	192
	VITA	203

LIST OF DIAGRAMS

<u>Plate</u>	<u>Figure</u>	<u>Description</u>	<u>Page</u>
7	24	Developmental stages of <u>P. hyoscyami</u> in susceptible host, <u>N. tabacum</u>	90
8	25-26	Early infection structures in the upper epidermis-germ tube, appressorium	92
9	27	Early infection structures in the upper epidermis-vesicle	94
10	28	Late infection structures in the upper epidermis	96
24	67	Haustorium and associated extra-haustorial matrix	124
37	95	Developmental stages in (bulb, cane and coil) haustorial formation	150

LIST OF PHOTOGRAPHIC PLATES

Note: Figures 12-23, 35-44, 68-77 are light micrographs.
 Figures 45-66, 78-94, 98-102 are electron micrographs.
 Figures 29-34 are scanning electron micrographs.

<u>Plate</u>	<u>Figure</u>	<u>Description</u>	<u>Page</u>
1	1-3	Infected tobacco from 1979 blue mould epidemic	78
2	4-5	Chlorotic, necrotic and sporulating lesions in <u>N. tabacum</u>	80
3	8-11	Upper epidermis, palisade, spongy parenchyma and lower epidermis	82
4	12-15	Early conidiophore development on susceptible tobacco	84
5	16-19	Late stages in conidiophore development on susceptible tobacco	86
6	20-23	Sexual structures	88
11	29-34	Scanning electron micrographs of conidia and infection structures formed during germination and penetration	98
12	35-40	Light micrographs of conidia, germ tubes, appressoria and vesicles	100
13	41-44	Germ tubes and appressoria	102
14	45-47	Cross sections of conidia	104
15	48-51	Cross sections of germinated conidia	106
16	52-53	Conidium with germ tube and appressorium	108
17	54	Appressorium, infection tube and vesicle in the upper epidermis	110
18	55-57	Infection tubes and plugs	112
19	58-59	Vesicle 'nipple' and hyphal branch	114

<u>Plate</u>	<u>Figure</u>	<u>Description</u>	<u>Page</u>
20	60	Hyphal branch in adjacent epidermal cell	116
21	61-63	Fungal nuclei , nucleoli and dictyosomes	118
22	64-65	Tubular vesicles and plasmalemmasome in fungal cytoplasm	120
23	66	Intercellular hypha	122
25	68-73	Intercellular hyphae and haustoria	126
26	74-77	Hauستoria and extrahaustorial matrices	128
27	78	Cane-shaped haustorium	130
28	79-80	Inactive haustorium and young haustorium	132
29	81	Host wall alterations adjacent to haustorium	134
30	82	Hauستorial electron-transparent and electron-opaque layers	136
31	83	Hauستorium with partial covering of the electron-transparent layer	138
32	84	Coiled haustorium	140
33	85	Young haustorium suspended in a cotyledonary cell vacuole	142
34	86-87	Hauستoria and adjacent intercellular hyphae	144
35	88-91	Developmental stages in intercellular hyphae	146
36	92-94	Collapsed and shrunken haustoria	148
38	96	Quantitative relationship between IKI and TSA tests	152
	97	IKI positive and IKI negative tobacco leaf tissue	152
39	98-99	Chloroplasts in healthy tissue	154

<u>Plate</u>	<u>Figure</u>	<u>Description</u>	<u>Page</u>
40	100-101	Chloroplasts in infected tissue	156
41	102	Infected tissue at 6 days post- inoculation	158

LIST OF GRAPHS

<u>Figure</u>	<u>Description</u>	<u>Page</u>
103	Starch formation in early infection	160
104	Starch degradation in early infection	162
105	Starch formation in late infection	164
106	Starch degradation in late infection	166
107	Enzyme activity in healthy and infected tobacco tissue	168
108	Total proteins in healthy and diseased tissue	168
109	Percent germination of conidia at constant temperatures	170
110	Cumulative percent germination of conidia	172
111	Total percent germination of conidia after exposure to high temperatures	174
112	Water potential and turgidity of conidia	176
113	Water potential and conidial germination	176
114	Ultraviolet irradiation of conidia	178
115	Ultraviolet irradiation of conidia and conidiophores	180

LIST OF TABLES.

<u>Table</u>	<u>Description</u>	<u>Page</u>
1	Time-course of infection of upper epidermal cells by <u>P. hyoscyami</u>	181
2	Starch formation in early infection (IKI test)	182
3	Starch degradation in early infection (IKI test)	183
4	Starch formation in late infection (IKI test)	184
5	Starch degradation in late infection (IKI test)	185
6	Storage of conidia at various temperatures and relative humidities	186
7	Inhibition of spore germination by carbon dioxide	187
8	Effect of flourescent light on germination	188

ABBREVIATIONS

A	Appressorium	L	Plasmalemmasome
AW	Anticlinal wall	LI	Lipid
B	Branch hypha	M	Mitochondrion
CH	Chloroplast	N	Nucleus
CO	Centriole	NI	Nipple
D	Dictyosome	NP	Nuclear pore
E	Epidermal cell	NU	Nucleolus
EHM	Extrahaustorial matrix	P	Plug
EM	Extrahaustorial membrane	PA	Palisade cell
ET	Electron-transparent layer	PM	Plasma membrane
EW	Epidermal wall	PP	Penetration peg
F	Flange	SG	Starch granule
FC	Fungal cytoplasm	SP	Spore (Conidium)
G	Germ tube	SV	Spherical vesicle
H	Hypha	T	Tubular element
HA	Haustorium	TO	Tonoplast
HC	Host cytoplasm	TSA	Total starch assay
HW	Host wall	V	Vesicle
I	Infection tube	VA	Vacuole
IKI	Iodine in potassium iodide test	Z	Electron-opaque layer
IN	Spore inclusions		

CHAPTER I .

INTRODUCTION

1.1. The History of Tobacco Downy Mildew

1.1.1. Taxonomy

The fungal organism, Peronospora hyoscyami f.sp. tabacina, is an Oomycete in the order Peronosporales. The order is characterized by the formation of biflagellate motile zoospores in the vegetative stage of the life cycle. Sexual reproduction is characterized by gametangial contact, which leads to the formation of oospores. All the species of the Peronosporaceae are obligate parasites. Diseases caused by this family of fungal pathogens are commonly referred to as the downy mildews.

Under optimal conditions P. hyoscyami forms asexual and sexual structures on the host tissue. Unlike most members of this group, P. hyoscyami lacks the motile zoospore stage. The hyaline, ellipsoidal conidia germinate directly and infect host tissue.

All members of the genus Nicotiana and certain members of the Solanaceae demonstrate varying degrees of susceptibility to P. hyoscyami.

In 1933, Adam (McGrath and Miller, 1958) closely examined herbarium specimens of the tobacco downy mildew

fungus. An attempt was made to classify the organism on the basis of shape, size and structure of conidia, conidiophores and oogonia. Adam concluded that classification could not be made on these characteristics. In addition, the pathogen failed to attack Hyoscyamus niger, as previously reported by de Bary (Wolf, 1939). The organism was re-named Peronospora tabacina Adam (Wolf, 1947), due to its ability to infect ~~the~~ Nicotiana species. Subsequent workers (Clayton and Stevenson, 1935; Wolf et al., 1936) in the field were in agreement with Adam and this name is widely used.

Today's protocol for scientific nomenclature requires the use of the original name. By convention the downy mildew of tobacco or the blue mould organism will be referred to as Peronospora hyoscyami f.sp. tabacina (Lucas, 1980).

1.1.2. Early History

The first record of tobacco downy mildew was made in 1863 by de Bary. He discovered it growing along the roadside in Europe, on Hyoscyamus niger (henbane plant) (Wolf, 1939). In 1885, in California, Farlow discovered a downy mildew growing on Nicotiana glauca near San Diego (McGrath and Miller, 1958; Wolf, 1939). Using the conidial stage, Farlow identified the pathogen and named it Peronospora hyoscyami de Bary (McGrath and Miller, 1958). In the late 19th century, Farlow had the foresight to express his concern over this pathogen of tobacco. He feared the

spread of the mildew from the wild tobacco, N. glauca, to the cultivated tobacco, N. tabacum (McGrath and Miller, 1958).

This organism was present in the cultivated tobacco fields in Australia in the 1890's. Wolf et al. (1934) postulated that the fungus was present 30-40 years prior to this date because cultivated tobacco had been grown in Australia since 1830.

In South America, Spegazzini described a species of Peronospora growing in N. longiflora, he named this organism Peronospora nicotianae, Spegazzini (McGrath and Miller, 1958). This organism was morphologically different from Peronospora hyoscyami described by de Bary (McGrath and Miller, 1958; Wolf, 1947). The vegetative stage of the South American Peronospora on tobacco was reported to contain motile zoospores (McGrath and Miller, 1958).

1.1.3. Tobacco Downy Mildew in the United States

In 1921 P. hyoscyami was discovered for the first time in commercially grown tobacco in Florida and Georgia (Stevens and Ayres, 1940). The losses caused by the disease were minimal. The reasons for the failure of the pathogen to establish itself in the Florida-Georgia region are not known. The next appearance of the fungus in commercial tobacco was in 1931 (Clayton and Stevenson, 1943; Stevens and Ayres, 1940; Wolf, 1947). Clayton and Stevenson (1943), believed that the failure to establish in the host in 1921 was due to the failure of pathogen to form oospores.

Effective eradication measures were taken in a small area where the pathogen occurred. Diseased plants were burned or drenched with formaldehyde (McGrath and Miller, 1958).

A number of theories existed as to the origin of P. hyoscyami in the U.S.A. The two main schools of thought were: (a) the organism was indigenous to the U.S.A. living on wild native tobacco and, (b) the fungus was introduced to California from Austrália (McGrath and Miller, 1958; Stevens and Ayres, 1940; Wolf, 1947). Upon the introduction from Australia, the organism established itself on wild tobacco, N. repanda (McGrath and Miller, 1958).

The eastward progression of the pathogen has been attributed to the increase in irrigation in Mexico and Texas, particularly in the Rio Grande Valley, after the first world war. Because of the increased water supply, the wild tobacco N. repanda, with its pathogen, P. hyoscyami, flourished and spread eastward (McGrath and Miller, 1958; Wolf, 1939; Wolf, 1947; Wolf et al., 1936).

Commercially grown tobacco was established in Florida and Georgia in 1910-1920's. The progression of the pathogen eastward, may have been attributed to wind borne spores. (Wolf, 1947).

Once it was established in the southern United States it spread northward as far as North Carolina and Virginia (McGrath and Miller, 1958). Losses were minimal and the disease was contained in the seedbeds (Dixon et al., 1935;



Dixon et al., 1936). Severe epiphytotics did occur in the seedbed for the years 1932, 1937 and 1938. In some communities 60-95% of the seedlings were killed (Anonymous, 1938). In 1938, infected tobacco plants were discovered in the field in North Carolina and Virginia (Pinckard and Shaw, 1943). The initiation of the disease in the field was attributed to widespread contamination of the seedbeds. After 1939, disease control was obtained in the tobacco seedbeds due to improved cultivation practices and the use of fungicides (Wolf, 1947).

The southwestern tobacco growing area of the U.S.A., has served as a continual reservoir of the blue mould organism. The pathogen is maintained in the conidial stage on plants and by oospores in the soil. It is the latter stage that is believed to guarantee continual propagation of the organism (Valleau, 1955).

The northward progression of the organism has been attributed entirely to the wind born conidia.

1.1.4. Tobacco Downy Mildew in Canada Prior to 1979

In 1938 during the period of an epiphytotic in the United States, P. hyoscyami appeared for the first time in southern Ontario (Stover and Koch, 1951). In 1940 infection of seedbeds at the same location as in 1938 occurred. At that time it was assumed that the pathogen had overwintered in Ontario.

The first record of a field infection in Canada was in 1945. It was attributed to the transfer of diseased plants

from seedbeds to the fields. Further infections of fields and seedbeds were reported in 1946 and 1948 (Stover and Koch, 1951). Improved farming practices and the use of fungicides prevented the development of P. hyoscyami in tobacco after 1949. Consequently, in Canada, tobacco growers and others associated with tobacco industry were not aware of the pathogen or thought that it was no longer a potentially hazardous tobacco pathogen.

1.1.5. Tobacco Downy Mildew in Europe, Australia and Cuba

In Australia, unlike North America, the blue mould organism caused damage in the field. Wolf et al. (1934) believed that P. hyoscyami had been present in Australian cultivated tobacco since 1850's. In Britain P. hyoscyami was discovered growing on tobacco cultivated for virus research. By 1959, the pathogen had spread to the Netherlands and West Germany, causing minimal damage. By 1960, most European tobacco growing areas were affected and the disease reached epiphytotic proportions due to the climatic conditions. Total losses due to the disease in 1960 were reported in Germany, France, Austria, Czechoslovakia as 70-85%, 90%, 60-70% and 80-90% respectively. Todd (1961), estimated that the total loss in the European crop in 1960 was 350 million dollars.

Blue mould was first reported in Cuba in 1957. Experts attributed this to wind borne spores from Florida. The organism did not appear again in that region until 1979 (Lucas, 1980). In 1980, 90% of the Cuban tobacco crop was destroyed.

1.1.6. Recent History of Downy Mildew of Tobacco in Canada

The 1979 Ontario blue mould epidemic demonstrates how the interaction between a vigorous fungal pathogen, an extremely susceptible host, ideal climatic conditions and human error resulted in enormous losses.

In 1979, Fernlea Flowers Inc. instituted a new procedure, avoiding the usual practice of growing plants in greenhouses in Canada. About 99,000 young plants or 'speedlings' were grown in individual V-shaped containers in Florida. While in Florida the young plants were infected by P. hyoscyami, where this pathogen was indigenous. The disease was not detected in shipment nor during planting in the Ontario fields. Growers reported that the plants appeared necrotic and unhealthy. Nonetheless these 'speedlings' were planted in the fields alongside locally grown tobacco. The temperatures were relatively low, in the 16-20°C range, during the day but much lower at night. These temperatures were optimal for the infection and development of the fungus in the host. (Figures 1, 2, 3)

On July 8th, 1979, the symptoms of the disease were diagnosed by the local tobacco research station as cold weather injury (McKeen, 1981; Schaus, 1980). In July the fungus survived a hot week of 30°C temperatures and continued to spread from the 'speedlings' to the local tobacco. Local growers were discouraged from employing eradivative or protective methods such as the fungicide, metalaxyl. The growers were advised to continue watering the crop

during the day for the high day temperatures would kill the fungus and the fungus would not grow at temperatures above 16°C. In contrast, this prolonged the infective period and established an exceedingly high inoculum potential in the centre of the tobacco belt. By the end of August of that year, blue mould was reported on 1,500 farms (McKeen, 1981; Schaus, 1980). The direct losses to farmers in southern Ontario were estimated to be greater than 100 million dollars, and in the United States and Canada together as 240 million dollars (Lucas, 1980). The monetary loss appeared to be greater than any previous plant disease loss in Canada.

Although some infection occurred in the field in Ontario in August 1980, most farmers sprayed their tobacco plants with metalaxyl, a systemic fungicide. Consequently the airborne conidia from United States caused no further damage.

1.2. Effects of the Physical Environment on the Disease Cycle

1.2.1. Germination, Penetration and Development in Host

On the host the first indication of germination was the formation of a small papilla at the side of the conidium. The papilla develops into a short germ tube (Shepherd and Mandryk, 1963). At the distal portion of the germ tube a club-shaped appressorium forms (Anonymous, 1938). An infection peg forms under the appressorium and penetrates the leaf tissue along the anticlinal wall (Lucas, 1980). Once inside the host the hyphae develop intercellularly or

intracellularly (Henderson, 1937; Milholland, et al., 1980). The intracellular hyphae or haustoria are specialized feeding structures which procure nutrients from the host. At a period 5-7 days following infection conidiophores develop on the lower leaf surface. The conidiophores are dichotomously branched structures bearing ellipsoidal conidia.

Different studies on optimal temperatures for conidial germination on the host have been reported at 10-20°C (Shepherd, 1962), 12.7-18.3°C (Wuest and Schmitt, 1965), 15-17.8°C (Cruickshank, 1958) and 15-25°C (Shepherd and Mandryk, 1963). The conidia were reported to be fragile, short-lived structures, extremely sensitive to ultraviolet radiation and high temperatures (Lucas, 1980). Shepherd et al. (1971) discovered that conidia were able to survive under diverse environmental conditions, surviving for 45 days at 5°C and 30 days at 80% relative humidity (RH) and 25°C.

Conidia attached to the conidiophores on the leaf are able to survive 34 days at 5°C and 100% RH. This survival is prolonged to 3 months if the conidia are maintained at -20°C (Cohen and Kuc, 1980). In contrast, Clayton and Gaines (1945) showed that conidia held at lower temperatures of 5-14 C survived the longest at 100% RH.

Erratic germination of the conidia on a day-to-day basis has been observed in most studies (Cruickshank, 1961a; Hill, 1966; Lucas, 1980; Shepherd et al., 1963; Shepherd et al., 1971). A decrease in conidial germination

following sporulation occurs within 24 hours (Hill, 1961). Clayton and Gaines (1945), also found that the highest mean percent germination was obtained on conidia collected at 6:00 a.m. in the field, by 11:00 a.m. most conidia were dead. Generations of conidia on the same conidophore drastically decrease in germinability when compared to the initial spore generation (Shepherd, 1962).

Washing conidia in water removed an intrinsic inhibitor (Hill, 1966; Shepherd, 1962) and provided higher and more uniform germination. Shepherd and Mandryk (1963), have shown that in addition to the intrinsic autoinhibitor, the conidia have a requirement for riboflavin when germinating in vitro. The host species, Nicotiana, produces a leaf inhibitor which prevents germination of P. hyoscyami conidia. The greatest concentration of the plant inhibitor was found on the upper leaves of the tobacco plant (Shepherd, et al., 1963, Cohen, et al., 1980).

1.2.2. Sporulation

The production of conidia in P. hyoscyami follows a diurnal cycle (Cruickshank, 1963). Sporulation occurs 5 to 6 days after infection. Sporulation requires a minimum of 2 h of darkness. Spore formation in P. hyoscyami is believed to result from a dark-induction phenomenon (Cruickshank, 1963). Optimum temperatures for sporulation have been reported as 15-23°C (Cruickshank, 1961b; Hill and Green, 1965). Hill and Green (1965), reported day/night temperatures of 24/20°, 20/20° and 16/16°C resulted in the highest spore production on infected leaf tissue. Day

temperatures of 28°C or higher and nights below 12°C retarded pathogen sporulation (Hill, 1965; Hill, 1966).

Mihailova (1972), named two critical periods in the life cycle of this pathogen. These are a period of massive spore release which occurs during low relative humidities and a period of massive spore formation which occurs at high relative humidities. Rapid change in the relative humidity and temperature induced spore release from the conidiophore. Wind, rain and mechanical shock may serve as additional means of spore release (Hill, 1961).

Cruickshank and Rider (1961), observed that infected plants had higher transpiration rates prior to sporulation, than healthy ones. The higher rates may create conditions in leaf tissue that favor sporulation. In an in vitro experiment Cruickshank and Mueller (1957) used infected non-sporulating leaf discs and floated them onto sucrose-mannitol solutions. This method allowed control of leaf diffusion pressure deficit (DPD) and the ambient relative humidity of the chamber was controlled by glycerol-water solutions. Results showed that the two factors controlling sporulation were relative humidity and the DPD of leaf tissue. A relative humidity less than 97% or a DPD greater than 3-4 atmospheres significantly reduced the degree of sporulation (Cruickshank, 1963; Cruickshank and Mueller, 1957). These experiments elegantly demonstrated that sporulation and spore discharge were governed by internal and external water conditions.

Cruickshank (1963), observed that light in the blue region of the spectrum inhibits spore formation and causes deformation in spore shape. Cohen (1976), confirmed these results and demonstrated that the inhibitory effect of light on sporulation was greatly influenced by temperature. Temperatures from 19-24°C increased the inhibition by light while at 8-15°C inhibition was not evident.

1.3. Morphological Aspects of Host-Pathogen Interaction

1.3.1. Structural Changes in Host Tissue

Morphological changes occur in tobacco plant tissue invaded by an obligate parasite. The physiological aspects of this interaction are not well understood. However, a great deal of investigation has been centered on the ultrastructural changes in the host-pathogen interaction.

In Uromyces phaseoli (Pers.) Wint. var vignae (Barcl.) (Heath, 1974), infection of cowpeas, a difference in chloroplast structure was observed following sporulation. In early stages of infection the ultrastructural changes resembled natural senescence. In later stages of infection the chloroplasts lost their shape and membrane organization (Heath, 1974). Heath (1974) related changes in chloroplasts in infected-tissue with senescence and ethylene production. Similar results were observed in rust infected flax and sunflower (Coffey et al., 1972) and in lettuce infected with beet western yellows virus (Tomlinson and Webb, 1978). In each case, large starch grains were present in chloroplasts of infected tissue.

Commonly associated with rust infections are 'green islands'. Harding et al. (1968), compared the chlorophyll content and ultrastructure of infected tissue in the 'island' and its vicinity. There were no changes in the ultrastructure in the 'green island', 84 h after infection. In tissue in the immediate vicinity of green islands considerable breakdown in the grana of the chloroplasts was evident (Harding et al., 1968). In infections of Peronospora parasitica on cabbage, 'green islands' were not found. Increases in respiration rate, soluble carbohydrate levels and starch content were evident in the infected tissue (Thornton and Cooke, 1974). Starch accumulation was common in tissues infected with rusts, powdery mildews and downy mildews (Coffey et al., 1972; Heath and Heath, 1971; Thornton and Cooke, 1974).

Host cells invaded by haustorial bodies were characterized by a thin band of host cytoplasm around the haustorium. As the haustorium developed there was a gradual increase in the volume of the host cytoplasm until the cell was filled (McKeen et al., 1966, Peyton and Bowen, 1963). The apparent increase in the cytoplasm indicates that the host has increased the synthesis of proteins. Such increased synthesis may compensate for the nutrients lost to the invading parasite (McKeen et al., 1968). Advanced stages of colony development were characterized by an increase in the ribosomal content of the host. This is another possible indication of increased host protein synthesis. In rust infections, host endoplasmic reticulum

is closely associated with the extrahaustorial membrane (or plasma membrane) (Berlin and Bowen, 1964; Bracker and Littlefield, 1973).

Clumps of tubules and vesicles are found adjacent to the fungal cell wall (Berlin and Bowen, 1964; Peyton and Bowen, 1963). The function of these vesicles or lomasomes is not known, however they are more numerous in haustoria than on the intercellular hypha (Berlin and Bowen, 1964).

1.3.2 Structure of the Host-Pathogen Interface

The invasion of host cells by P. hyoscyami leads to the production of specialized intracellular hyphae or haustorial bodies. Fraymouth (1956), studying haustoria in the Peronosporales, concluded that the shape of the haustorium reflects the quantity of nutrients it obtains from the host cell. The normally tubed-shaped haustoria coil and branch in nutritionally deficient cells.

The zone of interaction between the host and pathogen has been the basis of many investigations (Berlin and Bowen, 1964; Bracker and Littlefield, 1973; Bushnell, 1971; Chou, 1970; Coffey et al., 1972; Ehrlich and Ehrlich, 1963a,b; Heath and Heath, 1971). The sheath represented the response of the host to the fungal haustorium (Smith, 1900). Light microscopy studies by Fraymouth (1956) revealed that the sheath could entirely or partially enclose the haustorium of the Peronosporales.

Using the electron microscope, Ehrlich and Ehrlich (1963a) concluded that sheath formation in Erysiphe graminis

was a property of mature haustoria. In a succeeding paper on stem rust of wheat, Ehrlich and Ehrlich (1963b) changed the terminology and re-named the sheath, the zone of encapsulation.

Peyton and Bowen (1963), studying Peronospora manshurica on Glycine max stated that the sheath was dense staining material between the plasmalemma and the haustorial wall. The area was re-named the zone of apposition. The three terms: sheath, encapsulation and zone of apposition have unfortunately been used interchangeably. The confusion in the terminology was perhaps unavoidable, however, the problem was further complicated by the comparison of different taxonomic groups of fungi and different host combinations (Chou, 1970).

I shall use the terminology proposed by Bushnell (1972), where the extrahaustorial matrix, is the zone between the fungal wall and the plasmalemma of the host. The matrix itself may be composed of different layers or zones. The extrahaustorial membrane is a unit membrane which borders the host cytoplasm (Berlin and Bowen, 1964; Asada and Shiraishi, 1976; Bushnell, 1972; Heath and Heath, 1971; Hirata, 1971; Kohno et al., 1970; Peyton and Bowen, 1963). Bushnell (1972) concluded that the extrahaustorial membrane cannot be formed by stretching the existing plasma membrane. Instead, new membrane is laid down which is a direct product of the host-pathogen interaction. The dynamic nature of the extrahaustorial matrix is unknown. Studies are restricted to static electron-microscope pictures. Nonetheless, these

types of data enable us to postulate the degree of interaction between the host and parasite.

The sac (extrahaustorial matrix) can be extracted from cells infected by Erysiphe graminis (Hirata, 1971). The sac is elastic in nature because it can swell or shrink depending on the osmolarity of the suspending solution. The membrane of the sac (extrahaustorial membrane) is semi-permeable in nature and extremely sensitive to fixation (Bushnell, 1971; Hirata, 1971). Littlefield and Heath (1979), considered the possibility that the matrix was an artifact of fixation since it is so easily altered by fixation methods.

Ehrlich and Ehrlich (1963a), working with rusts, observed channels connecting the encapsulation layer, (or the extrahaustorial matrix), to the fungal cytoplasm. These channels have not been reported elsewhere. Peyton and Bowen (1963), working with Peronospora manshurica observed that the host plasmalemma around the haustorium had invaginations projecting into the host cell cytoplasm. These 'blebs' or secretory bodies were evident only in infected cells.

Peyton and Bowen (1963), hypothesized that 'secretory bodies' were formed on the host cell dictyosomes. From the dictyosomes they move to the plasmalemma and discharge contents into the zone of apposition (extrahaustorial matrix). In this manner the nucleus of the parasite, via messenger RNA, can direct the synthesis of proteins.

Vesicles have been observed around the haustorium, however

their origin is difficult to determine (Bracker and Littlefield, 1973; Ehrlich and Ehrlich, 1963a).

The infection of Pisum sativum with Peronospora pisi results in the formation of a penetration matrix. This electron-dense material represented a potential site for penetration (Hickey and Coffey, 1977). The papilla constituted the extrahaustorial matrix in P. pisi on P. sativum. Papilla formation was found to differ according to cell type (Kohno et al., 1970).

Working with Pseudoperonospora cubensis, Peronospora destructor, Peronospora brassicae and Peronospora spinaciae Kajiwara (1971), studied the ultrastructure of the haustoria. In each case, the haustoria contained an electron-dense layer on the outside of the fungal wall. Adjacent to the dense zone was the electron-transparent layer of the encapsulation.

Much controversy exists as to the origin of the electron-dense layer found on the surface of the fungal wall. Hickey and Coffey (1977) felt that this dense staining zone had a direct relationship with the penetration matrix observed near the penetration sites. Ingram et al., (1976) stated: "Whether the dark staining zone of the haustorial wall may be equated with encapsulation described as surrounding the haustoria of other members of Peronosporales by Peyton and Bowen (1963) or sheath around the haustoria of powdery mildews and rusts (Bracker and Littlefield, 1973) is a moot point, as is the question as to its origin in the host, fungus or both. The only reliable point of similarity between these structures is

that they occupy a similar position with regard to the haustorium and the protoplast of the host."

1.4. Objectives

The release of conidia of P. hyoscyami into the environment represents an important stage in the fungal life cycle. The effect of the environment on the airborne conidia determines if a mild disease or a severe epiphytotic will take place. Conidia are the principal means by which the continued survival and propagation of the pathogen are guaranteed. In the laboratory, an attempt was made to isolate the individual environmental factors and determine the effect of each on the spores. The three factors I worked with in various combinations were temperature, relative humidity and light. Each factor affected the germinability or viability of the conidium, thus it has a direct effect on the ability of the pathogen to continue its life cycle. This type of work has not been carried out on the P. hyoscyami f.sp. tabacina isolate obtained from the 1979 Ontario blue mould epiphytotic.

Investigations on the ultrastructure of P. hyoscyami conidium have not been carried out. Studying this problem will allow me to understand if the arrangement of membranes and internal structures contribute to the spore's ability to survive diverse conditions.

The colonization and development of P. hyoscyami f.sp. tabacina in the susceptible host, Nicotiana tabacum cultivar Virginia 115, has not been previously investigated by electron

and light microscopy. In an attempt to study the life cycle of this pathogen my work was subdivided into five major phases:

- a) pre-penetration,
- b) penetration,
- c) early development in the epidermal cell,
- d) development of intercellular hypha, haustoria, conidiophore and conidial formation and,
- e) formation of sexual structures.

Ultrastructural studies of penetration, early development and haustorial structure have been largely concentrated on the rusts and powdery mildews while very little information is available on the downy mildews.

The remaining objective of this work was to determine the effect of the obligate parasite on the ultrastructure of the host cells.

CHAPTER 2

MATERIALS AND METHODS

2.1. Conidial Inoculation

Conidia of Peronospora hyoscyami f.sp. tabacina vary in germination ability within the same spore population and between populations. In all experiments, unless otherwise stated, 5-10 week old plants of Nicotiana tabacum cultivar Virginia 115 were inoculated with a suspension of 10^8 - 10^{10} conidia per ml by means of sprayer with a fine nozzle. The inoculated plants were maintained in thermostatically controlled growth cabinets with day/night temperatures of 20/18°C, 100% relative humidity and a 12 h photoperiod at a light intensity (LI-COR LI 1905 quantum sensor) of 45 microeinsteins per m^2 per sec ($\mu Em^{-2} sec^{-1}$). At 5 days post-inoculation the relative humidity in the cabinets was lowered to 50-60% relative humidity, in order to prevent sporulation. Fifteen hours prior to an experiment which required conidia, plants were placed into plastic bags, tightly sealed and placed in the dark at 20°C. Following a 12-15 h incubation period, conidia and conidiophores formed a thin white lawn on the lower surface of the tobacco leaf.

Following the 12-15 h treatment, conidia were washed off the lower leaf surface with distilled water and centrifuged, at 250 rotations per min. for 15 min. The conidia were resuspended in distilled water and conidial counts were made

with a haemocytometer. In germination experiments, the conidial concentration was adjusted to 10^5 - 10^6 conidia/ml. One to 2 drops of this conidial suspension were placed on each 2 x 2 cm 1.5% Difco Bacto water agar block or 2 x 2 cm tobacco leaf section. A solution of 0.001% acid fuchsin in lactophenol was used as a conidial stain and to prevent further development or germination. Each experiment was repeated 4 times. In each experimental treatment 4 fields of 100 spores were counted. Controls were conidia germinated on water agar at 20°C. The viability of a conidium was determined by its ability to germinate. Conidia of P. hyoscyami were considered germinated if the length of the germ tube was equivalent to one-half the diameter of the conidium.

2.2. Temperature Experiments

2.2.1. Optimum Germination Temperatures

Conidia were prepared as outlined in Section 2.1. The conidia seeded agar blocks were placed in incubators at 5, 10, 15, 20, 25 and 30°C for 15 h and then the germination counts were made.

2.2.2 Determination of the Rate of Germination

The 'rate of germination' was defined as the number of conidia germinated in a given time period. It was determined at temperatures of 5, 10, 15, 20, 25 and 30°C. The blocks of seeded agar (as outlined in Section 2.1.) were removed from each incubator at 1 h intervals for 8 h. A final reading was obtained at 24h post-inoculation.

2.2.3. Exposure of Conidia to High Temperatures

In order to determine the effects of high temperatures for brief periods of time on conidia, seeded agar blocks were exposed to each of 25, 30 and 35°C for 1, 2, 3, 4, 5, 6, 7 and 8 h periods. Following the heat treatment, the agar blocks were placed at 20°C for 15 h and then percent germination was determined. Controls consisted of conidia kept at 20°C.

2.3. Control of Water Potential by Sucrose Solutions

Conidia (15 h old) were gently brushed off infected sporulating leaves into 1, 2, 3, 4 and 5 molar sucrose solutions. The molality at which the conidia became shrunken was recorded. Conidia were allowed to remain in their respective sucrose molarities for 24 h. Following this period percent germination was determined. To test the viability of the non-germinated conidia, the conidial sucrose solutions were centrifuged for 15-20 min. until a pellet was formed. The supernatant was decanted and the spore pellet suspended in distilled water. The procedure was repeated 4 times in order to remove sucrose from the conidia. The washed conidia were allowed to germinate on agar blocks and examined after 15 h.

2.4. Humidity Experiments

Sulfuric acid solutions and salt solutions (Appendix I) were used to control relative humidity in a sealed vessel. Coverslips (Corning No. 1, 22 mm²) were gently appressed to a lawn of conidia on the lower leaf surface. The cover slip

with the adhering conidia was inverted over tubes (diameter 20 mm, length 15 cm) containing sulfuric acid or salt solutions. The spores were placed at 0, 50 and 80% relative humidity. Zero percent relative humidity was obtained by placing the cover slips in containers filled with dry silica gel. The cover slips were sealed onto the tubes with sealing plastic (Elastoplast). The tubes were placed into sealed containers at 5, 15, 25 and 35°C. On consecutive days, samples were withdrawn from the treatments and percent germination determined. In germination experiments, the cover slips from the humidity experiments were placed on 1.5% water agar, so that the adhering spores were in contact with the agar surface. To facilitate germination 1 to 2 drops of water were added to the glass-agar interface. The samples were incubated at 20 C for 15 h and then the percent germination was determined.

2.5. Light Experiments

2.5.1. Fluorescent Light

Conidia were prepared as outlined in Section 2.1. The seeded agar blocks were exposed to fluorescent light at intensities of 45, 150, 300 and 600 $\mu\text{Em}^{-2} \text{sec}^{-1}$ in darkness at 20°C. The percent germination was determined after 15 h of incubation.

2.5.2. Ultraviolet Light

Suspensions of conidia 10^5 - 10^6 /ml were exposed to ultraviolet radiation of 120 $\mu\text{W cm}^{-2} \text{sec}^{-1}$ (General electric bulbs, 360 nm) for periods up to 1 h. The conidial solution was maintained

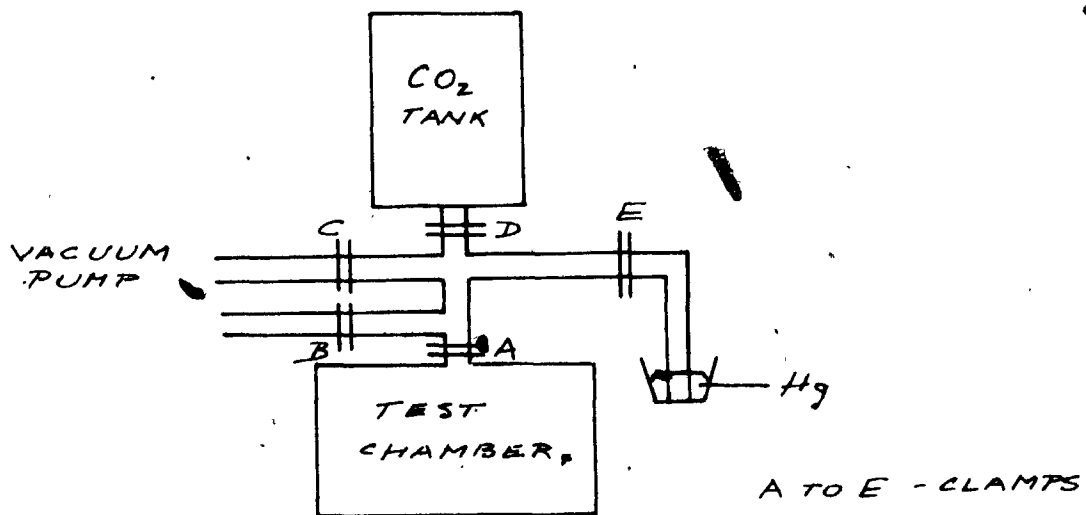
on a rotary shaker during ultraviolet radiation in order to keep the spores in suspension. One to 2 drops of the conidial suspension were removed at 10 min. intervals and placed in water agar. The same procedure was followed for controls which were not exposed to ultraviolet radiation.

Additionally, conidia attached to the conidiophores on 2 x 2 cm leaf sections were exposed to UV radiation at $120 \mu\text{W cm}^{-2} \text{ sec}^{-1}$ for periods up to 8 h. At specific time intervals leaf sections were removed from the UV light and placed in distilled water. The conidia were washed off the leaves and placed on water agar for 15 h at 20°C . Germination counts were made with a haemocytometer. Controls consisted of a similar treatment, however the conidia were not exposed to UV radiation.

2.6. Exposure of Conidia to Carbon Dioxide Enriched Air

To test the effect of carbon dioxide (CO_2) on conidial germination a closed chamber system was designed to enable control of CO_2 in the air. (Diagram 1)

DIAGRAM 1: Schematic Diagram of the CO_2 Apparatus



The actual quantity of CO₂ added to the test chamber depended on the atmospheric pressure for that day. For example, a barometric pressure of 705 mmHg, 9mmHg of CO₂ was required to give 1.3% CO₂ in the test chamber. This was accomplished by closing clamps B and D and evacuating the test chamber to 18 mmHg. This was monitored by a 30 in. (760 mm) manometer. With clamp B closed and D opened CO₂ equivalent to 9 mmHg was put into the chamber. Clamp E was closed and B opened to admit air into the chamber.

Conidia were seeded onto water agar and exposed to 1, 5, 7.5 and 15% CO₂. The controls were maintained in air at 20°C and atmospheric CO₂ concentration (0.03%). Following exposure to CO₂, for up to 18 h, the percent germination was determined. Spores which did not germinate in the CO₂ were placed in air at 20°C for 15 h to test germination. Each experiment was repeated 4 times, 4 fields of 100 spores each were counted at each treatment.

2.7. Light Microscopy

2.7.1. Leaf-clearing Solutions

To obtain a clear observation of conidia on the tobacco leaf surface two clearing methods were used.

1. Tobacco tissue was cleared in chloroform:lactophenol:methanol (1:1:1) solution for 0.5 to 2 h periods until all chlorophyll had been removed from the tissue sections. The sections were stained subsequently with 0.001% acid fuchsin in lactophenol.

2. A graded ethanol series of 20, 50 and 70% was used to clear the tobacco leaf tissue. The leaf sections remained

in 70% ethanol overnight. This clearing method was used prior to staining with Lacmoid (Sigma C.I. 51400).

2.7.2. Staining Procedures

Acid fuchsin (0.001%) in lactophenol and 0.01% Lacmoid (Sigma), acidified with 1 to 2 drops of glacial acetic acid, were used to stain the fungus during development, penetration and development in the host tissue.

Jacques' staining procedure (Jensen, 1962) was used to stain haustoria, extrahaustorial matrices intercellular hyphae and sexual structures. Leaf sections were dehydrated in a graded ethanol series (50, 70, 80, 90, 100, 100%), with 5 min. at each concentration. The ethanol clearing was followed by staining the leaf sections for 20-30 min. in a concentrated solution of methylene blue in absolute ethanol. Then the tissue was placed in a saturated solution of erythrosin B (Fisher) in clove oil for 5-10 min. The leaf sections were removed from the clove oil and placed in a wash solution composed of equal parts of xylene and ethanol. This wash removed the excess clove oil from the tissue. The final wash consisted of absolute xylene for 1-4 min. The staining tissue was mounted in 2:1 Canada balsam in xylene. The tissue was examined by means of a Zeiss light microscope.

2.8. Electron Microscopy

2.8.1. Transmission Electron Microscopy (TEM)

Discs 1 mm in diameter were cut from tobacco leaves and fixed for 2 h in 4% glutaraldehyde in cacodylate buffer at

pH 6.8. The material was rinsed twice in fresh buffer and post fixed for 1 h in 2% osmium tetroxide. After fixation the material was rinsed in water and stained in 5% uranyl magnesium acetate for 20 min. at room temperature, dehydrated in a graded acetone series of 20, 50, 70, 80, 90, 95 (20 min. each) and 100% acetone twice at 30 min. each. Following the final acetone series the material was placed in propylene oxide for 20 min. The propylene oxide was gradually replaced with Epon-Araldite plastic in varying proportions. Two hours at 3:1 propylene to plastic, 1:1 for 2 h and 2 changes of pure plastic 16 h each. During the embedding process the discs and the plastic:propylene solutions were placed on a rotary wheel to facilitate infiltration of the leaf tissue with plastic. The plastic was made by adding 4.4 ml EPON 812 (Ladd Sci. Co.) to 3.6 ml Araldite. The two chemicals were stirred slowly until they were totally mixed. To this mixture 20 ml DDSA (Dodecenyl succinic anhydride) was added and the entire mixture was stirred. To this final mixture 0.2 ml DBP (dibutylphthalate) and DMP-30 (tri-dimethylamio-methyl phenol) were added and mixed thoroughly. The fresh plastic and specimen were poured into moulds and placed in an oven for 24 h at 60°C. Thin sections were cut with a diamond knife on a Porter-Blum ultramicrotome. Silver or gold sections were mounted on uncoated 200 x 200 mesh copper grids and stained in lead citrate. The grids were examined in Philips 200 electron microscope operated at 60 kV with 50 μ m objective aperture.

Spurr's low viscosity embedding medium was used occasionally instead of Epon-Araldite (Spurr, 1969).

2.8.2. Scanning Electron Microscopy (SEM)

Infected tobacco tissue, 1 x 1 cm, was placed in 4% glutaraldehyde in 0.1 M sodium cacodylate buffer pH 6.8 for 2 h. The tissue was washed 5 times in buffer, 5 min. for each wash, and placed in 1% osmium tetroxide for 2.5h. The material was washed in distilled water, 3 times at 10 min. per wash, and passed through an ethanol series (50, 70, 80, 90, 95, 100, 100%), 5 min. per ethanol concentration. The material was then ready for critical point drying (see Section 2.8.3.).

To study the internal structures of the leaf infected with P. hyoscyami in the SEM the procedure was modified slightly. Plant tissue, 1 x 1 cm, was fixed in 1% osmium tetroxide in 0.1 M phosphate buffer pH 7.2 for 24 h at 0°C. The next morning fresh fixative was added for 4 h at 4°C. The material was rinsed 4 times, 15 min. per wash. The plant tissue was placed between two sections of pith tissue soaked in ethanol. Thin sections of pith tissue and infected tissue were made using a hand microtome. The thin sections of plant tissue were washed and separated from sections of pith in distilled water and added to 1% unbuffered osmium tetroxide for 60 min. The tissue was passed through a graded ethanol series (20, 40, 60, 80, 95, 100, 100%), 30 min. at each concentration. Following ethanol treatment the specimens were transferred immediately to the specimen chamber of the critical point drier.

2.8.3. Critical Point Drying (CPD)

Tissue from 100% ethanol was placed in the specimen

chamber of the Sorvall Critical Point drying apparatus. With the inlet and outlet valves closed, the tank valve was slowly opened to admit liquid carbon dioxide (CO_2) into the tubing. By slowly opening the inlet valve, the liquid CO_2 was admitted into the specimen chamber. When the chamber was full of liquid CO_2 , the inlet valve was closed and the system allowed to equilibrate for 15 min. Following equilibration, the inlet valve was opened first and then the outlet valve. The chamber was flushed with liquid CO_2 for 15 min. The CO_2 flow was monitored by observing the rate of bubble formation in the water created by the exhaust from the chamber. The above procedures of flushing and equilibration were repeated 6 times. During this period, the tank liquid displaced the solvent (ethanol) in the specimen. The chamber pressure was maintained at 800 psig (pounds per square inch-gauge). After the last flushing of the system, the inlet and outlet valves were closed and the specimen chamber was immersed in a beaker of water at 60°C . The pressure in the specimen chamber rose to 1,500-2,000 psig. The system was allowed to equilibrate for 5 min. At this point, the solvent in the plant tissue was replaced by CO_2 . At the critical temperature of CO_2 (45°C) the fluid in the chamber is at equilibrium and cannot separate into its respective vapour and liquid states. The fluid in the chamber was slowly exhausted at 100 psi/min. Once the chamber had been depressurized, the specimen preparation was complete. The dry tobacco tissue was mounted on SEM mounting stubs with double-sided adhesive tape. The specimens were then sputter-coated with a mixture of gold:paladium (1:1) for 10 min.

2.9. Starch Analysis in Infected Tobacco Leaves and Healthy Controls

2.9.1. Plant Pre-conditioning and Inoculation

Nicotiana tabacum, cultivar Virginia 115, plants were propagated in a greenhouse to the 4 leaf stage of development. To remove high starch levels from the leaves, the plants were transferred to dark growth cabinets. The temperature was 18°C and the plants remained in darkness for periods up to 3-4 days. The dark treatment was followed by a day/night regime of 12 h/12 h at $150 \mu\text{E m}^{-2} \text{sec}^{-1}$ for 1 to 2 days. The experimental plants were infected by using a conidial suspension of P. hyoscyami. Control plants were subjected to the same experimental treatments, except inoculation. The light/dark periods were adjusted as desired for each experimental treatment.

2.9.2. Macroscopic Detection of Starch

The detection of starch in whole leaves was achieved by placing the leaves in boiling water for 20 sec. The leaves were removed from the water and placed in a solution of 95% ethanol. The leaves remained in the ethanol solution until the chlorophyll had been removed from the plant tissue. Then cleared leaves were removed from the alcohol bath and placed in a 0.2% solution of iodine in potassium iodide (IKI). To prepare this solution, 2 g of potassium iodide was dissolved in 100 ml of water and then 0.2 g of iodine was dissolved in the potassium iodide solution. This method provided a semiquantitative measurement of small amounts of starch in the tobacco leaf. The presence of starch in the leaf was detected by the presence of a blue color in the alcohol

cleared leaves. After the leaf accumulated a limited amount of starch the blue color did not intensify. The presence of small amounts of starch in diseased and healthy leaves was measured quickly by this method throughout the day/night cycle and up to 6 days after infection.

2.9.3. Total Starch Assay

Tobacco leaves were collected from infected and control plants and tested with the IKI solution (see Section 2.9.2.). This gave a quick indication of the amount of starch accumulation/depletion in the test leaves. At 1, 3 and 6 days after infection with P. hyoscyami, 10 g of leaf tissue was ground in a Waring blender in 80% ethanol. This solution, containing macerated leaves, was centrifuged at 15,800 x g for 20 min. The supernatant was discarded but the pellet was resuspended in 80% ethanol. The washing of the pellet continued until all the traces of soluble sugars had been removed. The supernatant was tested with the Anthrone reagent for the presence of sugars. Washing continued until the supernatant did not turn blue when the Anthrone reagent was added. A blue color indicated the presence of soluble sugars. The remainder of the procedures for extraction of starch was followed as described by Jensen (1962). Glucose was used as a standard. The final results were recorded in terms of mg of starch/g of dry leaf tissue.

2.10. Enzyme Assay

In order to determine the activity of starch-degrading enzymes in diseased and healthy tobacco leaves 10 g of tobacco

leaf tissue was homogenized on ice in 0.1 M Tris-HCl buffer at pH 7.0. The homogenate was centrifuged at 14,460 x g at 5°C for 30 min. The protease inhibitor, phenylmethylsulfonyl fluoride (PMSF), which was added had no influence on the tobacco leaf extract containing the starch-degrading enzymes. The chemical was not added to the supernatant. Following centrifugation, the supernatant was mixed in equal proportions with saturated ammonium sulfate at 5°C for 30 min. The contents of the solution were centrifuged at 14,460 x g at 0°C. The pellet was resuspended in 5 ml of 0.1 M phosphate buffer at pH 6.0.

The enzyme activity of the starch degrading enzymes was assayed by adding soluble potato starch in 0.1 M phosphate buffer at pH 6.0 (Lintner soluble starch) to 3 ml of the reaction mixture. The mixture was placed on a shaker at 37°C. At 1 h intervals 1 ml aliquots of the mixture were removed and added to 49 ml distilled water. The relative enzyme activity was determined by measuring the amount of starch remaining following amyolytic activity. To the 50 ml starch and water solution 2 ml of the IKI solution were added. The blue color that resulted was measured at an absorbance of 620 nm. To quantify the starch, a starch standard curve was prepared. Excess IKI was used to prevent depletion of the IKI solution due to dilution. To each 25 ml of standard starch solution at different concentrations 1 ml of IKI solution was added. One ml IKI was added to 25 ml distilled water to zero the spectrophotometer (Bausch and Lomb).

Protein concentrations of the samples were determined according to Lowry et al. (1951).

CHAPTER 3

RESULTS

3.1. In Vivo Development

3.1.1. Disease Development in the Field and in Growth Chambers

The 1979 Ontario blue mould epidemic provided an opportunity to observe the development and progression of P. hyoscyami under field conditions. The tobacco crop in 1979 was damaged to such a degree that growers cut down the infected fields (Figure 1). The field symptoms in July and August were characterized by large numbers of chlorotic and necrotic lesions on the tobacco plants (Figures 2, 3). In the early dawn hours the fungus obtained sufficient moisture for sporulation. Conidia and conidiophores developed on the lower surfaces of plants infected for more than 5 days. Under continued optimal humidity the fungus sporulated on the upper surface of the leaf.

In growth chambers a similar disease cycle was obtained. In low light ($45\mu\text{E m}^{-2}\text{sec}^{-1}$), a 12 h day/night regime and day/night temperatures of 18/20°C, tobacco leaves infected with P. hyoscyami developed chlorotic lesions 2 to 3 days following infection (Figure 4). At 5 days or more following infection conidiophores and conidia developed first on the lower (Figure 7), then on the upper (Figure 6)

tobacco leaf surface. A drop in the relative humidity retarded the development of the fungus inside the host resulting in the production of large necrotic leaf lesions (Figure 5).

3.1.2. Host

Tobacco leaf tissue (Figures 8-11) observed by light microscopy exhibited large jigsaw-shaped upper and lower epidermal cells (Figures 8, 11), devoid of chloroplasts and containing a larger central vacuole. Immediately below the upper epidermis, the palisade cell layer (Figure 9) was composed of tubular cells arranged sparsely with large intercellular spaces between them. Below the palisade layer lay the spongy parenchyma cell layer. These cells were larger and interconnected (Figure 10), with extensive intercellular space between them. The lower epidermis (Figure 11) was similar to the upper epidermis in appearance.

3.1.3. Conidiophore and Conidial Formation

Conidiogenesis for the Ontario isolate of P. hyoscyami occurred in 5 days at 15/20°C day/night temperatures, a 12/12 h day/night regime and 100% RH. Under these conditions, fungal development in host tissue was extensive. The intercellular hyphae grew in the intercellular spaces of the host. The hyphae followed the host cell wall for long distances without haustorial formation. Division at the actively growing tips was always dichotomous (Figure 24). As the fungus invaded healthy tissue, the older sections of the intercellular hyphae became empty and devoid of

cytoplasm (Figures 86, 90). Within 5-6 days of inoculation in ambient relative humidity, segments of inter-cellular hyphae formed knot-shaped structures (Figure 12) in the stomatal chamber. Occasionally a single inter-cellular hypha was seen in the stomatal chamber (Figure 13). Conidiophore initials were present in the stomatal chamber. In darkness and high humidity the pre-emergent conidiophore developed into a conidiophore and emerged through the stomatal aperture (Figures 14, 16). One to 8 conidiophores were observed emerging from single stoma (Figures 14, 15).

The conidiophore initial elongation and branching commenced within 1 h (Figure 17). The branching was dichotomous, 4 to 5 dichotomous divisions were required prior to the initiation of conidial formation. The first indication of conidial formation was the appearance of small ball-shaped enlargements on the ends of the conidiophore branch (Figure 18). Conidial formation was not synchronous on all branches of a single conidiophore. Individual branches were observed to contain conidia of different sizes (Figure 19). Mature ellipsoidal conidia were released into the air once the relative humidity had dropped below 95%.

3.1.4. Sexual Structures

Sexual structures of P. hyoscyami were observed in 8-12 day old infected tobacco maintained in growth chambers at 20°C, 12/12 h day/night and ambient relative humidity.

The immature oogonium, 46 μm in diameter, appeared to conform somewhat to the shape of the intercellular space (Figure 20). Older oogonia appeared as spherical, thin walled, dark staining, structures. A small club shaped antheridium, 5 μm in diameter, was often observed adjacent to the oogonium (Figure 21). In the same host tissue fertilized oogonia were observed (Figures 22, 23). The oogonium had a well defined reserve globule and a thick oospore wall with a central globular body (Figure 22).

3.2. In Vitro Conidial Germination

The germination responses of P. hyoscyami conidia at constant temperatures are summarized in Figure 109. The minimum, optimum and maximum temperatures for conidial germination following 24 h incubation were 5, 10-20 and 30°C respectively. The fastest germination (Figure 110) occurred at 15 and 20°C. Germ tubes formed within 1 h of incubation at these temperatures. At 5 and 10°C a lag in germination of 6 and 2 h respectively was apparent. Maximum percent germination was obtained by 75 h at 10°C and 24 h at 5°C. At 25°C germination commenced within 1 h, however only 68% germination was obtained within a 24 h incubation period. At 30°C germination rate was very low, reaching 1.5% germination after 24 h of incubation.

Exposure of P. hyoscyami conidia to temperatures of 25, 30 and 35°C for 1 h intervals up to 8 h was followed by an incubation period of 15 h at 20°C (Figure 111). Exposure of conidia to 8 h at 25 and 30°C and 7 h at 35°C,

50% of the conidial population remained viable. An 8 h exposure at 35°C produced 0% survival of the conidia, however 50% of the conidial population remained viable after 1.5 h at exposure to 35°C.

Germination of P. hyoscyami conidia in fluorescent light of varying intensities from 45 to 600 $\mu\text{Em}^{-2}\text{sec}^{-1}$ and darkness had no effect on conidial germination (Table 8).

Ultraviolet irradiation ($120 \mu\text{Wcm}^{-2}\text{sec}^{-1}$) at 100% RH and 20°C resulted in a 50% reduction in viable conidia on glass slides after 5 min of exposure (Figure 114). For comparable exposure of conidia in water, 50% reduction in conidial germination was obtained following a 60 min. exposure period. Figure 115 shows the effect of UV ($120 \mu\text{W cm}^{-2}\text{sec}^{-1}$) irradiation on conidia attached to the conidiophore on a surface of a tobacco leaf. Following 3 h of UV irradiation 50% of the conidia remained viable. The control conidia remained 60% viable up to 8 h.

The swelling and shrinking of P. hyoscyami conidia was controlled (Figure 112), by sucrose solutions of varying molalities which exhibited differing water potentials. At water potentials up to -27 bars all conidia remained turgid while at -141 bars 98% of the conidia in the solution were shrunken. The conidia remained in the sucrose solutions for 24 h (Figure 113) and germination of 100% was obtained at 0 - .5 bars. Percent germination declined sharply reaching 0% germination at -141 bars.

Carbon dioxide enriched atmospheres of 1, 5, 7.5 and 15% inhibited germination of P. hyoscyami conidia (Table 7). A 2 h exposure of conidia to CO₂ enriched atmosphere led to gradually higher percent inhibition from 1 to 15% CO₂, the greatest inhibition occurred at 15% CO₂ the least at 1% CO₂. Holding the conidia in the CO₂ enriched environment for up to 18 h produced a decrease in the inhibition. Comparison with conidial germination by Botrytis cinerea and Aspergillus niger under similar experimental conditions was made. The spores of B. cinerea were slightly inhibited at 5% CO₂. Spores of Aspergillus niger were not inhibited at any CO₂ concentration used. Normal germination levels, equal to that of the controls, were obtained once the spores of P. hyoscyami, B. cinerea and A. niger were removed from CO₂ enriched atmosphere and placed in air.

Storage of conidia at relative humidities of 0, 55 and 81% and temperatures of 5, 10, 25 and 35°C (Table 6) showed that the highest percent spore survival occurred at 5°C, at all relative humidities. Factorial ANOVA analysis (Appendix 2) was performed on the storage data. This analysis showed that the length of storage of conidia was affected (at $p < 0.001$ level of significance) by temperature and relative humidity.

3.3. Germination, Penetration and Early Development

The conidia of P. hyoscyami are ellipsoidal (Figures 25, 30, 31, 32, 35), 15 x 22 μm in size, and tapered toward the attachment point (Figures 30, 33 - arrows). Prior to germination, the quiescent conidia were full of dark-staining protoplasm (Figure 35). Electron microscopy (Figure 45) showed that the quiescent thin walled conidia were filled with numerous nuclei, mitochondria and electron-dense particles. The conidial cytoplasm contained a few vacuoles and at the pointed end of the conidium a scar (Figures 30, 33) marked the point of attachment of the conidium to the conidiophore. Examination of the conidial scar in thin sections (Figure 46) showed a pore formed due to a break in the fungal wall. The conidium of P. hyoscyami does not have a papilla. Conidial shrinkage and collapse (Figure 50) of the conidial wall occurred when the conidium dried.

A summary of times required for infection of upper epidermal cells of a susceptible tobacco leaf are given in Table 1. Figures 25-28, graphically depict the process of germ tube formation (Figure 25), appressorium formation (Figure 26), penetration (Figure 26), vesicle formation (Figure 27) followed by hyphal growth through the epidermal cell and into the surrounding host cells or intercellular spaces (Figure 28).

Infection was rapid; the fungal hypha grew through the epidermis and into the adjoining tissue or intercellular

spaces by 2.6 - 4.1 h following inoculation.

The first indication of morphological changes in the germinating conidium was the change in the appearance of the spore protoplasm where small vacuoles coalesced to form larger structures (Figures 48, 49). The increasingly vacuolated conidial cytoplasm resulted in the displacement of the cytoplasmic contents to the periphery of the conidium (Figure 49).

Conidia from the inoculation drop lodged in the depressions of the epidermal cells (Figures 29, 32, 33) where water collected and remained for the longest period of time. The lowest leaf depressions were directly above the anticlinal wall (Figures 32, 33). It was in this constricted space that the conidium produced a germ tube, 3-4 μm in diameter (Figures 25, 31, 33, 36). The germ tube formed near the pointed tip of the conidium (Figures 31, 32). On susceptible tobacco, the germ tube usually remained short, not more than 10 μm in length. Germination of conidia in water on glass slides, lead to production of germ tubes up to 400 μm in length (Figure 41). On 1.5% Difco Bacto agar, the germ tubes branched and formed long hypha (Figure 42). Occasionally an appressorium developed without the formation of a germ tube (Figures 43, 44). The germ tube was always constricted at its point of origin (Figures 33, 53). Sufficient protoplasm to fill the germ tube flowed from the conidium (Figure 36). The club-shaped appressorium formed at the end of the germ tube and

was filled with cytoplasm (Figures 37, 38, 53).

At this stage the conidium was devoid of cytoplasm (Figure 51). Occasionally, small circular structures or conidial inclusions remained in the conidium (Figure 38). These structures were not observed in the electron micrographs, only in conidia stained with Lacmoid and observed by means of the light microscope.

The protoplasm that flowed from the conidium into the germ tube and appressorium contained electron-dense granules, cytoplasm full of free ribosomes and large numbers of mitochondria (Figure 47). The plasma membrane of the conidium remained in the empty conidium (Figures 52, 53). The spore wall broke (Figure 53) and new wall material was formed around the germ tube. The plasma membrane of the conidium was continuous with that of the germ tube and appressorium (Figure 53). The portion of the appressorium in contact with the leaf and adjacent to an anticlinal wall, developed an infection tube about 2 μm in width, which passed through the host epidermal wall (Figures 54, 55, 56), but produced no change in the wall electron-density. A flange was present around the penetration tube between the epidermal and appressorial walls (Figures 34, 39, 55).

Following penetration, a large spherical vesicle 10-15 μm in diameter formed in less than 5 min, at the tip of the infection tube inside the epidermal cell (Figure 27). While the protoplasm moved into this vesicle, a plug began to form at the inner end of the infection tube (Figures 27,

55, 56). The contents of the appressorium emptied into the vesicle and plug formation was completed (Figure 57). Small amounts of cytoplasm remained in the tube and the appressorium (Figures 54, 57). The plug consisted of small pieces of electron-dense material (Figure 57). A wall, surrounded the vesicle and was continuous over the plug (Figure 57).

Hyphal growth was initiated as the vesicle formed a 'nipple' like projection at the end distal to the epidermal wall (Figures 40, 58). The 'nipple' and the vesicle were filled with numerous nuclei, with closely associated dictyosomes and large numbers of mitochondria (Figure 58). In the 'nipple' itself, large numbers of spherical and tubular vesicles were observed (Figure 58). The nipple usually developed into a lobulate carrot-shaped body (Figures 28, 58). The ultrastructure of the carrot-shaped body showed it was filled with large numbers of mitochondria and nuclei. The host plasma membrane surrounded the carrot-like vesicle (Figure 54).

A small quantity of the host cytoplasm was found in a thin layer between the host plasmalemma and the tonoplast (Figures 54, 58). A break in the plasma membrane due to fungal penetration was never observed. Occasionally a branch formed and invaded an adjacent epidermal cell (Figures 28, 60). After growing through the epidermal cell, the hypha grew into a palisade cell (Figure 59) or intercellular space. This was made possible by the morphology

of the tobacco leaf where the palisade cells (Figure 9) were separated from each other and projected from the epidermal cells somewhat like pegs on a drying board. The chloroplasts, mitochondria and cytoplasm in the infected host cells appeared to be healthy (Figure 59). Host cytoplasm accumulated at the point of entry of the fungus (Figure 59), but in other regions of the host cell, it formed a thin band around the invading fungal structures (Figure 54, 60).

Actively growing regions of the fungus were always packed with dense protoplasm (Figures 58, 59, 60). Fungal nuclei were about 3 μm in diameter, and each contained a small nucleolus (Figure 61). Several nuclei were present in the ungerminated conidium, germ tube, appressorium, vesicle (Figure 45), and hyphae. A dictyosome was always at the side of each nucleus (Figures 28, 60, 61). Blebs on the nuclear envelope were observed projecting into the adjacent dictyosomes (Figure 62). The tubular elements were numerous in the cytoplasm (Figures 58, 60) and often projected through the plasmalemma into the fungal wall (Figure 64). The fungal plasmalemma was always convoluted (Figures 57, 60, 64).

A few lipid bodies were found in the conidia and hyphae (Figures 45, 54). No glycogen or protein crystals were detected in any part of the fungus. The mitochondria were elongated, contained distinct cristae (Figures 58, 60) and were abundant, especially near the growing hyphal tips.

Vacuoles occupied at least one half of the space in each conidium but were not plentiful in cytoplasm in actively growing regions (Figures 58, 59).

Small electron-transparent vesicles were numerous in the cytoplasm in the actively growing regions (Figures 58, 60). Occasionally a distinct centriole was observed beside a nucleus (Figure 61). A dictyosome was always found adjacent to a centriole (Figure 61). Plasmalemasomes were often observed (Figure 65) in close proximity to the fungal wall.

3.4. Haustorial Formation

3.4.1. Light Microscopy

Bulb shaped incipient haustoria of P. hyoscyami (Figures 68, 69, 95A) were present in several kinds of cells of the tobacco leaf; the upper epidermis, palisade, spongy parenchyma and lower epidermis. Fungal intercellular hyphae followed closely the cell walls of the host cells (Figures 68, 70). Haustoria formed along certain portions of the intercellular hypha. Long stretches, 400 - 800 μm , of hyphae were observed without haustorial bodies. Haustorial formation was occasionally observed to consist of clusters of haustoria radiating from terminal portions of intercellular hypha into adjacent cells (Figure 72).

The bulb-shaped incipient haustorium developed into a cane-shaped body (Figures 67, 71, 74) which reached up to 10 - 15 μm in length. Branching of the cane-shaped structure was occasionally observed (Figures 71, 73). Continued

growth and development of the haustorium resulted in a torulose and spiralling structure reaching lengths up to 50 μm (Figure 73).

In infections 7 days and older, some shrunken or collapsed haustoria (Figure 77) were observed in host cells. The shrunken haustoria were often found adjacent to turgid haustoria in the same host cell.

A dark staining layer immediately adjacent to the haustorium (Figures 74 - 77) was evident when sections of leaf tissue were stained with Jacque's stain. The dense layer partially (Figures 74, 75) or entirely (Figure 76) enclosed the haustorium and the dark staining layer was present around shrunken haustoria (Figure 77). The intercellular hypha of the fungus did not have a dense layer on the periphery of the fungal wall (Figure 75).

3.4.2. Electron Microscopy

Haustoria developed only from hyphae that were in contact with the host wall. However a hypha might be in contact with the host wall for a long distance (200-400 μm) without haustorial formation. The first sign of haustorial formation was a slight bulging of the hyphal wall into the host wall. Serial sections of haustorial penetrations did not contain evidence of papillae. By the time the incipient haustorium had been formed, the fibrils in the host wall (Figure 81 - arrow) had reoriented in the vicinity of the haustorial neck. The host-wall pore was about 1 μm in diameter. At the edge of the pore a small amount of host wall was out-turned around the neck of the haustorium

(Figure 81). The cane-shaped haustorial body (Figure 95B) enlarged until it was about 3 μm in diameter (Figure 78). The haustorial wall was continuous with that of the mother hypha (Figures 67, 78). The young haustorium was characteristically full of cytoplasm (Figures 78 to 85) which contained mitochondria (Figures 83, 85), nuclei and endoplasmic reticulum (Figure 82). Occasionally atypical mitochondria were observed in irregularly shaped young haustoria (Figure 91). A large dictyosome was always present adjacent to the fungal nucleus (Figure 85). Vacuoles were not observed in the incipient haustorium (Figures 79, 80) and in the mother hyphae adjacent to the haustoria. Vacuolated haustoria were observed in the later stages of haustorial development.

Due to coiling of the haustorial body (Figure 95C) more than one section through the fungal body was observed (Figure 84). Associated with the haustorium was material located between the fungal wall and the host cytoplasm. The zone was characterized by two layers. Immediately adjacent to the fungal wall was an electron-opaque layer (Figure 67) and an outer electron-transparent layer (Figure 67). The electron-dense layer, 0.3 - 0.5 μm in thickness, encased the entire haustorium (Figures 78, 79, 80, 94). The electron-transparent layer, up to 3 μm in diameter, enclosed the haustorium entirely (Figures 78, 81, 84) or partially (Figure 83). Dark-staining membrane-bound vesicles were interspersed in this zone. Pores were observed in the inner opaque layer (Figures 67, 82). This layer was

usually somewhat thicker near the base of the haustorium (Figure 81). Projections from the host cytoplasm (Figure 82, curved arrow) were in contact with the electron-dense layer. Haustoria developing in the large central vacuole of the host cell contained cytoplasmic strands which connected the cytoplasm around the haustorium to the layer of cytoplasm lining the inside of the host cell (Figure 85).

The host plasma membrane was not broken by the fungus, instead the membrane covered the haustorial body (Figures 81, 85). Host cytoplasm was located in a band between the host plasma membrane and the tonoplast (Figure 78). In sections it formed a thin layer around the fungal body (Figures 67, 78, 83).

Up to 8 days post-inoculation, degradation and disorientation of host tissue was not observed. Host cytoplasmic organelles, mitochondria, chloroplasts and nuclei (Figures 80, 83, 84), had a normal structural appearance. As the haustoria matured they became longer and more vacuolated (Figures 81, 84).

Ultrastructural changes were apparent in the adjoining mother hyphae. Young hyphae (Figure 66) contained a densely staining cytoplasm full of mitochondria, nuclei and dictyosomes. As the hyphae matured increasing number of vacuoles were observed in the cytoplasm (Figures 86, 87, 88, 89). Eventually the hyphal cytoplasm was devoid of contents (Figure 90).

48

Collapsed or shrunken haustoria were occasionally observed in cross section (Figures 92, 93, 94), while the mother hypha which produced the collapsed haustorium remained turgid (Figure 94). In cross section and longitudinal section the electron-opaque layer and electron-transparent layer were prominent (Figure 92) and the fungal wall was convoluted (Figure 93). The host cytoplasm adjacent to collapsed haustoria appeared normal (Figure 94).

3.5. Starch Accumulation and Degradation in Infected and Healthy Host Tissue

During electron microscopic studies of development of P. hyoscyami in susceptible tobacco, diseased leaves were fixed in the morning following a dark period at 1 to 2 days after infection. More starch was observed in chloroplasts of diseased (Figures 100, 101) than healthy leaves (Figure 98) for periods up to 4 days post-inoculation. However, when the leaves were examined on day 5 or thereafter the reverse was true (Figure 102). Abundant starch granules were found in healthy leaves (Figure 99) while at the same time starch granules were not present in the 6 day-infected tissue.

The IKI test (Section 2.9.2) enabled the investigator to follow starch accumulation/degradation throughout the infection cycle. Plants inoculated for 36 h were placed in darkness with uninoculated control plants. In infected plants, starch formation was similar to that in the healthy controls (Table 2). This profile was maintained for up to

cells (Sargent et al., 1973).

The intimate association of tubular elements and spherical vesicles, which bleb from the dictyosomes, with the fungal wall, and their great abundance in growing hyphae, indicated that they play a role in wall synthesis as several investigators have claimed (Groves et al., 1970; Mollenhauer and Moore, 1966). Groves et al. (1970) have suggested that the vesicular membrane fuses with the plasma membrane, and the vesicular contents are used as wall components.

Frey-Wyssling and Mühlethaler (1965) claimed that carbohydrates appeared to be produced in Golgi vesicles. Perhaps the tubular vesicles were filled with soluble cytoplasmic β -1, 3-glucan (mycolaminaran), which Wang and Bartnicki-Garcia (1980) claimed may be the reserve carbohydrate of oomycetes. It may be coincidental that the dictyosomes generally are restricted in the fungi to the oomycetes (Bracker, 1967a) and they are the ones which contain mycolaminaran.

Powell and Bracker (1977) showed that the so-called 'finger print' vacuoles of zoospores of Phytophthora palmivora have a high content of mycolaminaran and mycolaminaran phosphate. 'Finger print' vacuoles were not observed in P. hyoscyami hyphae and myelin bodies were seldom found.

The intimate association of the dictyosome and nucleus was similar to that in other oomycetes (Mollenhauer and Moore, 1966) and lends support to the work of Moore and

remained significantly higher in healthy tissue than 6 day inoculated tissue (Figure 105).

Starch degradation monitored with the TSA test exhibited a slightly different profile. In early infection (Figure 104) total starch quantities were not significantly different between healthy and 2 h infected tissue. A marked difference in total leaf starch was apparent at 6 days following inoculation. Starch levels were significantly higher in healthy tissue than 6 day infected tissue (Figure 106).

Crude enzyme extract from healthy leaves degraded potato starch at the same rate as extract from the diseased leaves up to 3 days after infection (Figure 107). On the fifth day and thereafter, extract from the diseased leaves degraded potato starch more rapidly than extract from the healthy leaves.

Total proteins (Figure 108) in the enzyme extracts were significantly greater in the infected tissue starting at 4 days and thereafter.

CHAPTER 4

DISCUSSION

4.1. In Vivo Development

In growth cabinets under optimal conditions fungal development was examined in the host tissue. This marks the first time that this process has been documented for this species. The hyphae of P. hyoscyami grew in the intercellular spaces of the host tissue. Due to the nature of tobacco tissue, with its abundant intercellular spaces in the palisade and spongy parenchyma, fungal development was not constrained. The hyphae closely adhered to the host cell walls. Within 5 days of development and relative humidity below 98%, hyphal knots were observed in the stomatal chamber. This marks the first report of this type of structure in the downy mildews. At low relative humidities, below 98%, the hyphal knots form in the stomatal chambers, acting as reservoirs of fungal material. An increase in relative humidity to 100%, resulted in an immediate formation of conidiophore initials from the hyphal knots.

An attempt was made to study sexual development in P. hyoscyami. Oospores, oogonia and antheridia were observed in heavily infected host tissue. My isolate of P. hyoscyami lost the ability to produce sexual structures in 1980. Work

in this area has been limited. Kröber (1969) using tobacco infected with P. hyoscyami could not produce infection with oospores. He concluded that field infections by oospores do not occur in this species of Peronospora.

In Peronospora parasitica Pers Ex. Fr. (Ohguchi and Asada, 1981) oogonia are rarely found. Michelmore (1981), showed that Peronospora parasitica contained homothallic and heterothallic isolates. Additionally Bremia lactucae was observed to be heterothallic with two distinct compatible types. Mycelia of two opposite compatibility types needed to be established in the same tissue zone to obtain oospore formation.

I believe a similar situation may exist in P. hyoscyami f.sp. tabacina. The loss in the ability of the 1979 Ontario isolate to produce sexual structures may be attributed to the loss of a compatible mating type required for the sexual phase in the life cycle of this pathogen of tobacco.

4.2. In Vitro Conidial Germination

A dual purpose existed in conducting basic germination experiments under varying temperatures, light, relative humidities, and concentrations of CO₂ on the atmosphere. First the experiments allowed me to describe the relation of conidia to the varying environmental factors. The isolate of P. hyoscyami used in my experiments was obtained during the 1979 blue mould epidemic in Ontario. The data on this isolate were compared to data from current studies

of P. hyoscyami in Europe and Australia where field infections are more common than in North America.

The second reason for the study of conidia, was that airborne conidia are the main inoculum of this obligate parasite. The distribution, disease cycle, epidemiology and problems associated with control P. hyoscyami are all factors directly associated with the ability of the conidium to germinate.

Optimal temperatures for germination of the Ontario isolate of P. hyoscyami were at 15 to 20°C and an optimal germination rate was obtained at the same temperatures. Cruickshank (1961a) found that for an Australian isolate of P. hyoscyami, after 1 h the same total germination occurred at 20, 24, 28 and 30°C. The percentage germination at 27°C was significantly greater than at any other temperature. Clayton and Gaines (1945) found that the optimal temperatures for germination were 1.5 - 10°C and 17 - 26°C while Wolf et al. (1934) discovered that germination of this species started within 2 h at 7 - 15°C and 5 h at 21°C. They obtained no germination at 26°C. Shepherd (1962) and Hill (1969) reported optimal germination temperatures at 15 to 20°C, (Kröber (1981) in Europe) obtained optimum germination at temperatures from 18 to 22°C. The considerable difference in germination data may represent real differences in germination ability from isolate to isolate.

Conidia can withstand high temperatures of 25 - 35°C for periods of up to 8 h. The experiment shows that while germination is not possible at 30 and 35°C, conidia are not

destroyed at these temperatures, they retain their ability to germinate at lower temperatures.

Germinability of P. hyoscyami conidia was not influenced by light or darkness. In contrast Fried and Stuteville (1977) showed that spores of P. hyoscyami germinated equally well in diffuse light and darkness but were inhibited by direct light.

In my experiments ultraviolet irradiation proved to be detrimental to the survival of the conidia. The degree of the effect depended on the conditions of the conidia during UV irradiation. The most complete eradication of conidia occurred in air, while water provided a protection layer. The least effect was observed for conidia which remained on the conidiophore. In contrast, Shepherd et al. (1971) showed that conidia in dry air at 0% RH were more resistant to UV irradiation than conidia in water.

As sucrose molarity increased from 1 to 5 resulting in a decrease in the water potential of the solutions, there was an increase in the percentage of shrunken conidia. A similar response curve was obtained when the conidia were allowed to germinate in their respective sucrose solutions. An increase in sucrose concentration and thus a decrease in water potential, led to an increase percentage of shrunken and ungerminated conidia. Germination of P. hyoscyami conidia, a downy mildew, unlike germination of some conidia of powdery mildews, requires moisture.

Conidial longevity was greatest at low temperatures regardless of relative humidity. At a temperature of 25°C

and a high relative humidity of 80% conidia survived for less than 3 days. Hill (1962) and Kröber (1981) found that spore survival of P. hyoscyami was favoured by low temperatures, and low relative humidities. Clayton and Gaines (1945) observed that spores at cooler temperatures, regardless of relative humidity, survived the longest. Cohen and Kuč (1980) were able to store conidia for 3 months at -20°C and 34 days at 5°C and 100% RH.

The extreme sensitivity of P. hyoscyami conidia to CO_2 in the air came to my attention upon accidental incubation of conidia with yeast cultures. The apparent problem with germination of P. hyoscyami was shown to be due to the production of CO_2 by the yeast cultures. In the literature Botrytis cinerea (Brown, 1922) has been recorded as one of the most sensitive fungal organisms to CO_2 . My experiments have shown a remarkable sensitivity of germinating conidia of P. hyoscyami to 1% CO_2 while B. cinerea was slightly inhibited at 5% CO_2 . Alternatively, CO_2 from 1 to 15% had no effect on germination of the spores of Aspergillus niger. The physiological nature of the inhibition remains unknown, however the inhibiting effect of CO_2 on conidia may be reversed to a large degree if the conidia are allowed to incubate in air at 20°C .

4.3. Germination, Penetration and Early Development

To determine if the spores of downy mildews should be classed as sporangia or conidia requires morphological examination. Viennot-Bourgin (1981) stated that, sporangia of

the Peronosporaceae have a distinct apical modification of the wall, the operculum. The operculum or papilla, swells during final stages of maturation. With the loss of the operculum there has been a concomitant loss in the ability to produce zoospores (Shaw, 1981). Electron micrographs (Figures 45, 46) show the absence of papilla in the asexual propagules of P. hyoscyami. This downy mildew has lost its ability to produce zoospores. Consequently, the asexual propagule is a conidium.

A small amount of information was available on the development of P. hyoscyami in the susceptible host N. tabacum. Kröber and Petzold (1972) conducted electron and light microscope studies on susceptible and resistant tobacco, however their investigations were carried out on leaves 12 - 120 h after inoculation. My work centered on morphological changes in conidia and host tissue invaded by P. hyoscyami 0 to 6 days post inoculation.

The cytoplasm which at first was dense and full of nuclei, mitochondria, dictyosomes and electron-dense granules, was characteristic of a metabolically active protoplasm. With increased formation of vacuoles, the cytoplasm was pushed to the perimeter of the spore. The vacuoles may increase the pressure on the cytoplasm thus allowing the flow of materials into the newly formed germ tube and appressorium.

The production of the germ tube and the appressorium on the viable spores and the lack of appressorial formation

on media or water, indicated that appressorium formation was a reaction to the host. Shepherd and Mandryk (1963) only observed the branching of the germ tube of the tobacco mildew when spores were germinated under optimal conditions. The long and torulose germ tubes seen in water on glass slides were attributed to a lack of riboflavin. Spores of Peronospora parasitica inoculated on liver medium, produced germ tubes which grew towards the liver and formed swellings or lobes in the agar (McMeekin, 1981).

Because the leaf surface was very uneven, the conidia probably rolled into, and lodged in, the depressions that followed the lines of juncture between epidermal cells. This fact has never been observed before. As a result, appressoria, which were produced with or without short germ tubes, were usually above or adjacent to the anticlinal walls. The infection pegs, which originated on the lower surface of the appressoria, were close to the anticlinal walls because of the position taken by the conidia on the tobacco leaf and because the germ tubes and appressoria grew from the lateral wall of the conidia directly to the leaf.

Fungal penetration at the junction of epidermal cells has been reported in many parasitic fungi (Cunningham and Hagedorn, 1962; Pierre and Millar, 1965; Young, 1926). Brown and Harvey (1927) mentioned that it was a well known tendency and considered the junction between epidermal cells to be a point of weak mechanical resistance, allowing easier mechanical penetration than elsewhere.

My studies showed that the epidermal wall was thickest

above the anticlinal wall. Electron microscopic studies of wall penetrations in tobacco indicated a chemical penetration process because there was no infolding of the wall and the opening had a smooth margin.

Wood (1967) suggested the possibility of wax ducts in the cuticle and ectodesmata in outer epidermal cell walls forming a passage for the fungal penetration tube. I did not observe wax ducts or ectodesmata in the tobacco epidermal wall.

Water appears first and remains longer in the depression between the cells than on other leaf areas and consequently development readily occurred above the anticlinal wall.

The chemical composition and function of the flange around the infection pore between the appressorium and epidermal wall was unreported previously. The flange may be cuticle and wall material that has been degraded by P. hyoscyami enzymes and pushed up around the infection tube as it pressed through the wall.

I found that P. hyoscyami passed through the epidermal wall into the epidermal cell and not between the anticlinal walls as Lucas (1980) reported recently. Henderson (1937) discovered that in addition to penetration through the epidermis, P. hyoscyami penetrated leaf hairs on the tobacco. In my work penetration via the latter route was not observed. Chou (1970) reported that P. parasitica passed between the anticlinal walls of the epidermal cells. The apparent blueprint for the mechanism of entry must differ among species of Peronospora.

The fact that protoplasm from the appressorium and germ tube was able to 'surge' into the epidermal cell to form a vesicle indicates that turgor pressure was greater in the appressorium than in the epidermal cell. It may be postulated additionally that the pressure was equalized by the time most of the cytoplasm was forced into the epidermal cell. My hypothesis must be tested in the future.

A small amount of protoplasm with a nucleus was left in the infection tube and appressorium. The protoplasm left in the penetration tube appeared to continue its activity and synthesize a wall on the outer side of the plug. The plug protected the fungus from the external environment and allowed it to increase its turgor pressure. All obligate fungi either form a plug (Chou, 1970) or a septum in the infection tube (McKeen and Rimmer, 1973).

The fact that the infection vesicle was spherical probably indicated that its wall was flexible while the vesicle was enlarging. If a wall were not present at all times, we should have detected its absence in some of our sectioned material unless the wall was formed extremely quickly. Formation of a vesicle in the epidermal cell has been observed in a number of downy mildews. The downy mildew of grape, Plasmopara viticola, forms a vesicle in the stomatal chamber (Langcake and Lovell, 1980). Bremia lactucae (Sargent, 1981) forms primary vesicles in the epidermal cells of lettuce. Unlike P. hyoscyami, the vesicle of B. lactucae developed into a secondary vesicle which left the epidermal cell and invaded the adjoining

cells (Sargent et al., 1973).

The intimate association of tubular elements and spherical vesicles, which bleb from the dictyosomes, with the fungal wall, and their great abundance in growing hyphae, indicated that they play a role in wall synthesis as several investigators have claimed (Groves et al., 1970; Mollenhauer and Moore, 1966). Groves et al. (1970) have suggested that the vesicular membrane fuses with the plasma membrane, and the vesicular contents are used as wall components.

Frey-Wyssling and Mühlethaler (1965) claimed that carbohydrates appeared to be produced in Golgi vesicles. Perhaps the tubular vesicles were filled with soluble cytoplasmic β -1, 3-glucan (mycolaminaran), which Wang and Bartnicki-Garcia (1980) claimed may be the reserve carbohydrate of oomycetes. It may be coincidental that the dictyosomes generally are restricted in the fungi to the oomycetes (Bracker, 1967a) and they are the ones which contain mycolaminaran.

Powell and Bracker (1977) showed that the so-called 'finger print' vacuoles of zoospores of Phytophthora palmivora have a high content of mycolaminaran and mycolaminaran phosphate. 'Finger print' vacuoles were not observed in P. hyoscyami hyphae and myelin bodies were seldom found.

The intimate association of the dictyosome and nucleus was similar to that in other oomycetes (Mollenhauer and Moore, 1966) and lends support to the work of Moore and

McLear (1963) who claimed that the dictyosome were formed by a series of vesiculations of the outer component of the nuclear envelope. Although P. hyoscyami does not produce zoospores it has retained its centrioles.

The hyphae in the epidermal cells caused only a slight modification and no apparent damage to the host cytoplasm. There was an increase in the amount of host cytoplasm around the point of entry, and a thin layer of cytoplasm covered the hypha. Sargent (1981) reported the close association of the host nucleus and the primary vesicle infection on lettuce by B. lactucae. This positioning of the nucleus relative to the vesicle was observed occasionally in P. hyoscyami infections of tobacco epidermal cells.

The formation of a plug in the infection tube, once the appressorium's cytoplasmic contents formed a vesicle in the epidermal cell, represents a unique adaptation of this pathogen to its environment. I believe that the plug protects P. hyoscyami from an unfavourable external environment and allows an increase in the turgor pressure inside its vesicle.

The rapidity of germination, appressorial formation, penetration of cuticle and epidermal wall, and vesicle formation was impressive. P. hyoscyami was able to send its hypha through the epidermal cell and into a palisade cell or intercellular space within 2.6 h after inoculation. P. hyoscyami infected its host much more rapidly than other fungal pathogens. The imperfect fungus, Botrytis cinerea,

required 7 h for penetration (McKeen, 1974), while the ascomycete Erysiphe graminis required about 10 h (McKeen and Rimmer, 1973), Peronospora parasitica (Chou, 1970) required 6 h and Bremia lactucae about 5 h (Sargent et al., 1973). Plasmodiophora brassicae (Aist and Williams, 1971) infected its host in about 3 h after zoospore encystment; this was approximately the time required for P. hyoscyami. The very short infection time enabled the tobacco pathogen to escape desiccation and to commence a new life cycle inside the host.

4.4. Haustorial Ultrastructure

4.4.1. Penetration of the Host Wall

Prior to haustorial formation in P. hyoscyami there was no host reaction or papilla formation in susceptible tobacco. Accumulation of electron-dense material between the host plasma membrane and the host cell wall was an early sign of penetration in some Phycomycetes. A host reaction, often called a papilla, forms in the infection of potato by Phytophthora infestans (Hohl and Strössel, 1976), and of peas by Peronospora pisi (Hickey and Coffey, 1980), Peronospora viciae (Beakes et al., 1982).

Both mechanical and enzymatic action appear to have been involved in the passage of P. hyoscyami hyphae through the tobacco cell wall during haustorial formation. The infection pore was clear-cut except for a small amount of out-curling of the host wall towards the intercellular hypha which could be caused by the pressure of the haustorial

neck. Thigmotropism does not appear to be responsible for penetration of the host wall during haustorial formation. The intercellular hypha of P. hyoscyami were frequently in contact with host cell walls for long distances without haustorial formation.

4.4.2. Terminology

In the description of the haustorial apparatus an attempt has been made to use general descriptive terms rather than conflicting and confusing terminology. The confusion has resulted in part because the coating around the haustorium was first observed by means of the light microscope (Fraymouth, 1956; Rice, 1927; Smith, 1900) and later by means of the electron microscope (Berlin and Bowen, 1964; Bracker, 1967b; Chou, 1970; Coffey, 1976; Heath and Heath, 1971; Hohl and Strössel, 1976; Ingram et al., 1976; Littlefield and Heath, 1979; McKeen, 1974; McKeen et al., 1966; Peyton and Bowen, 1963). The interface between the haustorium wall and the plasma membrane (the extrahaustorial membrane) may be composed of a variable number of components in different host-pathogen combinations. A great problem with the current terminology is that the greatest number of the host-pathogen studies have been carried out using rusts and powdery mildews (Berlin and Bowen, 1964; Chong and Harder, 1982; Coffey, 1976; Heath and Heath, 1971; Littlefield and Heath, 1979), and as a result, workers studying the downy mildews have attempted to use the same terminology. The author agrees with Chou's

(1970) statement that confusion in terminology was perhaps unavoidable because the origin, nature and function of the various structures were largely unknown, and the use of terms was complicated by comparison of taxonomically different groups of fungi. Components within this interface between the fungus and its host have been called: zone of apposition (Chou, 1970; Peyton and Bowen, 1963), encapsulation (Berlin and Bowen, 1964; Ehrlich and Ehrlich, 1963a; Ehrlich and Ehrlich, 1963b; Heath and Heath, 1971), sack (Bushnell, 1971; Hirata, 1971), sheath (Bracker, 1967b; Chou, 1970; Fraymouth, 1956; Peyton and Bowen, 1963), collar (Beakes et al., 1982, Langcake and Lovell, 1980), extrahaustorial matrix (Beakes et al., 1982; Bracker and Littlefield, 1973; Bushnell, 1972) and encasement (Hickey and Coffey, 1980; Hohl and Strössel, 1976).

Smith (1900) working with the Erysiphae used the term sheath in reference to a sac-like covering around the haustorium on the powdery mildews. The term encapsulation should be reserved for the zone between the inactive or shrunken haustorium and its host. In today's research, sheath and encasement are occasionally used as synonyms or to depict the formation of a collar-like area around the neck of the haustorium (Berlin and Bowen, 1964; Bracker and Littlefield; 1973; Peyton and Bowen, 1963). Bracker (1967b) recommended that sheath be used in its original sense as first described by Smith (1900). Bushnell (1972) stated that the sheath was produced as the extension of the papilla, while Kohno et al. (1970) stated "thus, we distinguish the

sheaths from the papillae tentatively until we can clarify the origin of the sheaths'. In 1976 Ingram et al (1976) summarized the situation in the following manner, "whether the dark staining zone of the haustorial wall may be equated with encapsulation described as surrounding the haustoria of other members of the Peronosporales by Peyton and Bowen (1963) or sheath around the haustoria of powdery mildews and rusts (Bracker and Littlefield, 1973) is a moot point as is the question as to its origin in the host, fungus or both. The only reliable point of similarity between these various structures is that they occupy a similar position with regard to the haustorium and the protoplast of the host".

I have adopted the terminology originally defined and used by Bushnell (1972). The extrahaustorial matrix (EHM), is the liquid or solid substance between the extrahaustorial membrane (or plasma membrane) and the haustorial wall. Bushnell stated that it was equivalent to the sheath matrix of Bracker (1967b), the encapsulation of Ehrlich and Ehrlich (1963a, 1963b), the zone of apposition of Peyton and Bowen (1963) and the encapsulation described by Berlin and Bowen (1964). Heath and Heath (1971) use the term extrahaustorial matrix in their diagrammatic representation of the fungal and host structures associated with a dikaryotic haustorium in rust infection of cowpea leaves. Hickey and Coffey (1977) and Beakes et al. (1982) present strong circumstantial evidence of direct ontogenic relationship between the penetration matrix (papilla) and the extrahaustorial matrix.

4.4.3. Haustorial Electron-Opaque Layer

The electron-opaque matrix surrounding the haustorium in the susceptible leaf of N. tabacum occupied a similar position and resembled the zone of apposition around the haustorium of P. manshurica as described by Peyton and Bowen (1963). However, the zone of apposition did not appear as dark and had smooth inner and outer surfaces, while the electron-opaque matrix around the P. hyoscyami haustoria varied in thickness and the outer surface was irregular. Chou (1970) showed the presence of an electron-dense layer on the surface adjacent to the haustorial wall of P. parasitica. He considered this zone an integral part of the haustorial wall. Since the electron-opaque zone is opaque, of variable thickness and has an irregular outer surface, I believe it is not part of the wall, but part of the interface.

Kajiwara (1971) reported the presence of an electron-dense layer, .15 to .20 μm in thickness, as an integral component of certain downy mildews. In Peronospora destructor, P. brassicae and P. spinaciae the electron-dense zone was similar in appearance and position to the electron-opaque matrix in P. hyoscyami. The electron-dense layer in P. brassicae was composed of membrane-bound vesicles which were not present in the dense matrix of P. hyoscyami. In pea infected with P. pisi, a dense-staining haustorial matrix was frequently much thicker at the proximal end of the haustorium. Apparently the electron-opaque matrix adjacent to the haustorial wall is characteristic of the downy mildews and serves some function. A similar dense layer was observed

around the haustorial wall of rust fungi. Coffey (1976) postulated that this material was a major determinant in resistance. This was not the case in our susceptible tobacco.

4.4.4. The Electron-Transparent Haustorial Layer

The outer matrical layer, the electron-transparent layer, did not always extend to the end of the haustorium. It was found in the neck region, middle portion and/or the distal portion of the haustorial body. Fraymouth (1956) used the light microscope to study the haustoria of the Peronosporales and made a similar observation. She believed that the sudden increase in growth of the fungus burst the sheath (or the extrahaustorial matrix).

The electron-transparent matrix appears to be a very important layer. It is a transmission zone between the host and the fungus. My electron micrographs show the blebbing of host cytoplasm into this zone. It was through this layer that channels of host cytoplasm ran and were connected to the electron-dense layer.

The matrix was always present around young haustoria. It appeared to be similar in appearance to the collar and encasement in the pea downy mildew (Hickey and Coffey, 1977), encapsulation in P. destructor on onion (Kajiwara, 1971) and the electron-transparent matrix in P. viciae on pea (Beakes et al., 1982).

In P. hyoscyami the electron-transparent matrix contained membrane-bound inclusions and the host cytoplasm

blebbed into this layer. Beakes et al. (1982) also observed membrane-bound vesicular inclusions in the electron-transparent zone. Soybeans infected by Phytophthora megasperma var sojae (Strössel et al., 1982) and treated with the systemic fungicide metalaxyl had electron-transparent wall appositions. In metalaxyl-treated peas infected by Peronospora pisi, the encasement (my electron-transparent matrix) was present around the haustorial body. The zone had three distinct profiles; bilayered, unilayered or vesicular-layered (Hickey and Coffey, 1980). In contrast, in susceptible tobacco infected by P. hyoscyami the electron-transparent zone had a uniform appearance.

The extrahaustorial matrix (Hickey and Coffey, 1977) around Uromyces phaseoli var vignae haustoria in the susceptible cultivar appeared to be somewhat similar to the electron-transparent layer of P. hyoscyami. Both were apparently formed by deposition from the host cytoplasm.

At present very little information exists on the chemical composition, physiology and origin of the extrahaustorial matrix. In powdery mildews the haustorial body can be separated from the matrix (Bushnell, 1971; Hirata, 1971). Such experiments have revealed that the extrahaustorial matrix behaves as a semi-permeable membrane (Bushnell, 1971) and is composed of an elastic material (Hirata, 1971). When labeled ^{14}C glucose was given to the host, radioactivity accumulated in the haustorial wall and not in the extrahaustorial matrix (Bushnell, 1971).

Certain investigators have suggested that the electron-lucent layer in rusts may be an artifact of preparation because

its size and composition varies with the fixatives used (Littlefield and Heath, 1979).

4.4.5. The Extrahaustorial Membrane

A unit membrane was present around each haustorium of P. hyoscyami. The membrane was continuous with the plasma membrane of the host. Bracker and Littlefield (1973) proposed that the extrahaustorial membrane is the plasma membrane. The membrane cannot be formed by stretching the existing host plasma membrane, instead new membrane was synthesized around the haustorium. The newly formed membrane is characteristic of the host-parasite interface. In powdery mildews the strength of the extrahaustorial membrane allows the excision of the extrahaustorial matrix from the haustorium (Hirata, 1971).

Chou (1970) showed a considerable proliferation of host plasmalemma at the time of incipient haustorium formation in P. parasitica (Fr.) Tul. on cabbage. In P. viciae infection of peas, the extrahaustorial membrane became increasingly lobed and the lobes extended into the host cytoplasm (Beakes et al., 1982). Beakes et al. (1982) believed that the convoluted plasma membrane may serve to increase the absorptive capacity of the haustorium. Ingram et al. (1976) attributed the lobing of the plasmalemma to progressive aging of the haustorium.

In downy mildews of turnip and grape Kajiwara (1971) and Beakes et al. (1982) had no clear evidence of plasmalemma around the haustorial body. Infections of P. spinaciae and P. parasitica on spinach and radish respectively were

characterized by a break in the plasmalemma around the fungal haustorium (Asada and Shiraishi, 1976; Kajiwara, 1971), resulting in direct contact between the host and pathogen.

The extrahaustorial membrane of P. hyoscyami was continuous around the intracellular hyphae. Contact between the host cytoplasm and the haustorium was restricted to the cytoplasmic strands connecting the host cytoplasm to the electron transparent layer of the haustorium. Convulsions and lobes were not present in the membrane at any stage of haustorial development.

Occasionally a membrane on the outer surface of the electron-opaque matrix was observed. It was sandwiched between the electron-opaque layer and the electron-transparent layer. I consider this to be a remnant of a membrane from the breakdown of the blebbing vesicles, and not the host plasma membrane.

4.4.6. Host Response to Fungal Invasion

The response of the susceptible host to the presence of haustoria and intercellular hyphae appeared to be minimal up to 8 to 9 days following inoculation. The host cytoplasm formed a thin layer around the periphery of the epidermal, palisade and spongy parenchyma cells. The mitochondria, nuclei and chloroplastids showed no structural signs of degradation or distortion.

In B. lactucae on lettuce, Sargent (1981) frequently observed a close association between the host endoplasmic reticulum and the mature haustorium. A similar close

association of host endoplasmic reticulum and extrahaustorial membranes was shown in infected peas by Peronospora viciae (Beakes et al. 1982) and occasionally in the infection of tobacco by P. hyoscyami.

The most striking observation in my work on the haustoria of P. hyoscyami, was the blebbing of the vesicles from the plasma membrane of the host to the electron-transparent layer of the fungal extrahaustorial matrix. This provided evidence for the proposed theory that the haustorial matrix, particularly the electron transparent layer, may be of host origin.

4.4.7. Ultrastructural Changes in Aging Haustoria and Intercellular Hyphae

Most investigators will agree that dense cytoplasm in young haustoria is an indication of metabolically active haustorial bodies (Langcake and Lovell, 1980; Tommerup, 1981). In P. hyoscyami the young haustoria and adjoining intercellular hyphae were characterized by abundant mitochondria, dictyosomes, endoplasmic reticulum, nuclei and associated nucleoli and few small vesicles. The maturing haustorium was characterized by a change in shape from a cane to a coil. In P. hyoscyami plasmalemmasomes were observed adjacent to the haustorial fungal wall. Plasmalemmasomes were present in abundance on Maro cultivar of pea which is less susceptible to P. viciae (Beakes et al., 1982). Their function and significance has not been established.

Shrunken and collapsed haustoria were observed in cells which also contained turgid haustoria. The cause of the collapse was not known. Beakes et al. (1982) maintained

that the loss of haustorial turgor may result in hyphal collapse as a result of pressure exerted by the host protoplast, or alternatively, the impairment of haustorial function, to absorb and translocate nutrients, may cause premature senescence and lysis of intercellular hyphae resulting in haustorial collapse. I maintain that if pressure was exerted by the host protoplast it would be equal on all walls of the host cell. It would be expected therefore that all haustoria in a particular host cell would be collapsed. In P. hyoscyami collapsed haustoria were observed adjacent to healthy haustoria in the same host cell. Thus the hypothesis proposed by Beake's et al. (1982) does not apply in this case. I suggest that the collapse of the haustorial structures represents a natural stage in the aging of the haustorium. This hypothesis allows for the presence of healthy and collapsed haustoria in the same host cell.

4.5. Starch Accumulation and Degradation in Infected and Healthy Tissue

In my preliminary investigations I observed a greater abundance of starch in infected leaves during the electron microscopy investigations. This phenomenon has been quite commonly observed by investigators working with rusts and powdery mildews. The seldom used iodine test provided a quick method for determining the presence or absence of starch in whole leaf tissue. The test had a limited sensitivity for concentrations above approximately 110 mg. of starch per gram of dry leaf tissue, there was no further intensification

of blue color. However, the IKI test indicated that starch accumulation was not a constant characteristic of the disease. By following starch formation/degradation it became apparent that healthy and infected tissues differed in their respective ability to accumulate starch.

The highly specific TSA test revealed that in early and late stages of infection the infected tissue contained lower starch levels during starch degradation and accumulation phases.

In a recent review of starch in plant tissues Preiss (1982) noted that, "very little is known about the initiation or regulation of starch degradation in the chloroplast". Sucrose acts as the major carbon source for the synthesis of starch in the chloroplasts (Preiss, 1982). Starch degradation/accumulation is controlled by enzymes located in the cytoplasm and the chloroplasts of plant cells (Preiss, 1982). In turn light controls and regulates enzyme activation and inhibition in the chloroplast (Buchanan et al., 1981). A number of enzymes seems to be involved in starch degradation and formation (Abbott and Matheson, 1972; Kakie and Sugizaki, 1970; Okita and Preiss, 1980). Dunn (1974) believed that in vivo α -amylase is the only enzyme that has the ability to initiate degradation of the starch granule.

In infected host tissue invaded by a biotrophic parasite the normal cycle of accumulation/degradation of starch is disrupted (Preiss, 1982). Whipps and Lewis (1981) described several factors that influence the amount of storage carbohydrates in infected tissue including; the stage and

intensity of infection, the rate of photosynthesis of infected host tissue, the rate of translocation of sucrose from other parts of the plant, the activity of synthetic and degradative enzymes and the loss of soluble carbohydrates from the host to the fungus. Tissues invaded by fungal parasite often undergo changes in chlorophyll content (Harding et al., 1968; Misra and Biswal, 1981), change in the levels of soluble and non-soluble sugars (Inman, 1962), necrosis and starch accumulation and/or degradation (Inman, 1962; Tomlinson and Webb, 1978; Tu, 1979). Diurnal cycling of starch and soluble sugars has been observed in some healthy plants (Chang, 1979; Kakie and Sugizaki, 1970). Differences additionally exist between young and old healthy tobacco plants. Younger plants degrade starch more efficiently than older plants (Preiss, 1982).

Increased amounts of starch have been reported in rust, powdery mildew and virus infected leaves (Allen and Dunkle, 1971; Coffey et al., 1972; Jones and Dainello, 1982; Okita and Preiss, 1980). Tentoxin, a toxin extracted from Alternaria alternata has a marked influence on the degradation/accumulation of starch in host tissue. Its action, an increase in synthesis or increase in degradation, is influenced by the host plant (Hanchey, 1981).

The starch-degrading abilities of extracts from healthy and diseased tobacco tissue were tested on potato starch. This simple test was carried out to give a quick indication as to which extract exhibited higher amylolytic activity. Extracts from infected tissue at 4 days and thereafter showed

significantly greater amylolytic activity than the controls. Simultaneously, the extract from infected tissue had a considerable increase in total proteins.

These results indicated that the behaviour of the enzymes in the course of an infection is very complex and requires an experimental design in which the starch-degrading enzymes can be purified and their respective specific enzymatic activities determined for healthy and infected tissue.

Increases in enzymatic activity in infected tissues have been observed in a number of host-parasite systems (Voliva et al., 1982). Increased levels of peroxidase, β -glucosidase and RNase in tissue infected by P. parasitica were observed at 3 to 4 days following infection (Kluozewski and Lucas, 1982). Tobacco infected by P. hyoscyami f.sp. tabacina contained high levels of β -glucosidase, peroxidase and phenoloxidase (Edreva, 1974; Edreva, 1975; Edreva and Georgieva, 1980). The significance of these enzymes is not understood. Reports of starch-degrading enzymes in healthy plants of Nicotiana tabacum are varied. Thorpe and Meier (1974) reported high levels of the starch degrading enzyme phosphorylase and low activity of α -amylase, maltase and R-enzyme. Abbot and Matheson (1972) found low and constant levels of α -amylase and no β -amylase in tobacco.

The significant change in total starch content in infected leaves of N. tabacum in comparison to that in healthy leaves, an apparent increase in amylolytic activity and the increase in total protein with infection indicate that

P. hyoscyami has an immediate and continuing effect on the starch degrading enzymes of Nicotiana tabacum.

4.6. Effects of Fungus on Host Chloroplast Ultrastructure

My electron micrographs of N. tabacum plants infected with P. hyoscyami up to 6 days after inoculation, indicated that the fungus has no deleterious effect on the chloroplasts and host organelles in general. Sections of leaf tissue at 6 days post-inoculation had chloroplasts that retained their normal appearance. Chlorosis may occur while the chloroplasts still retain their normal stacking of the thylakoid membranes. Chlorosis in infected tissues was not caused by degradation of the chloroplast as suggested by Edreva and Georgieva (1980). The fungus possibly destroys the chlorophylls in the host tissue, leading to the production of chlorotic areas.

In contrast Georgieva and Edreva (1974) showed that the initial growth of hyphae of P. hyoscyami f.sp. tabacina in the parenchyma causes, first chlorosis then nuclear damage, resulting in further chlorosis.

In my work degeneration of the chloroplast and host cell contents occurred 11-12 days post-inoculation. In agreement with this finding Heath (1974) observed no difference between the ultrastructures of healthy and diseased tissues in early infection. In contrast, Coffey, et al., (1972) working with Melampsora lini on flax and Puccinia helianthi on sunflower, showed that at 8 days post-inoculation changes in chloroplast ultrastructure occurred.

2

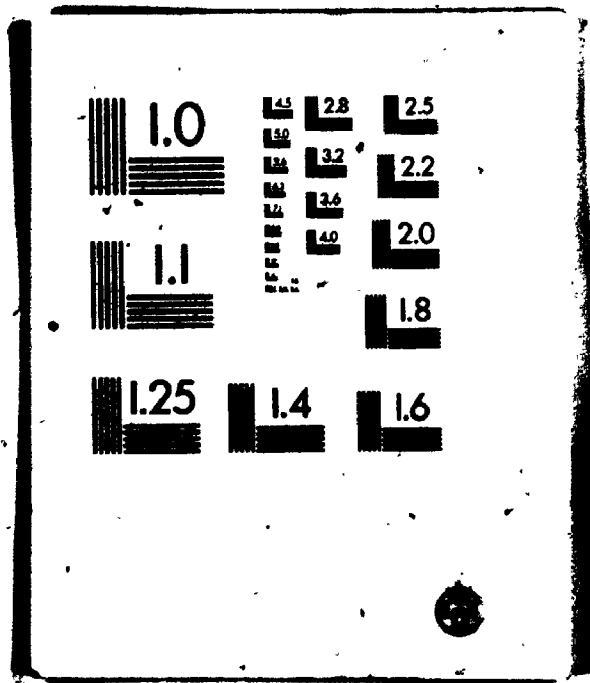


PLATE 1

Figure 1. A field of tobacco cut down during the 1979 blue mould epidemic.

Figure 2. Mature tobacco leaf infected with P. hyoscyami f.sp. tabacina. Observe the large number of necrotic and chlorotic lesions on a single leaf surface.

Figure 3. Mature tobacco plant with necrotic lesions on the lower leaves. The photograph was taken during the blue mould epidemic in 1979.

x2.5



PLATE 2

Figure 4. Chlorotic lesions on leaf of Nicotiana tabacum infected with P. hyoscyami f.sp. tabacina at 3-5 days following infection.

Figure 5. Chlorotic and necrotic lesions on tobacco leaf infected with P. hyoscyami f.sp. tabacina at 8 days post-inoculation.

Figure 6. Upper surface of tobacco leaf infected with P. hyoscyami at 7 days following infection and 100% relative humidity. Observe the mat formed by the conidia and conidiophores.

Figure 7. Lower surface of tobacco leaf infected with P. hyoscyami f.sp. tabacina. Chlorotic areas (arrow) in the leaf were often associated with mats of conidia and conidiophores.

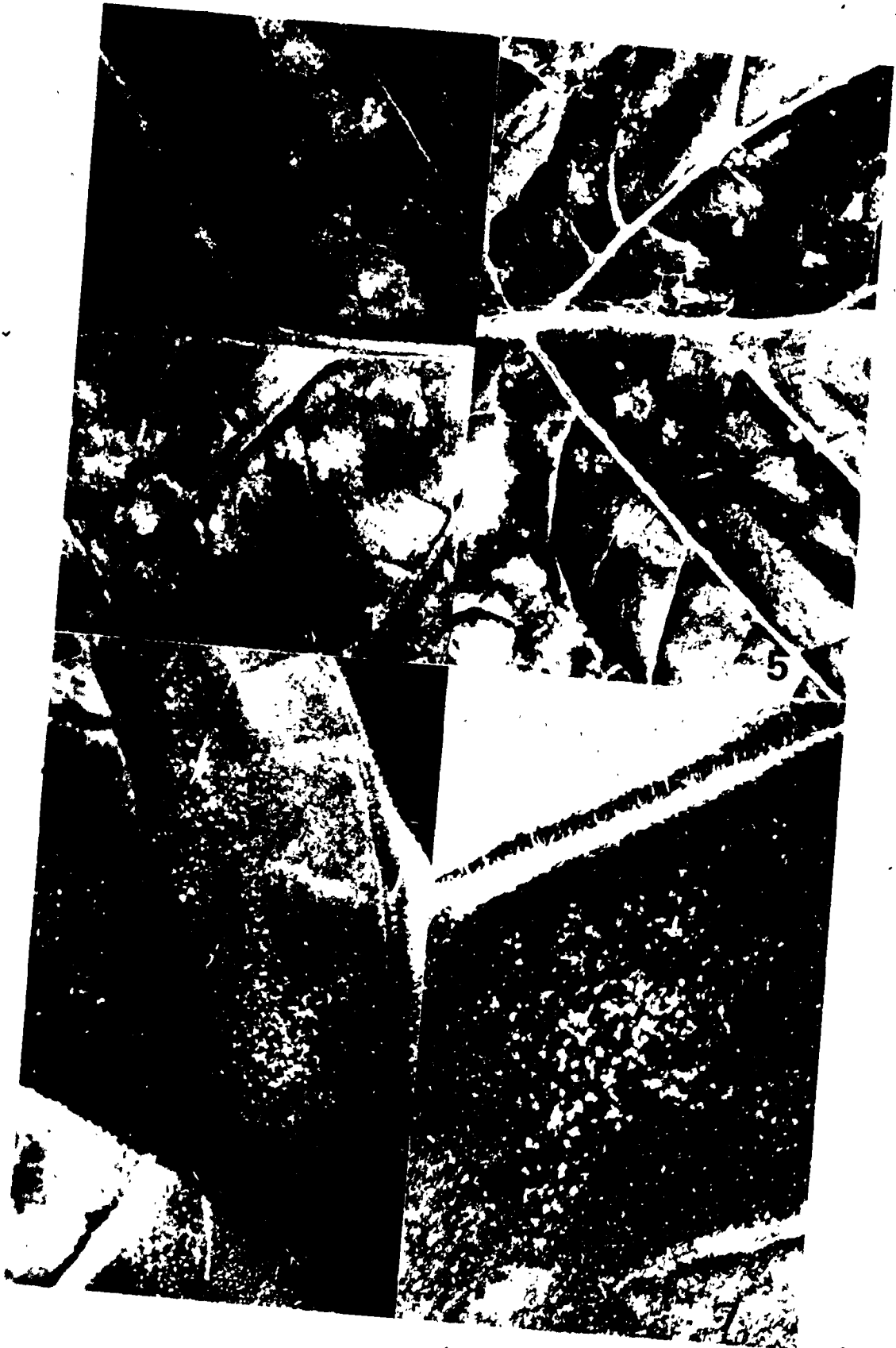


PLATE 3

Figure 8. Top view of upper epidermal cells in N. tabacum. x850

Figure 9. Palisade cells in N. tabacum. Observe the large intercellular spaces between adjoining groups of palisade cells. x1,100

Figure 10. Large cells of the spongy parenchyma forming a jigsaw-like network of cells below the palisade layer, in a healthy N. tabacum leaf. x1,500

Figure 11. Lower epidermal cells in N. tabacum, similar in appearance to upper epidermis (Fig. 8). x1,100



R

P

PLATE 4

Light micrographs of conidiophore development
in P. hyoscyami on susceptible tobacco.

Figure 12. Hyphal knot, in infected N. tabacum leaf.

x1,500

Figure 13. Fungal hypha in the stomatal chamber of

the tobacco leaf. x1,800

Figure 14. Young conidiophore initial emerging from the

stoma of a susceptible tobacco leaf. x1,500

Figure 15. Eight conidiophore stems emerging from a
single stoma on the lower tobacco leaf

surface. x750



PLATE 5

Figure 16. Young unbranched conidiophore on the lower surface of a leaf of N. tabacum formed at 6 days post inoculation and after 4 hours of darkness at 100% relative humidity. x1,500

Figure 17. Branched P. hyoscyami f.sp. tabacina conidiophore. Branching commences after 4-5 h in the dark and 100% relative humidity. x900

Figure 18. Swellings at end portions of the conidiophore branches, at 5-6 h of darkness and high relative humidity. Mark beginning of conidial formation. x300

Figure 19. Mature conidia on the conidiophore of P. hyoscyami f.sp. tabacina. x600

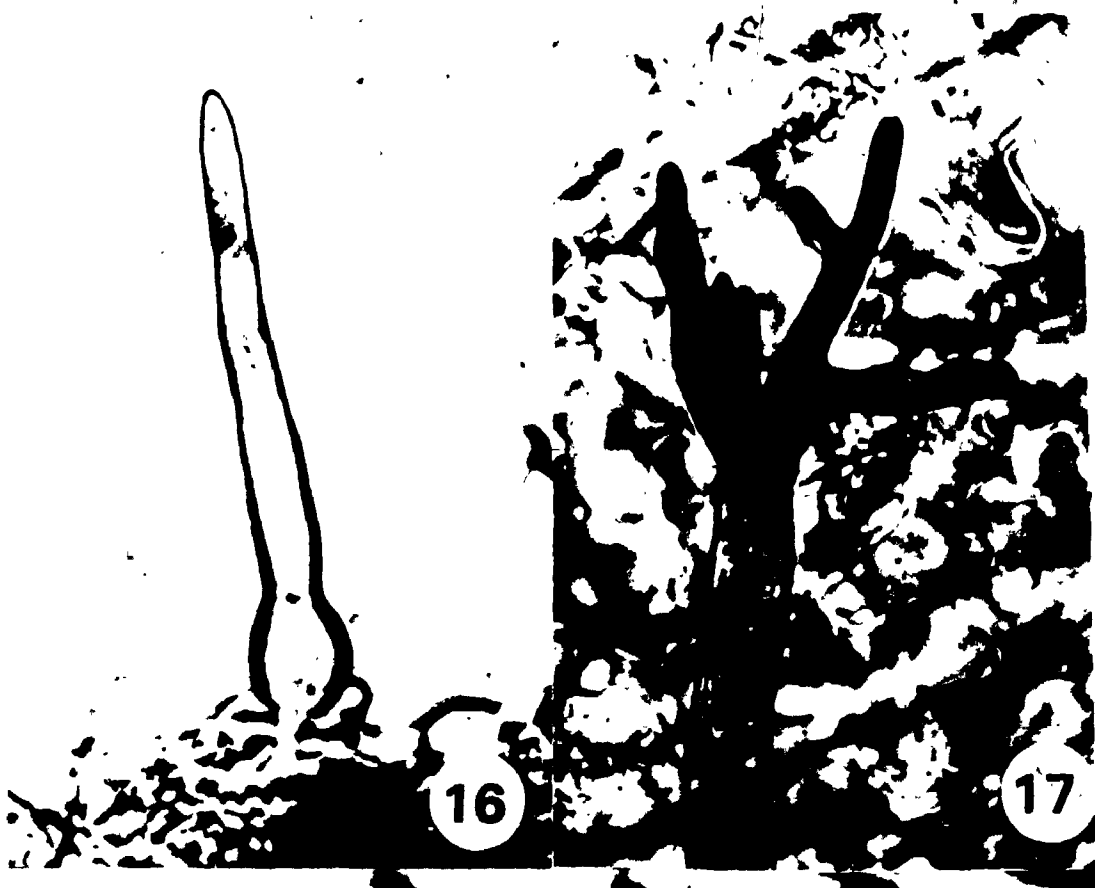


PLATE 6

Formation of sexual structures of P. hyoscyami
f.sp. tabacina in the tobacco leaf.

Figure 20. Young oogonium of P. hyoscyami f.sp. tabacina
in the host tissue. Observe the darkly
stained cytoplasm. The oogonium wall conforms
to the shape of the intercellular space. xl,100

Figure 21. Mature oogonium and antheridium of P. hyoscyami
f.sp. tabacina. The antheridium (arrow) lies
on top of the oogonium. xl,100

Figure 22. Oospore of P. hyoscyami f.sp. tabacina in the
tobacco leaf. Observe the light staining
periplasm (arrow) that surrounds the oospore.
xl,100

Figure 23. Oospore of P. hyoscyami in tobacco. Observe
the large granules in the centre of the
oospore. xl,300



20



21



22



23

PLATE 7

Figure 24. A schematic diagram depicting the developmental stages of P. hyoscyami.f.sp. tabacina in the susceptible host, N. tabacum.

- A. Empty conidium on the surface of the host leaf.
- B. Primary vesicle and branches in the epidermal cell.
- C. Intercellular hyphae follow the intercellular spaces of the host.
- D. Haustorium forms in host cell.
- E. Hyphal knots in the stomatal chamber precede conidiophore formation.
- F. Branched conidiophores form on the lower epidermal surface.
- G. Mature conidia form in darkness and high relative humidity within 6-7 h.
- H. Heavily infected host tissue at 6 days following inoculation was characterized by conidiophores on the lower and upper epidermal surface.

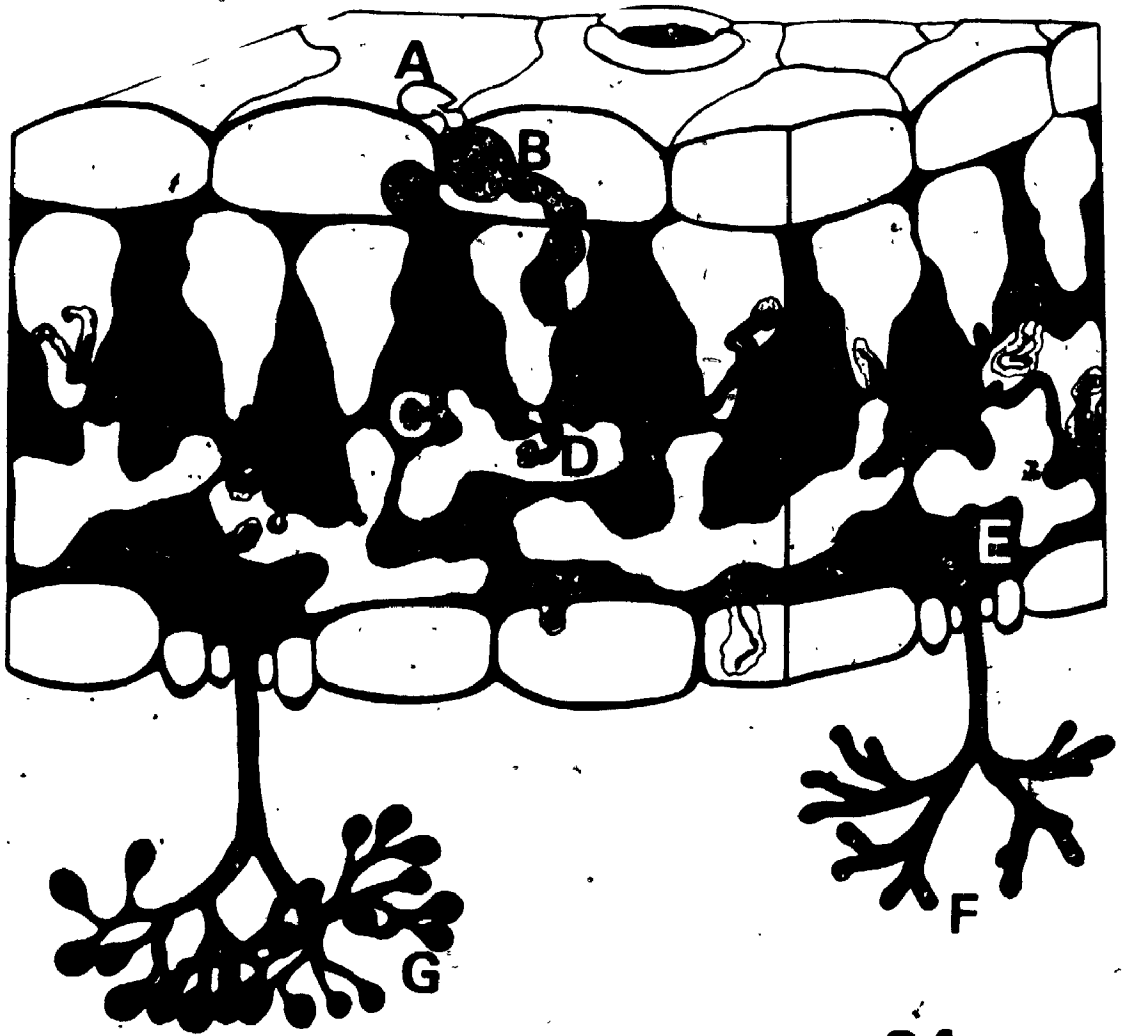


PLATE 8

Diagrams depicting structures formed during germination, penetration and development of P. hyoscyami f.sp. tabacina in the epidermal cells of N. tabacum.

Figure 25. A conidium with a germ tube (G) on the upper epidermal cell surface. TO-tonoplast, PM-plasma membrane, CW-cell wall.

Figure 26. A conidium that is partially filled with cytoplasm and opaque globules (IN). The germ tube is short and the appressorium (A) has a fine infection peg (PP) which has pushed host wall material aside (F). The infection peg is adjacent to the anticlinal wall of the epidermal cells.

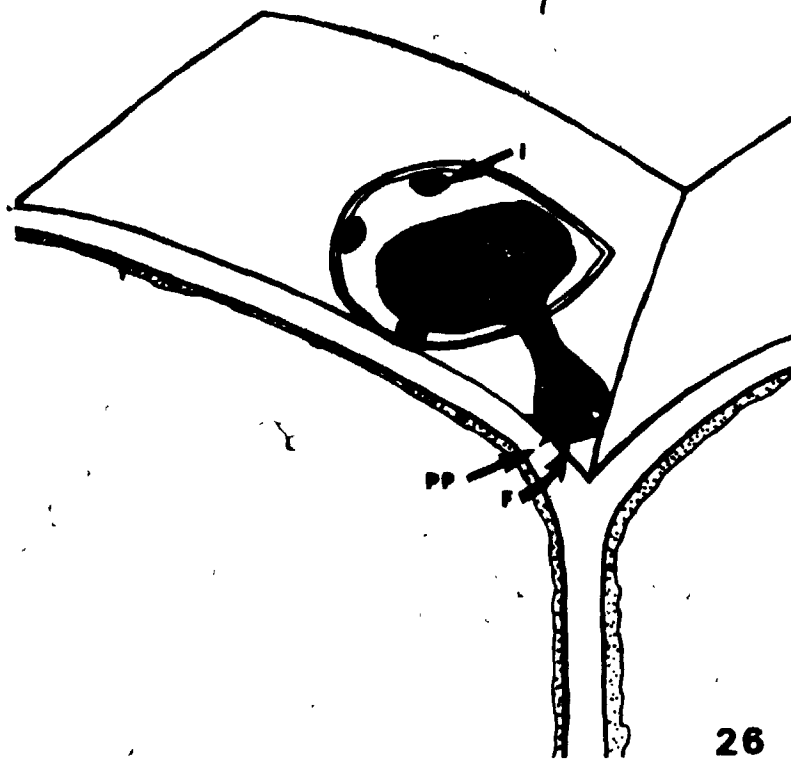
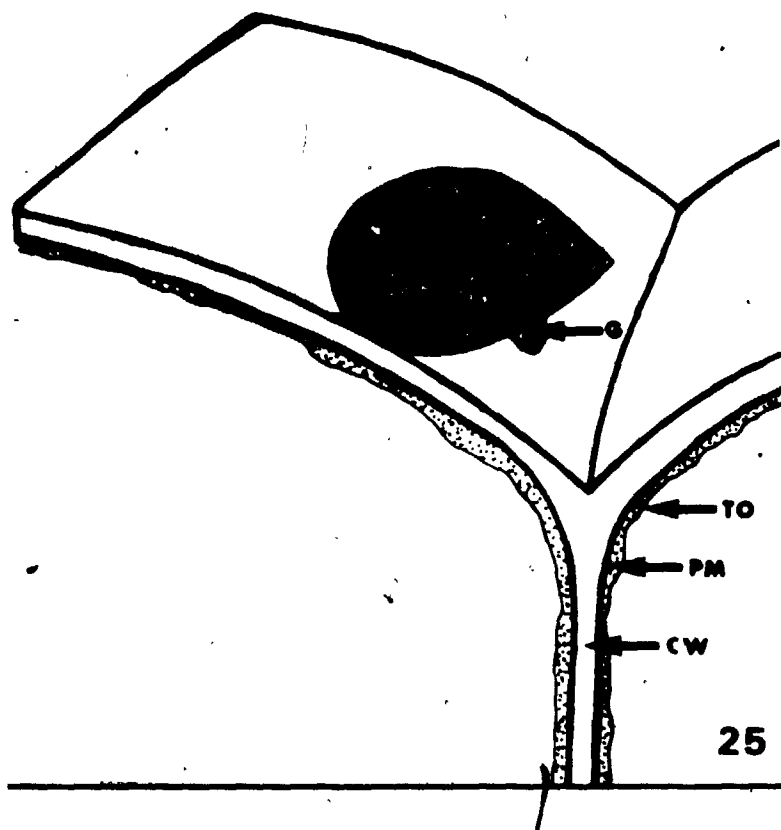
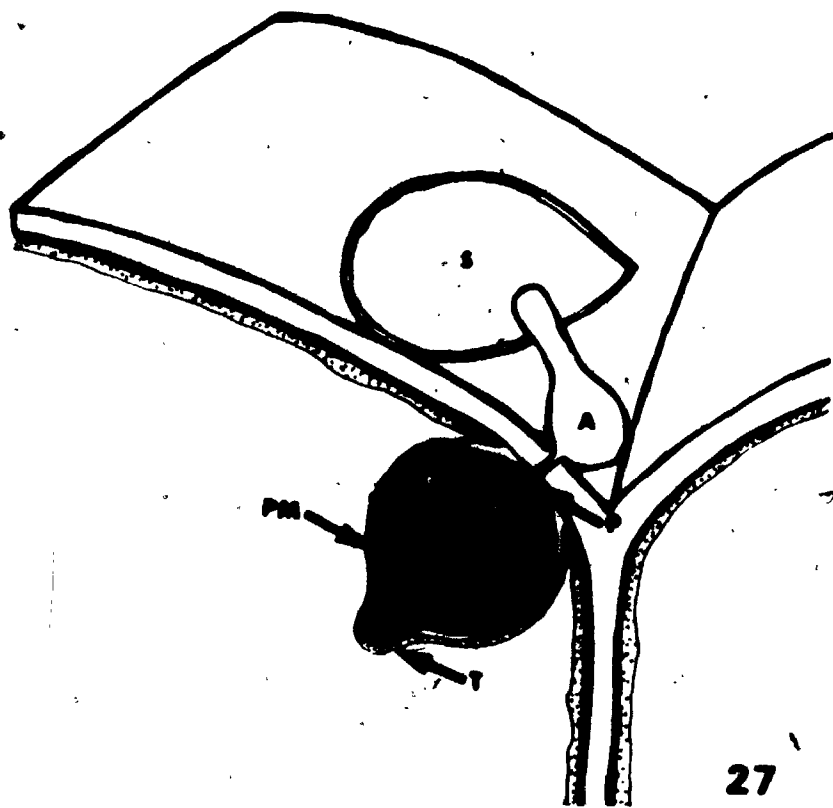


PLATE 9

Same series as Plate 8 (cont'd)

Figure 27. A spherical vesicle (V) joins to an empty infection tube, appressorium (A) germ tube and conidium (S). There is a plug (P) in the infection tube next to the vesicle.



27

PLATE 10

Same series as Plate 8 (cont'd)

Figure 28. Early infection bodies of P. hyoscyami f.sp. tabacina in a susceptible tobacco leaf.

Observe the intracellular hypha in the tobacco cell and the large amount of intercellular space between the palisade cells:

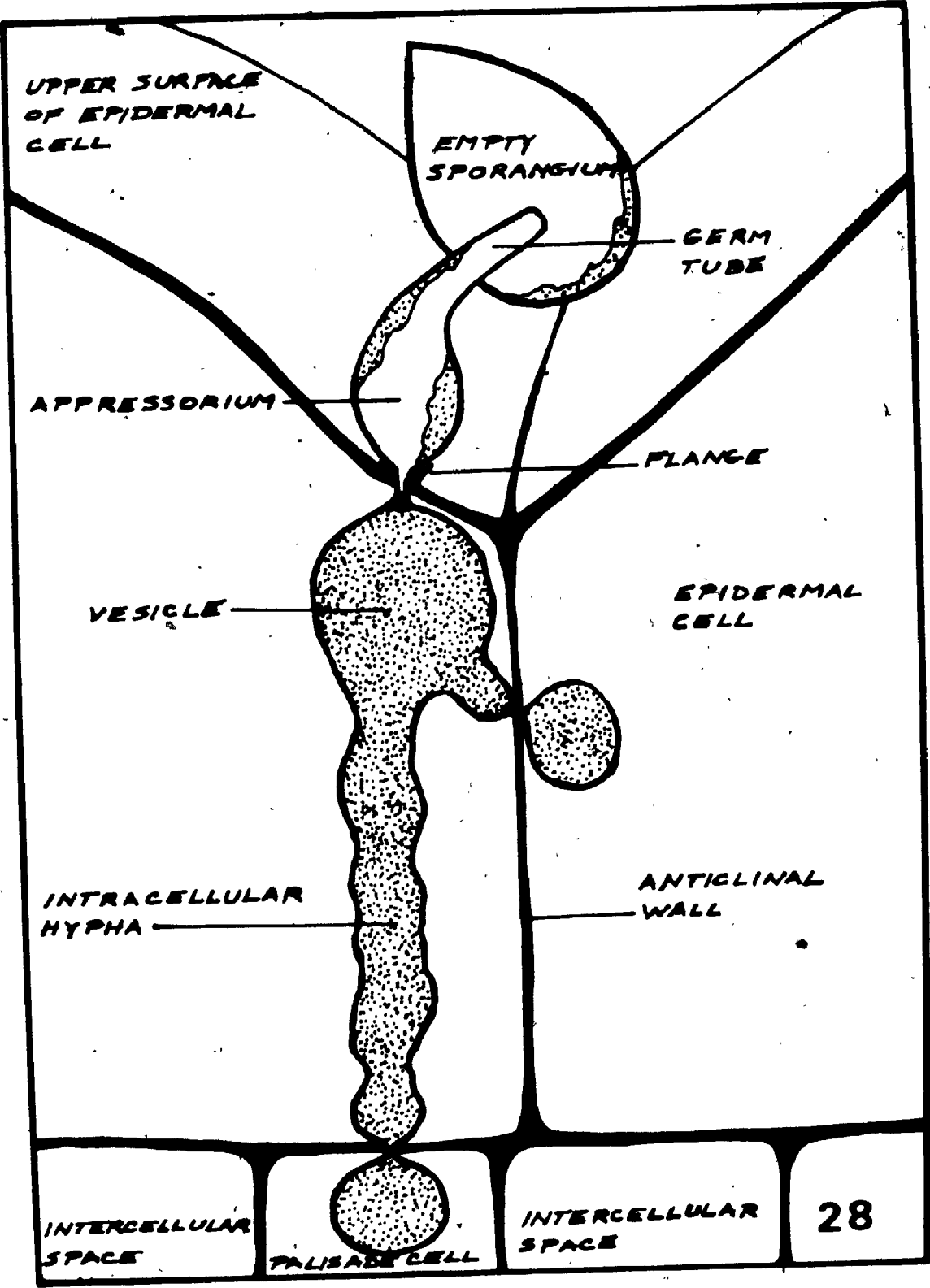


PLATE 11

Scanning electron micrographs of P. hyoscyami
f.sp. tabacina conidia infecting susceptible N.
tabacum var Virginia 115 leaves.

- Figure 29. A low power view of the surface of tobacco leaf supporting conidia. The conidia are lodged in the depressions above the anticlinal walls of the epidermal cells. x500
- Figure 30. A conidium with a prominent scar (arrow) at the tip. This marks the point of attachment of the conidium to the branch of the conidiophore. x2,000
- Figure 31. A conidium with a lateral germ tube. Observe that its connection to the conidium is restricted in size.
- Figure 32. A small germ tube and curved appressorium. Observe that the conidium lies in the depression of the leaf. x2,000
- Figure 33. A conidium with the appressorium growing down into the depression of the leaf. Observe the attachment scar (arrow) and the emergence of the germ tube at the side of the conidium. x2,000
- Figure 34. A part of an appressorium that has broken away from the infection tube in the tobacco leaf. Observe the flange (F) around the perimeter with a core of cytoplasm or plug, the width of the infection tube, in the centre. x5,000

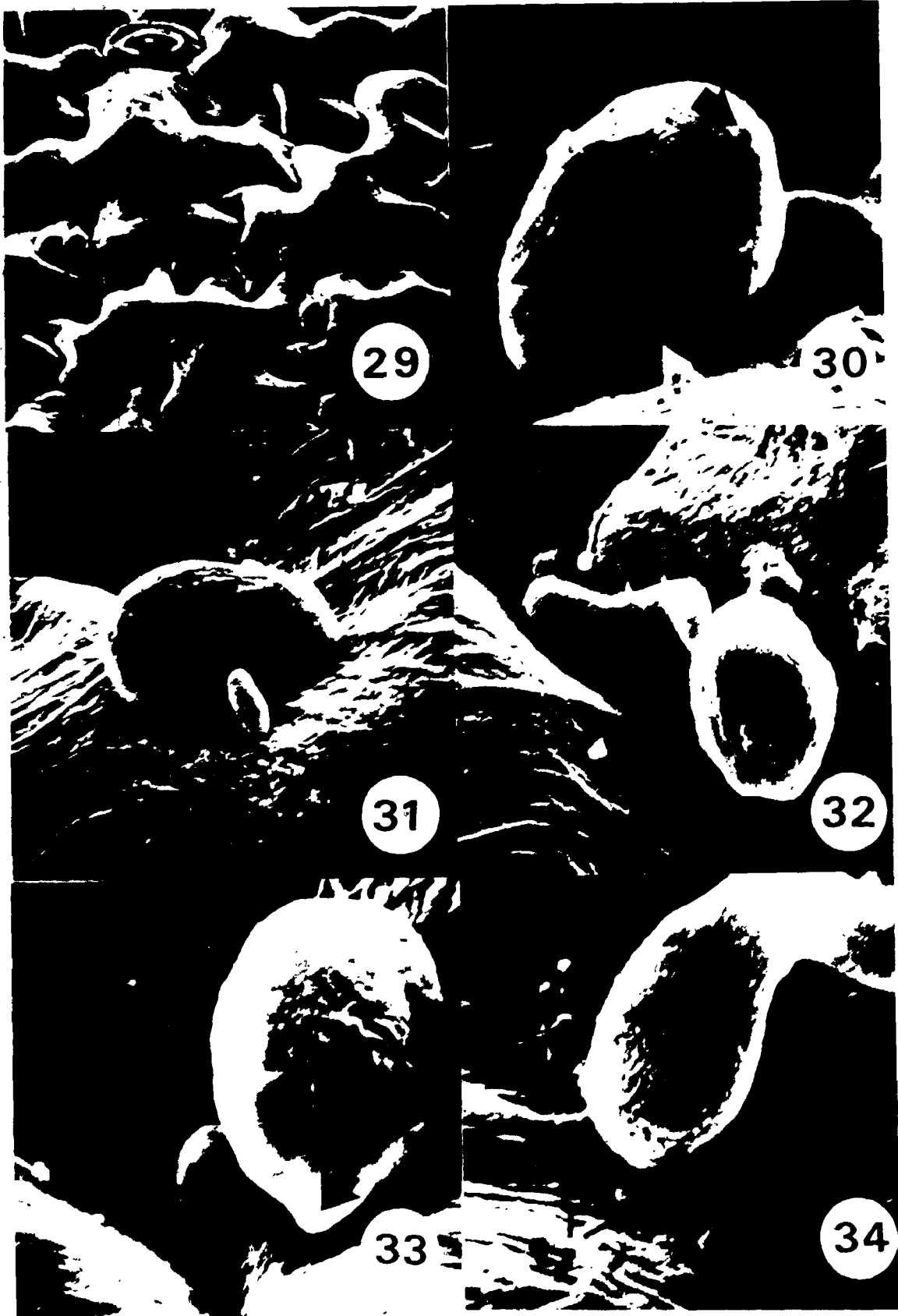


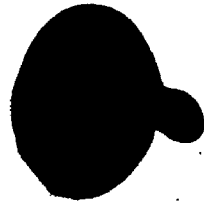
PLATE 12

Light micrographs of conidia, germ tubes, appressoria and vesicles formed on the surface of a susceptible tobacco leaf.

- Figure 35. A quiescent conidium with dark staining cytoplasm. x1,200
- Figure 36. A conidium with a short germ tube emerging from its lateral wall. x1,200
- Figure 37. A club shaped appressorium attached to a conidium. The dark staining cytoplasm has migrated from the conidium into the appressorium. x1,200
- Figure 38. A conidium and appressorium. The appressorium is full of cytoplasm while the conidium contains some cytoplasm and circular inclusions (IN). x1,200
- Figure 39. A flange (F) stained with acidified Lacmoid at the end of an appressorium. The clear tube between the conidium and appressorium is the infection tube. x1,200
- Figure 40. A vesicle with a 'nipple' in an epidermal cell. The spherical body outside the epidermal cell is the appressorium. The arrow points to the 'nipple' or branch of the vesicle. x1,200



35



36



37



IN

38



F

39



40

PLATE 13

Figure 41. A conidium germinated in water on a glass slide. Observe the long germ tube. x1,200

Figure 42. A germinated conidium on 1.5% Difco Bacto agar. It has a long germ tube. x700

Figure 43. An uncharacteristic germ tube and appressorium which occasionally formed on susceptible tobacco leaves. x1,200

Figure 44. An uncharacteristically long appressorium which had the ability to produce a successful infection in the tobacco leaf. x1,200

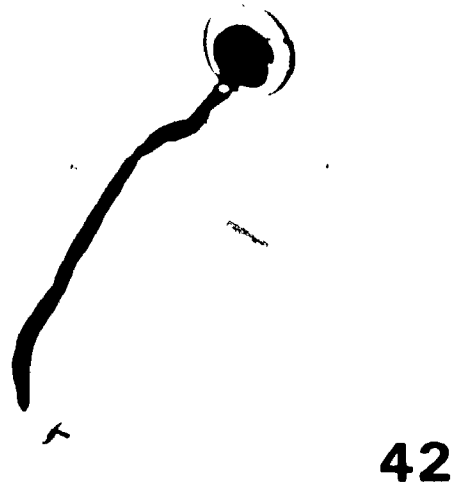
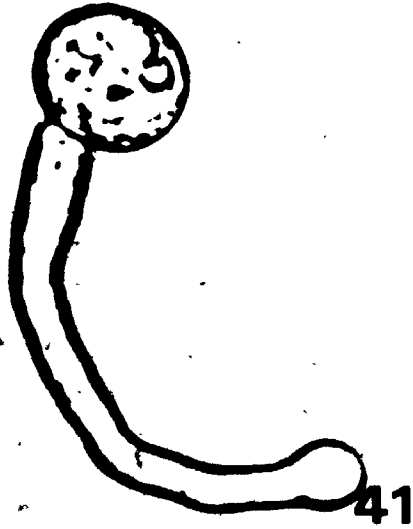


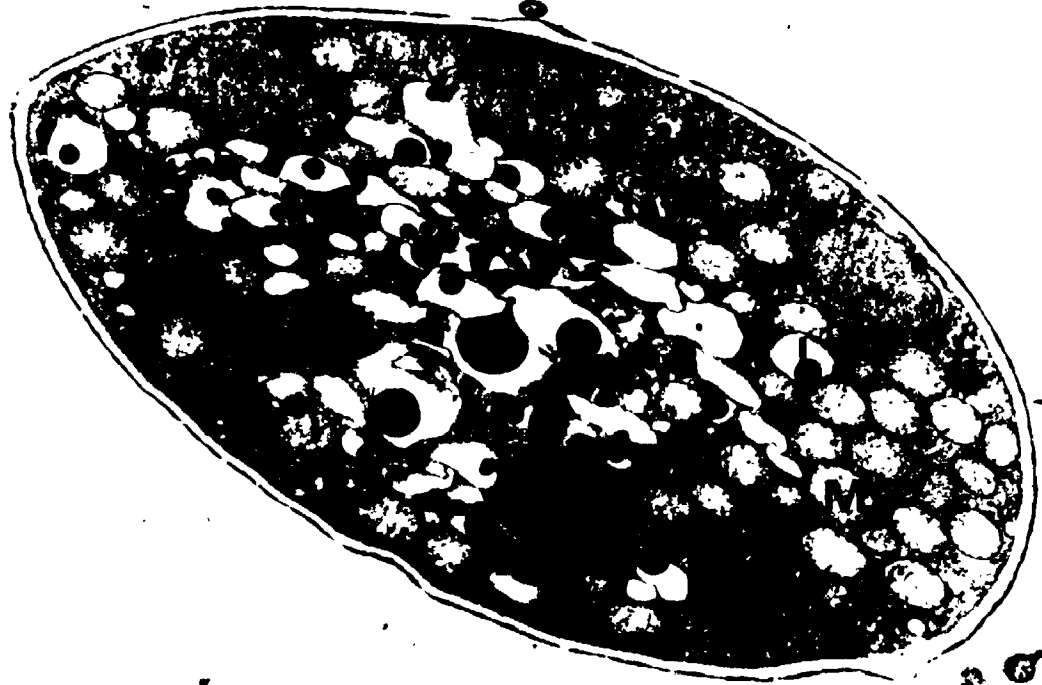
PLATE 14

Transmission electron micrographs of conidia of P. hyoscyami f.sp. tabacina on susceptible tobacco leaf.

Figure 45. A section of ungerminated conidium. Observe the thin wall, large numbers of mitochondria (M), lipid bodies (L), and five nuclei (N).
x7,200

Figure 46. A section through the attachment scar of the conidium. x15,300

Figure 47. A section through part of a conidium which has germinated and some cytoplasm has emptied into the germ tube. Observe the large numbers of mitochondria (M) and an abundance of free ribosomes. x18,500



45



47

PLATE 15

- Figure 48. A section of an ungerminated conidium, 1 h post-inoculation. Observe the large numbers of vacuoles (VA) and small amount of protoplasm which is adjacent to the cell wall. Several electron-dense bodies are present in the conidium. x6,300
- Figure 49. A section of a nongerminated conidium, 2.5 h post-inoculation. The small vacuoles (VA) have coalesced into large vacuoles. The protoplasm at the periphery of the conidium is granular in appearance. x6,700
- Figure 50. A section of a non-germinated conidium, the convoluted cell wall of the conidium indicates the loss of turgidity due to water loss. x6,700
- Figure 51. A section of a germinated conidium. The protoplasm has migrated to the appressorium. Observe that the plasma membrane (PM) has remained in the empty conidium. x7,000

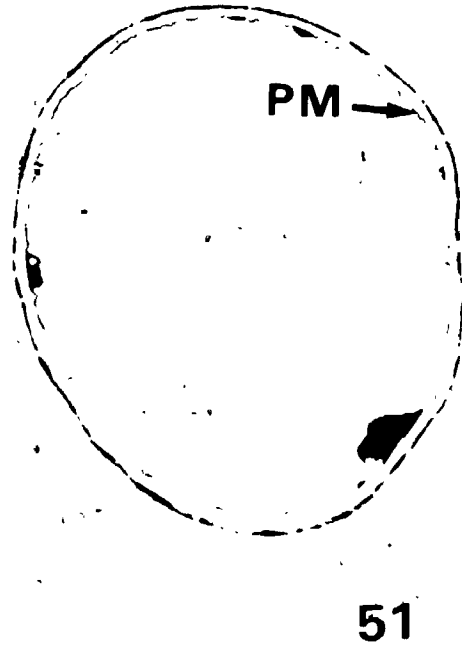
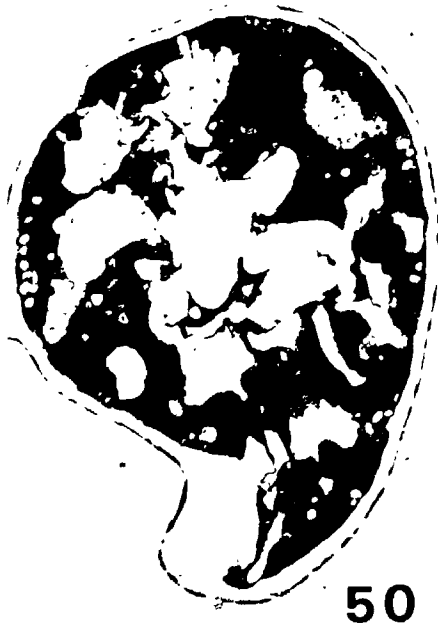
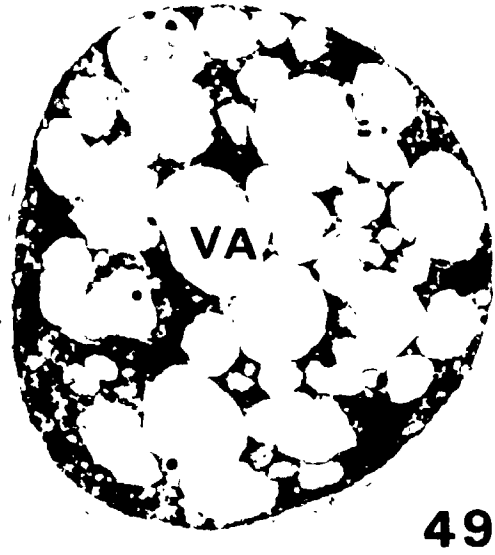
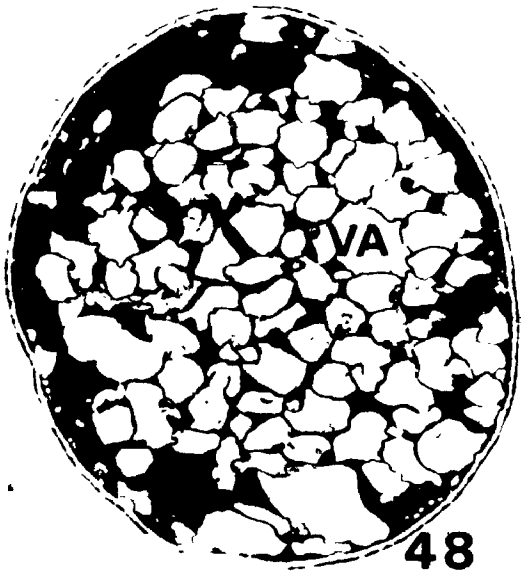


PLATE 16

Figure 52. A section through a conidium that has germinated and produced a germ tube and an appressorium. The plasma membrane (PM) and a large central vacuole (VA) remained in the conidium. x9,300

Figure 53. A section of an empty conidium and part of an appressorium (A). Observe the continuation of plasma membrane (PM) into the appressorium and the break in the spore wall at the point where a germ tube forms. A large vacuole (VA) remains in the conidium. The protoplasm in the appressorium is densely packed with nuclei, mitochondria and electron-dense particles. x9,300

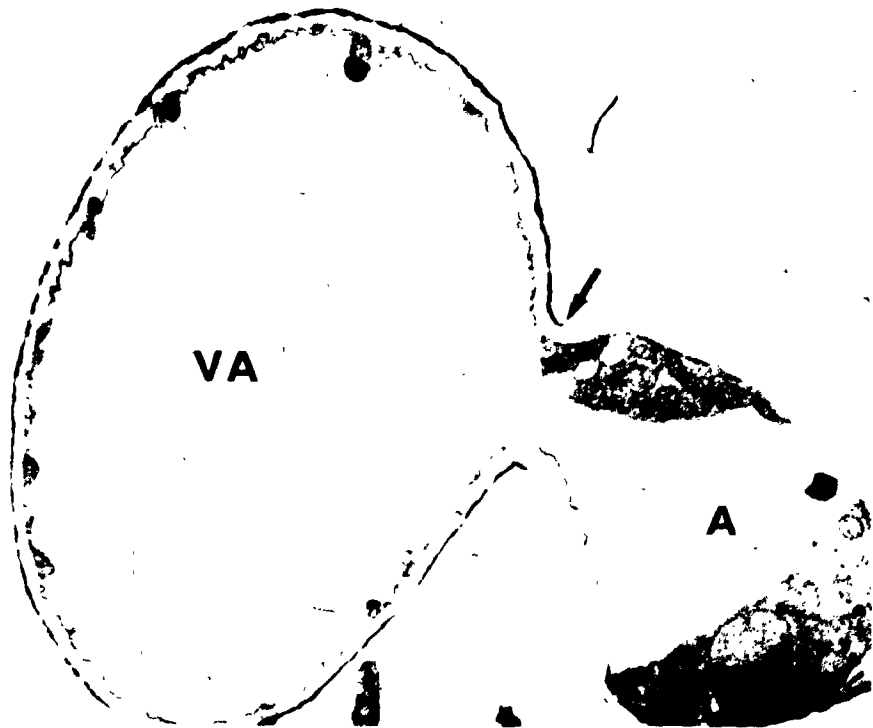
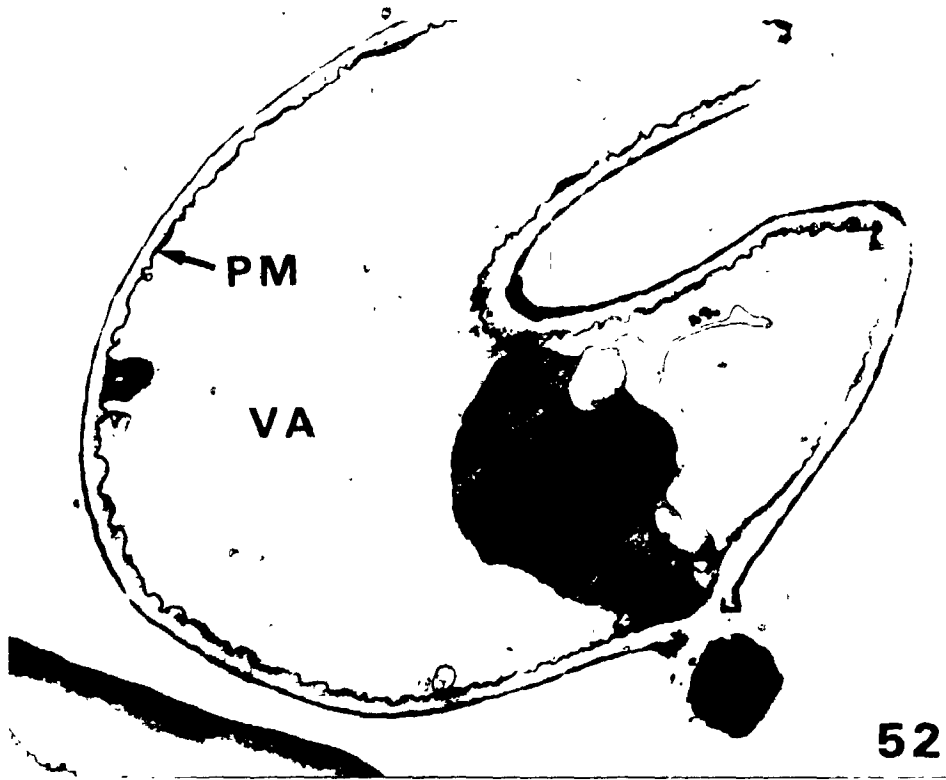


PLATE 17

Transmission electron micrographs of structures formed in susceptible tobacco epidermal cells infected with P. hyoscyami f.sp. tabacina.

Figure 54. A section through an empty appressorium (A), an infection tube and a vesicle. Observe the thin layer of cytoplasm in the appressorium and the electron-transparent plug that fills the inner end of the infection tube. The infection hole is adjacent to an anticlinal wall (AW). The vesicle contains a few vacuoles, two nuclei (N) with nucleoli and numerous mitochondria (M). A thin layer of host cytoplasm (arrow) surrounds the vesicle.
x20,400

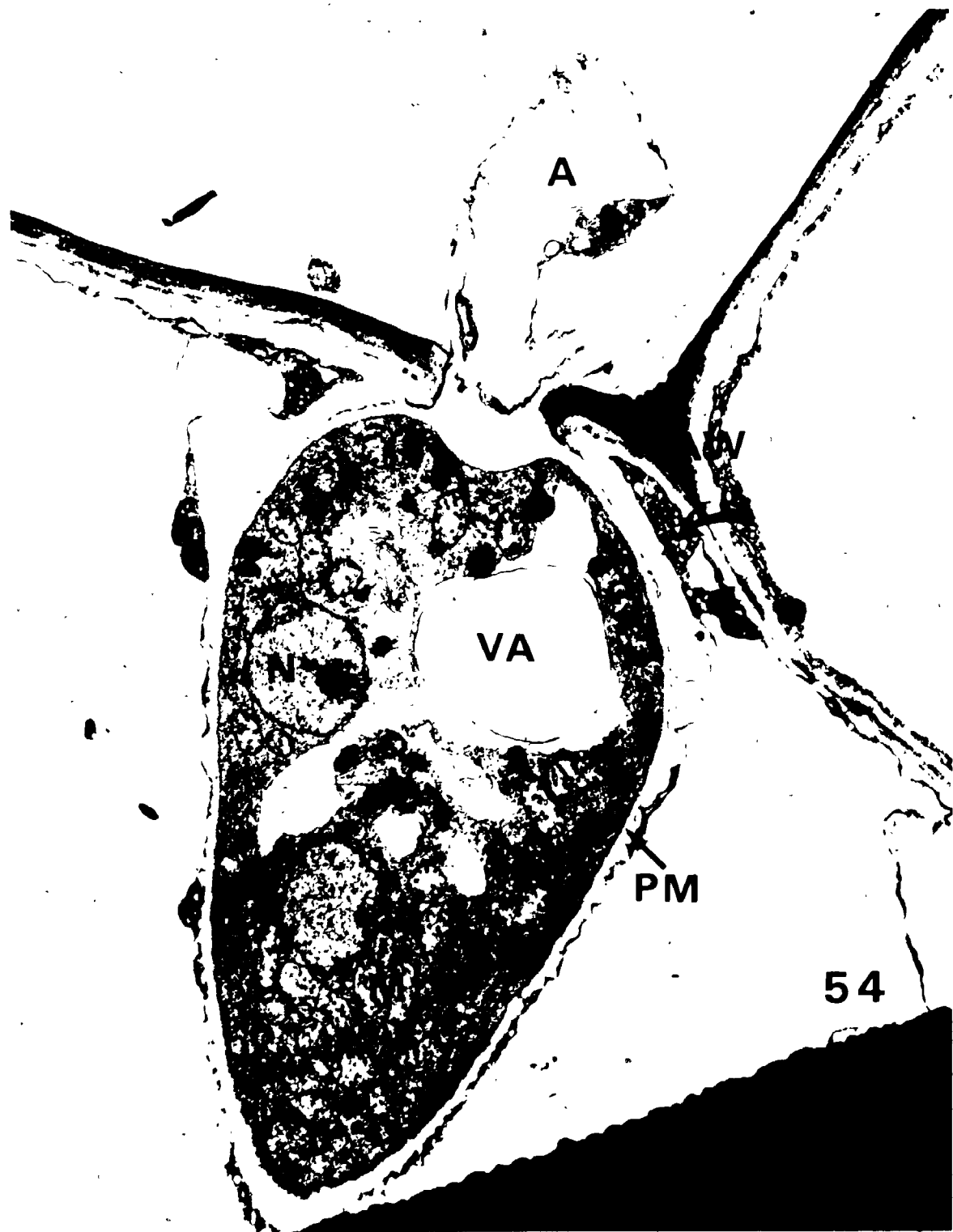


PLATE 18

Same series as Plate 17 (cont'd)

Figure 55. A section through part of the appressorium, partial plug in the infection tube (P) and part of the vesicle (SV). The electron-dense flange (F) is present between the appressorium and host wall. x19,400

Figure 56. A section through the appressorium (A), infection tube, plug (P) and vesicle (SV). x24,000

Figure 57. A section through a plug (P) and a portion of the infection vesicle. Observe the plug which is electron-transparent except for scattered electron-dense particles. A fungal wall (FW) separates the plug and cytoplasm. The fungal cytoplasm (FC) contains many tubular vesicles and the plasmalemma (PM) adjacent to the vesicular wall is irregular and tubules project into the fungal wall (FW). x70,000



PLATE 19

Same series as Plate 17 (cont'd)

Figure 58. Micrograph of a part of vesicle and a 'nipple' (NI). The cytoplasm is dense and contains numerous round tubular vesicles. Observe the two dictyosomes (D) beside the nucleus (N) with its associated nucleolus (NU). Host cytoplasm (HC) surrounds the fungus. The host plasma membrane, host cytoplasm (HC) and tonoplast membrane (T) encase the fungus in the epidermal cell. x16,000

Figure 59. A section of hyphal branch (B) which has penetrated a palisade (PA) cell. Observe the healthy host chloroplasts (CH) while the fungal hypha contains few vacuoles, dense cytoplasm and numerous mitochondria. x11,300

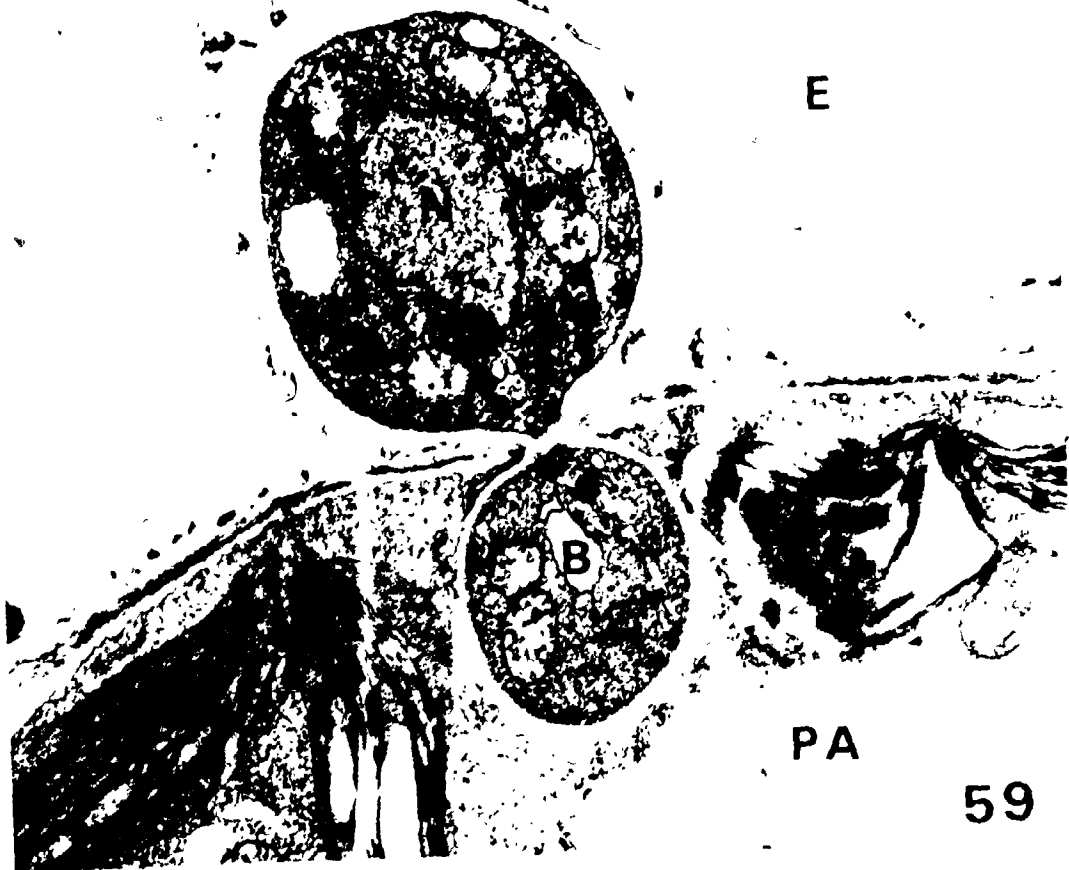
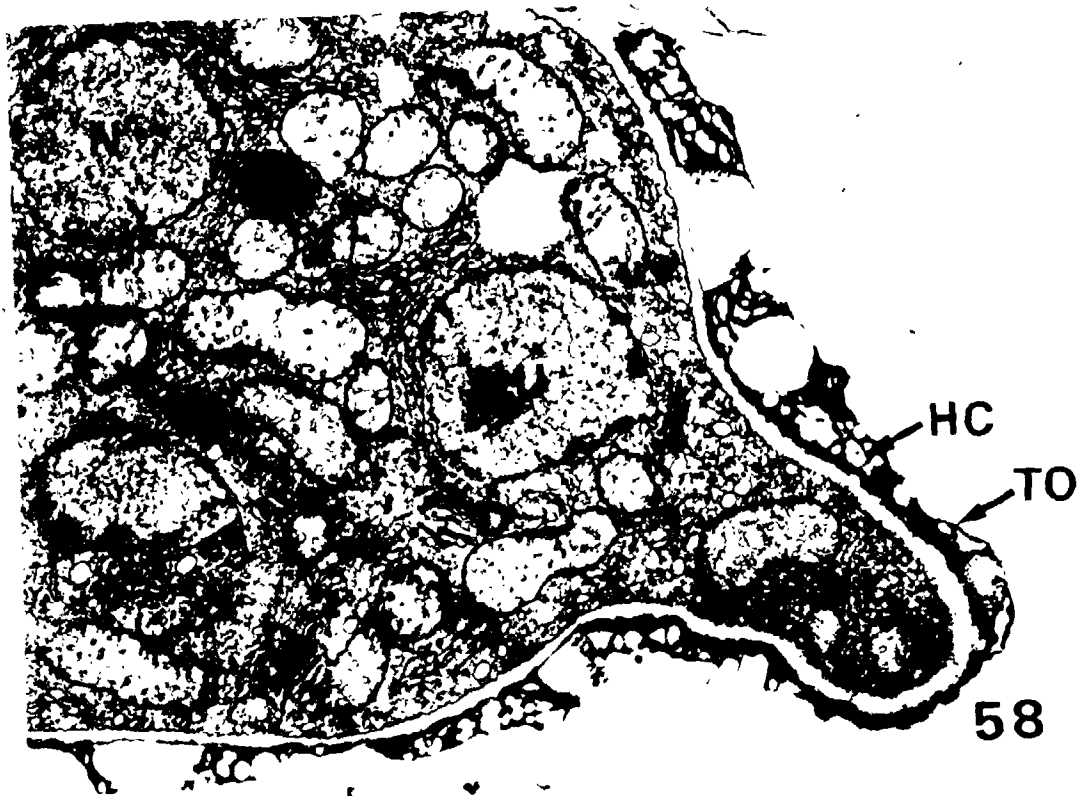


PLATE 20

Same series as Plate 17 (cont'd)

Figure 60. A hyphal branch (B) that has passed through an anticlinal (AW) into an adjacent epidermal cell. The fungal plasmalemma is very uneven and convoluted. Numerous tubular elements (T) are present in the densely packed cytoplasm. Two dictyosomes (D) are adjacent to the nucleus. Host cytoplasm, adjacent to the fungal wall (FW) forms a thin layer around the branch. The tonoplast (TO) membrane forms the outer membrane layer on the hyphal branch. x15,300

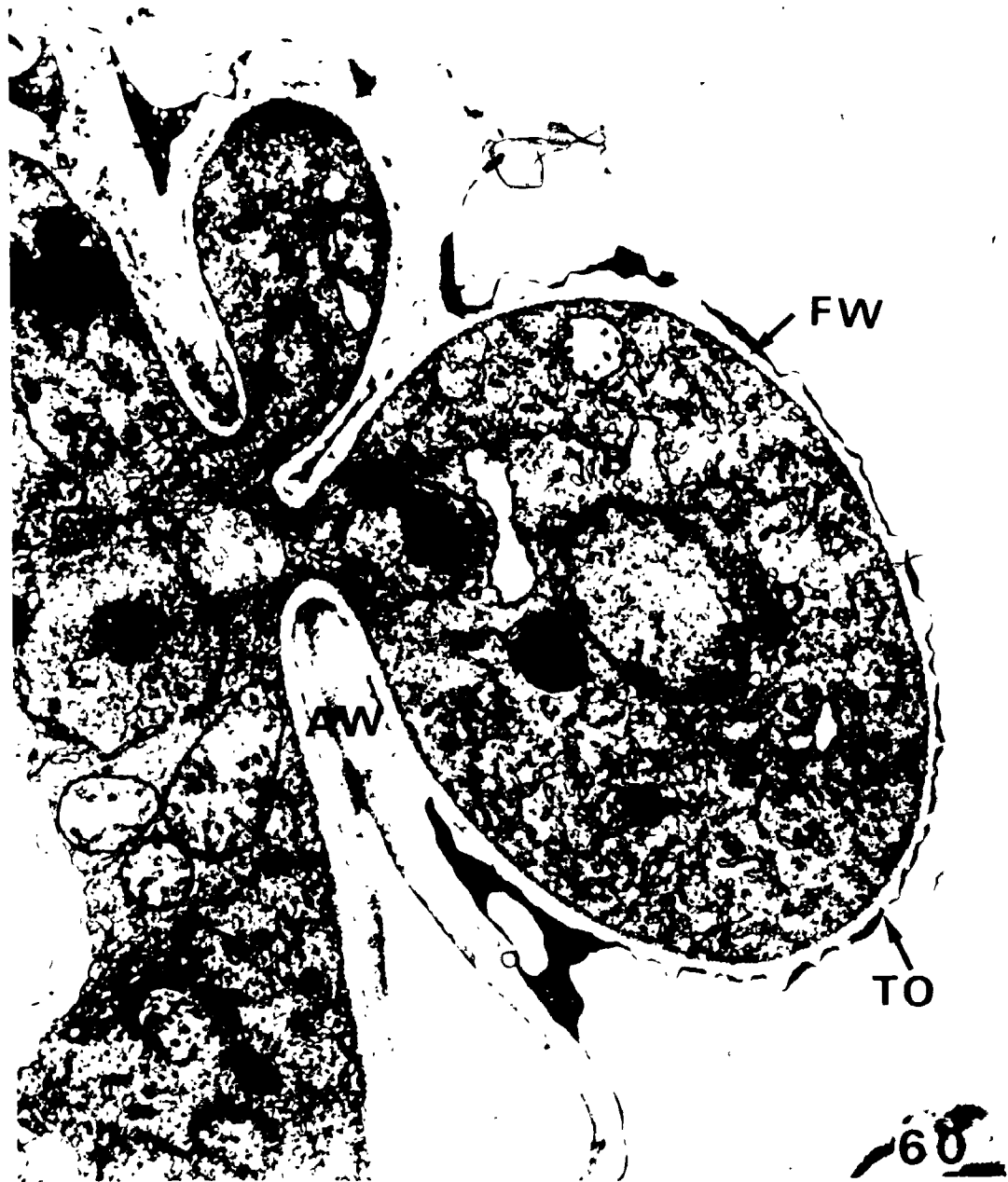


PLATE 21

Same series as Plate 17 (cont'd)

Figure 61. A thin section through a fungal nucleus (N) and its nucleolus (NU). Dictyosomes (D) are frequently associated with the nucleus. Spherical and tubular vesicles are associated with the dictyosome. Observe a distinct centriole (CO) adjacent to the nucleus. Note the nine groups of centripetal tubes in a cartwheel structure. x37,000

Figure 62. A section through a nucleus (N) that is blebbing off vesicles. The arrow points to a bleb on the nuclear envelope. x47,300

Figure 63. A section through part of a nucleus (N) and surrounding cytoplasm in a growing hypha. Note the large distinct nuclear pore (NP) in the nuclear membrane. x71,700



PLATE 22

Same series as Plate 17 (cont'd)

Figure 64. A thin section through a vesicle.

Observe the large number of spherical and tubular vesicles (T) adjacent to the convoluted plasma membrane of the fungus.

Arrow points to a vesicular element passing through the plasmalemma opening into the fungal wall (FW). x43,700

Figure 65. The large cluster of tubules (L) (plasmalemmasome)

adjacent to fungal wall. A small number of lipid droplets are seen in the vesicle.

x43,700

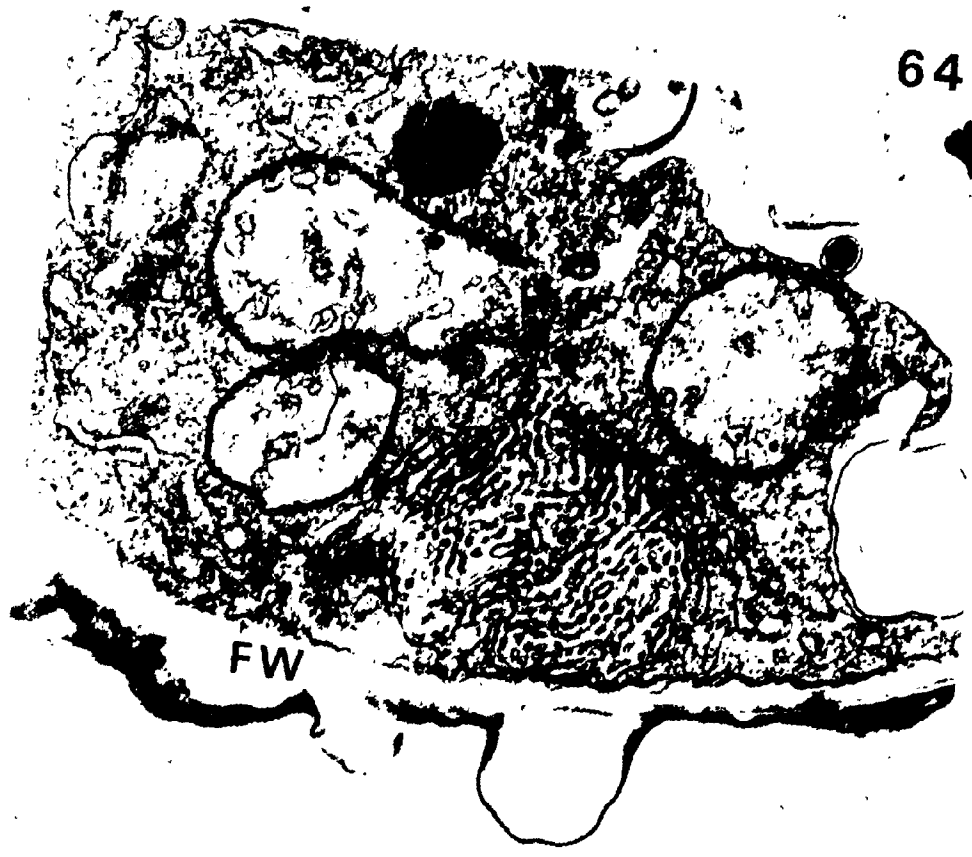
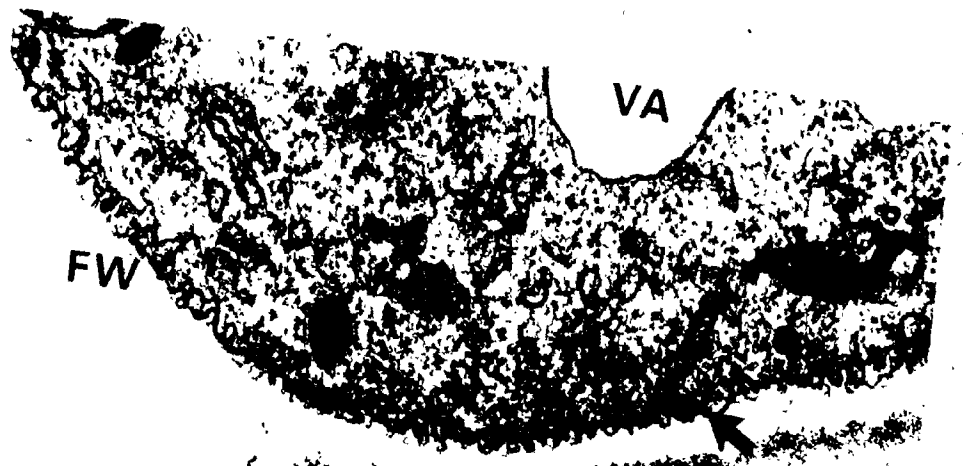


PLATE 23

Figure 66. A thin section of an intercellular hypha of P. hyoscyami f.sp. tabacina. Observe the many nuclei (N) each with a nucleolus (NU). The hyphal cytoplasm is densely packed containing large numbers of mitochondria (M) and a few vacuoles. x13,300



PLATE 24

Figure 67. A diagram of a cane-shaped haustorium which is constricted at its neck where it passes through the host wall (HW). The extrahaustorial matrix is adjacent to fungal wall (FW), and is composed of two layers that vary in thickness, an electron-opaque layer with pores (arrow) and an electron-transparent layer. The extrahaustorial matrix is surrounded by the plasma membrane (P, extrahaustorial membrane), a thin layer of host cytoplasm (C), and by the tonoplast (T). The host cells of N. tabacum contain a large central vacuole (VA).

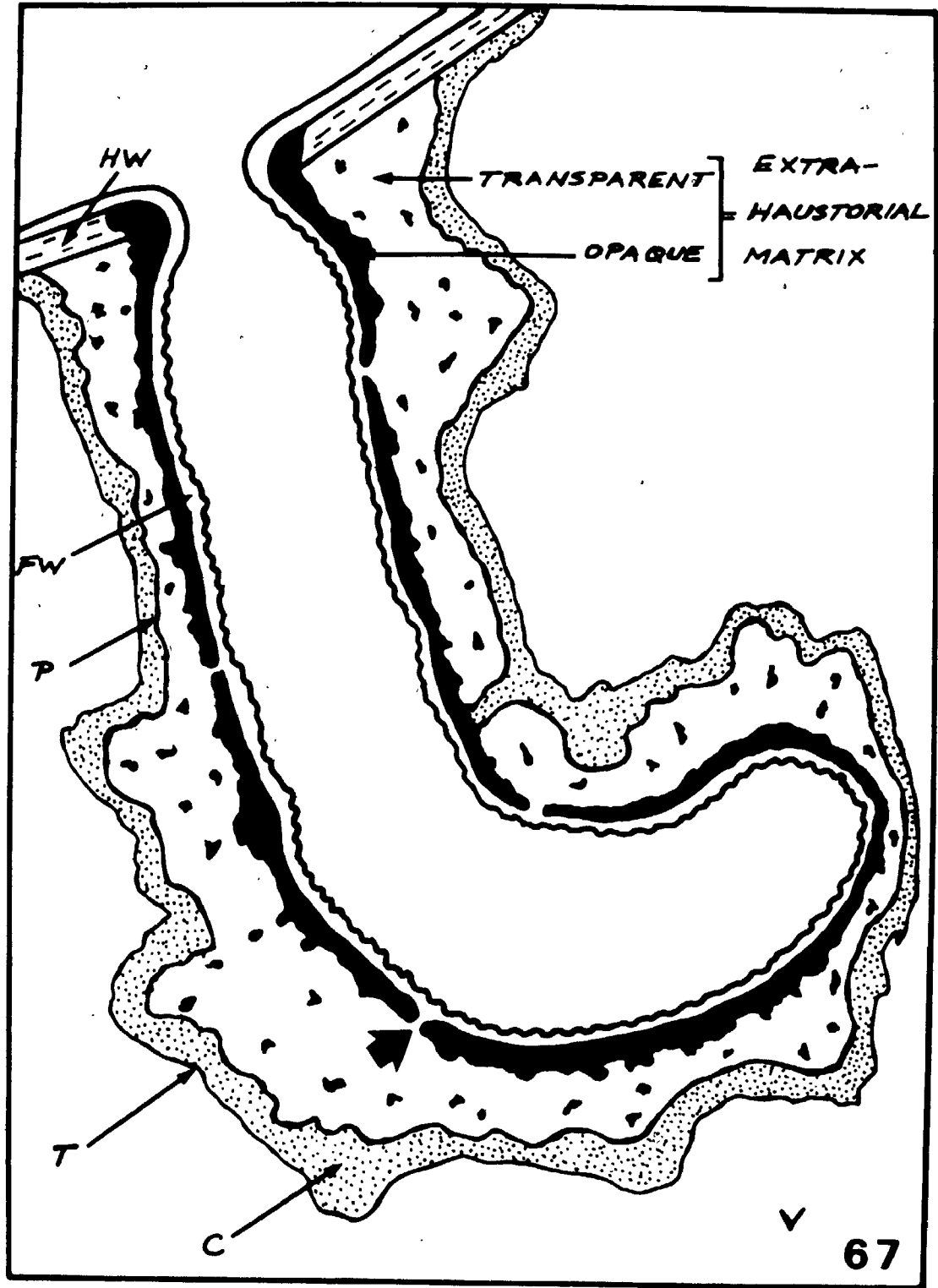


PLATE 25

Light micrographs

- Figure 68. Intercellular hypha (H) with a cluster of young haustoria. Most of the young haustoria (HA) are surrounded by an extrahaustorial matrix that is deeply stained with methylene blue and erythrosin. x1,200
- Figure 69. Section of intercellular hypha (H) a bulb-shaped haustorium (HA). x1,500
- Figure 70. Intercellular hyphae which closely follows the host cell walls. Arrow points out a haustorium in the epidermal cell. x800
- Figure 71. An intercellular lobulate hypha that has produced a long branched haustorium (HA). x1,500
- Figure 72. A cluster of haustoria in epidermal cells (arrow). x1,000
- Figure 73. A long torulose haustorium stained with acid fuchsin. x1,600

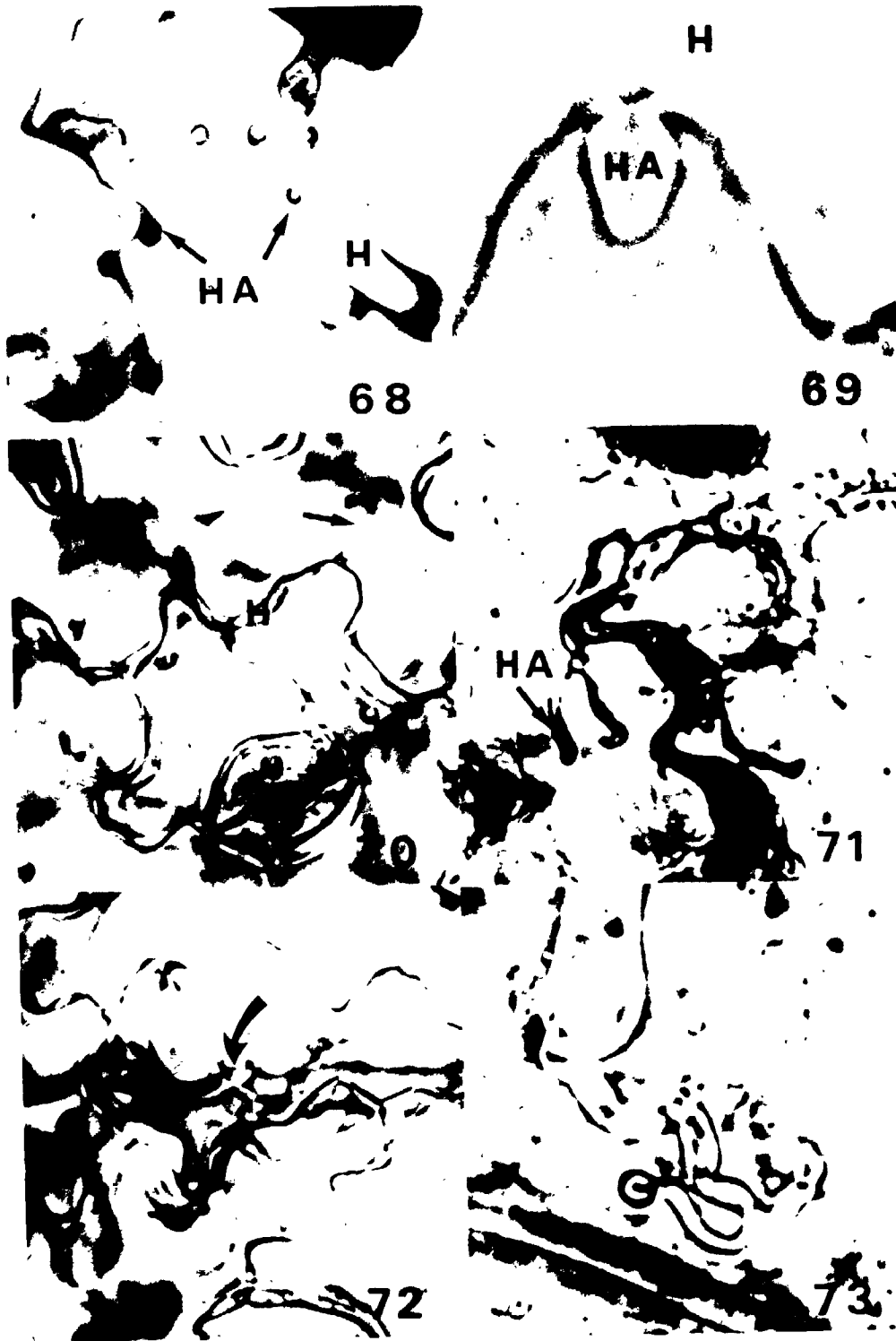


PLATE 26

Same series as Plate 25 (Cont'd)

Figure 74. A haustorium with a large darkly stained extrahaustorial matrix (EHM) at its base. x2,500

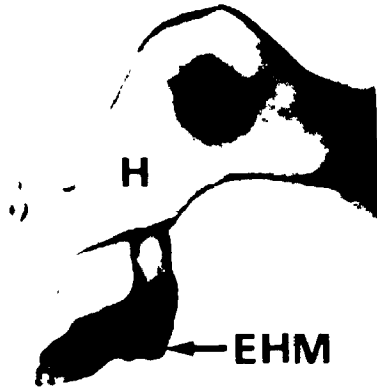
Figure 75. A haustorium with a darkly stained extrahaustorial matrix (EHM) except at its tip and base. x2,500

Figure 76. A haustorium with a thin extrahaustorial matrix (EHM) in some regions. x2,500

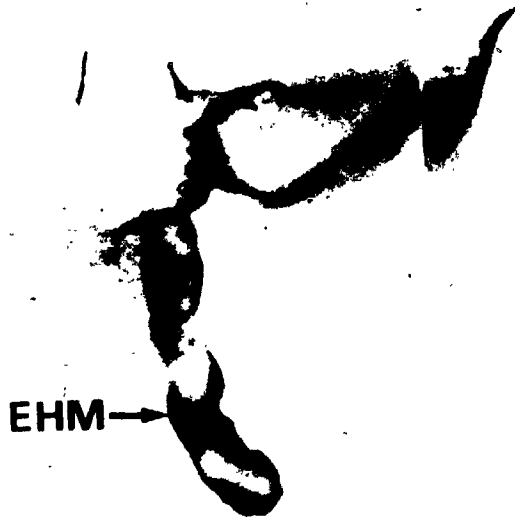
Figure 77. A shrunken haustorium (HA) with an extrahaustorial matrix (EHM) at its base. x2,100



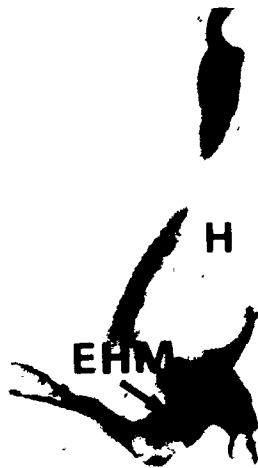
74



75




76



77

PLATE 27

Figure 78. A section through a cane-shaped haustorium which is constricted at its neck where it passes through the host wall. The haustorial wall is covered with a thin electron-opaque layer (Z) that is surrounded by an electron-transparent layer (ET) containing electron-opaque particles. Next to the extrahaustorial matrix (EHM) is a very thin layer of host cytoplasm which is bounded by the tonoplast (TO). x17,400



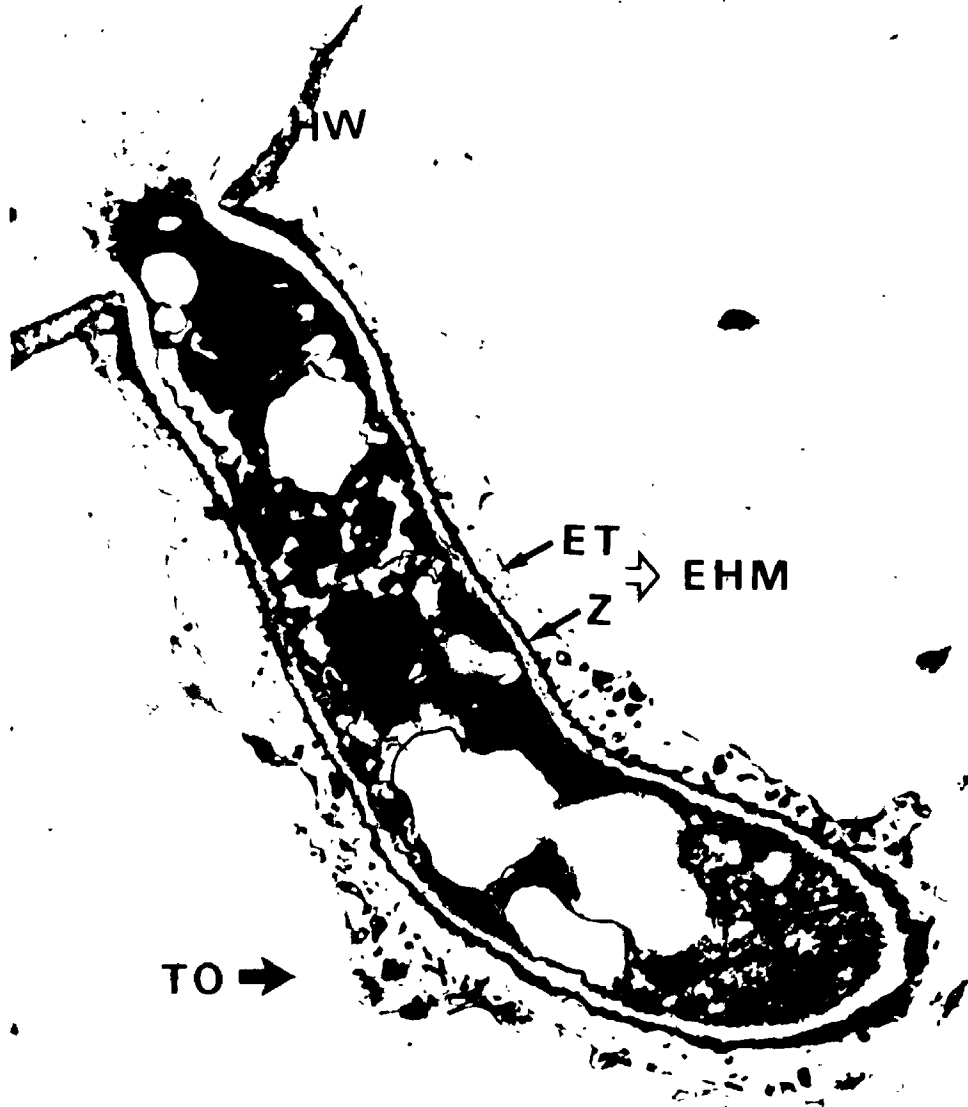


PLATE 28

Figure 79. An apparently inactive haustorium. It does not contain organelles and is surrounded by an electron-opaque layer (Z). The fungal wall (FW) continues from the hypha (H) to the haustorium. x10,100

Figure 80. Intercellular hypha and young haustorium (HA). The haustorium is bulb-shaped, contains dense cytoplasm, and is surrounded by an electron-opaque layer and host cytoplasm. A host nucleus and two chloroplastids with large starch granules (SG) are present in the host tissue. x12,400

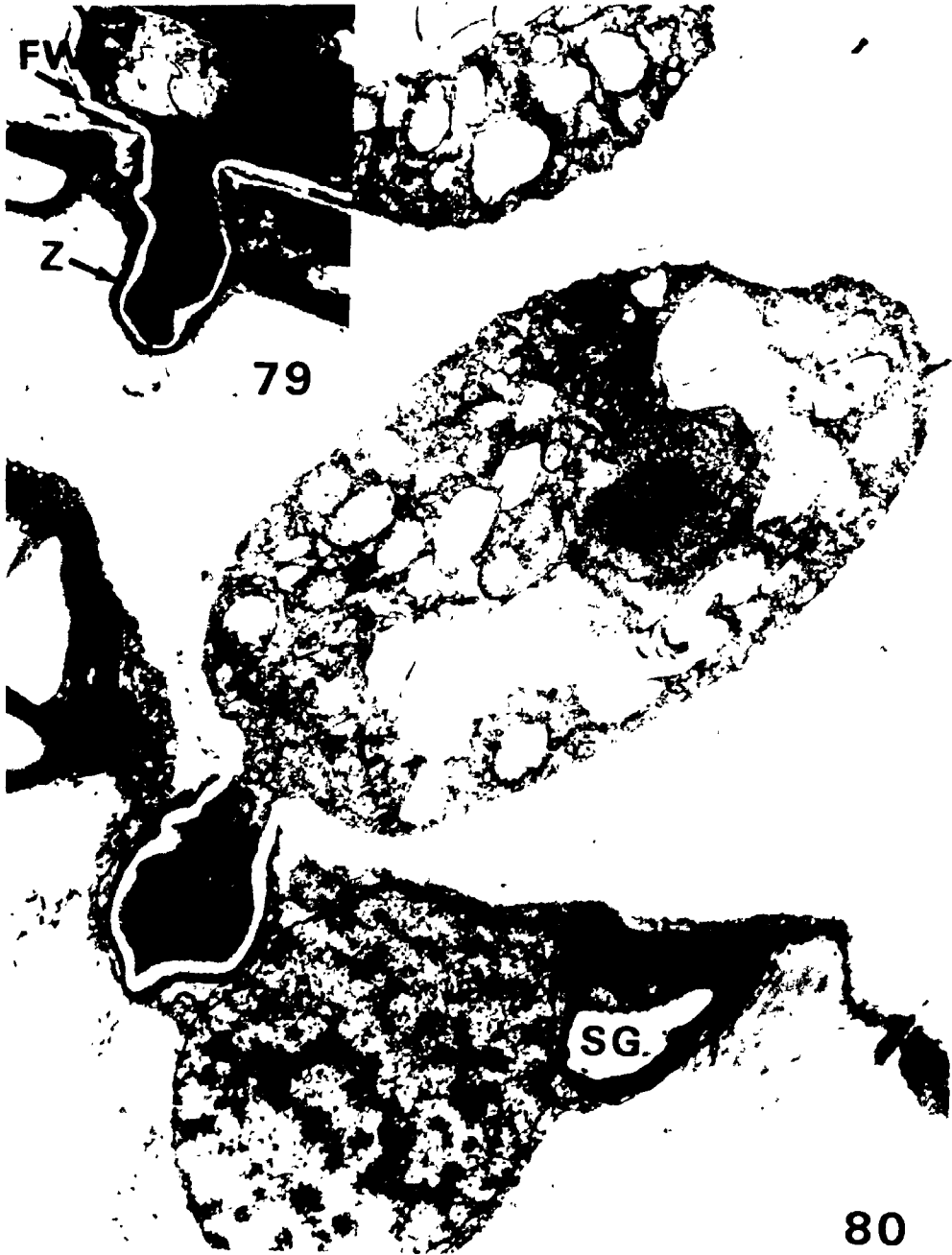


PLATE 29

Figure 81. Section through a young haustorium (HA).
The host wall is turned toward the inter-
cellular hypha (arrow) while the host wall
adjacent to the haustorial neck undergoes a
change in the orientation of microfibrils.
Immediately adjacent to the plasma membrane
(PM) lies the host cytoplasm (HC). x31,900

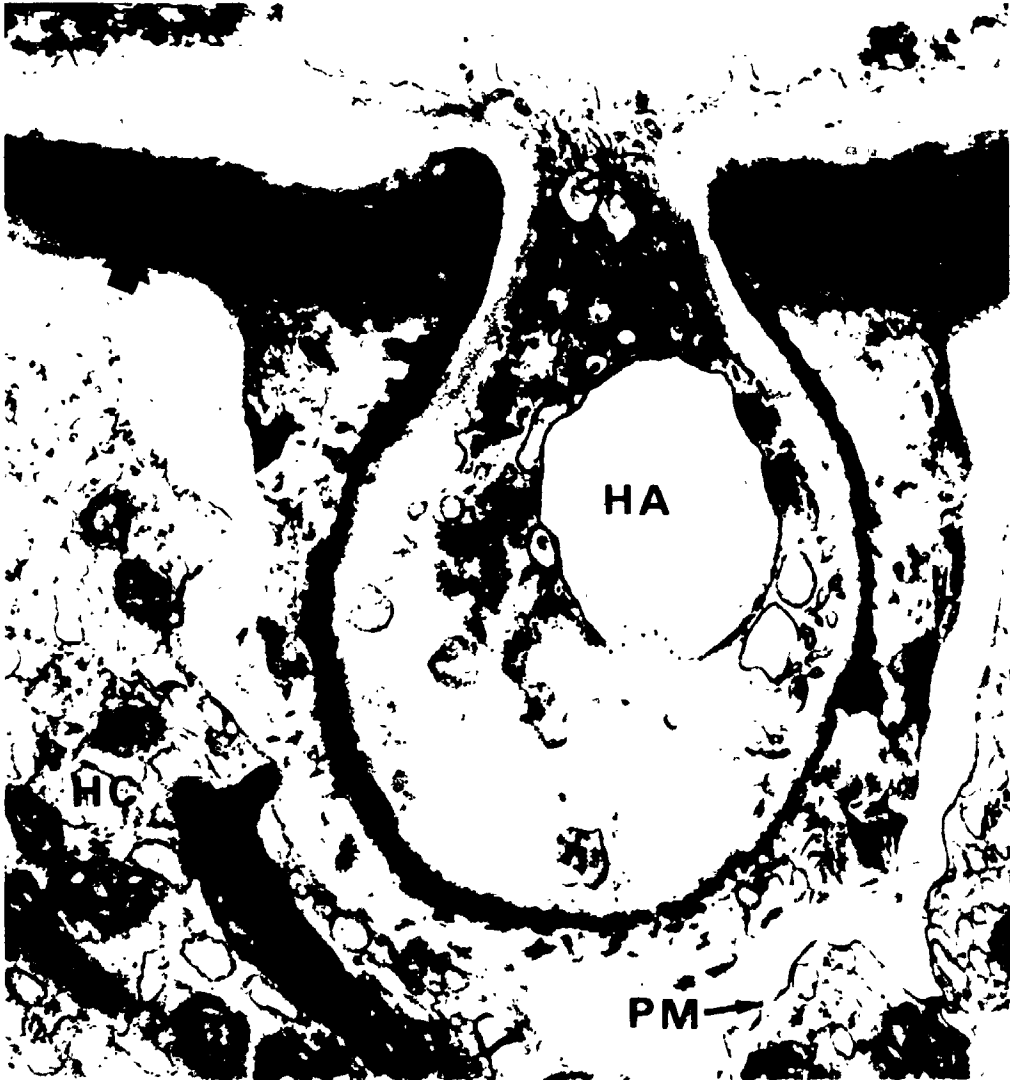


PLATE 30

Figure 82. A cross section of haustorium that contains long strands of endoplasmic reticulum, three mitochondria (M), lipid (LI) and large vacuole (V). The haustorial plasmalemma is markedly indented. The electron-opaque layer (Z) has pores (arrowhead) and is in contact with elongated blebs or vacuoles. The thick electron-transparent layer (ET) contains many vacuoles or blebs and in some instances has strands of cytoplasm through the electron-transparent layer that make contact with the electron-opaque layer (Z) (curved arrow). The host cytoplasm appears to be blebbing into the electron-transparent layer (ET) of the extrahaustorial matrix (EHM). x10,700



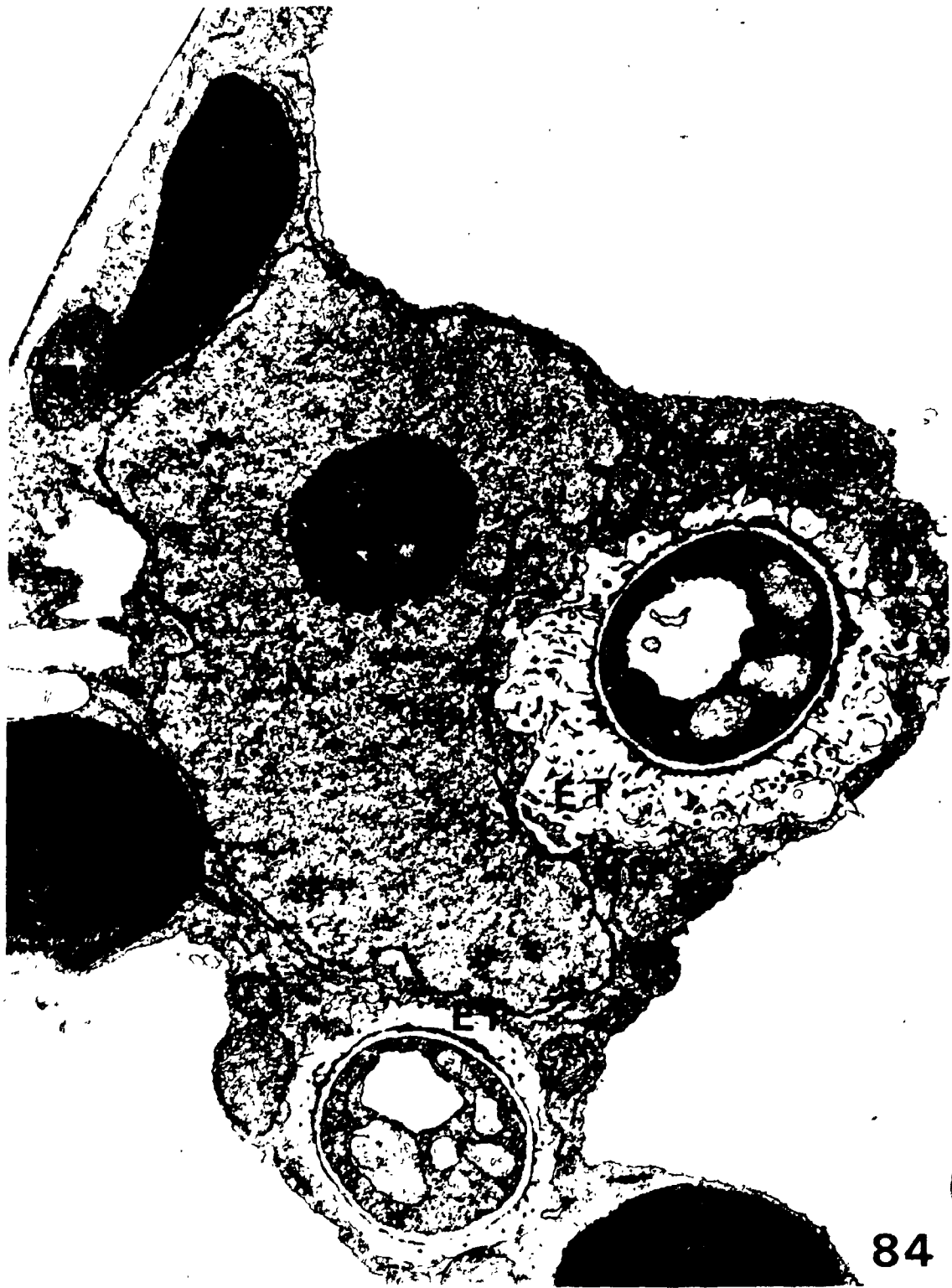
PLATE 31

Figure 83. A longitudinal section through a portion of the haustorium (HA) that contains mitochondria, vacuoles and dense cytoplasm. The electron-opaque layer (Z) is continuous along the haustorial wall but the electron-transparent layer (ET) only extends part way along the haustorium. A thin layer of host cytoplasm (HC) surrounds the haustorium. x25,400



PLATE 32

Figure 84. Two cross sections of a coiled haustorium. One section is surrounded by a greater quantity of electron-transparent material (ET) than the other. Dense host cytoplasm (HC) surrounds the extrahaustorial matrix. Host chloroplasts (CH), mitochondria (M), and a large host nucleus (N) and nucleolus (NU) are adjacent to the haustorial segments. x14,000



84

PLATE 33

Figure 85. A young haustorium suspended in a cotyledonary-cell vacuole (V). Cytoplasmic strands connect it to the relatively thick layer of cytoplasm (HC) that surrounds the extrahaustorial matrix of the haustorium. The electron-opaque layer (Z) has pores or gaps. The host cytoplasm (HC) passes through the electron-transparent layer (ET) in several places and comes in contact with electron-opaque layer (Z). A large nucleus (N) with an adjacent dictyosome (D) is present in the haustorium. Observe the haustorial plasmalemma is very irregular. x38,200

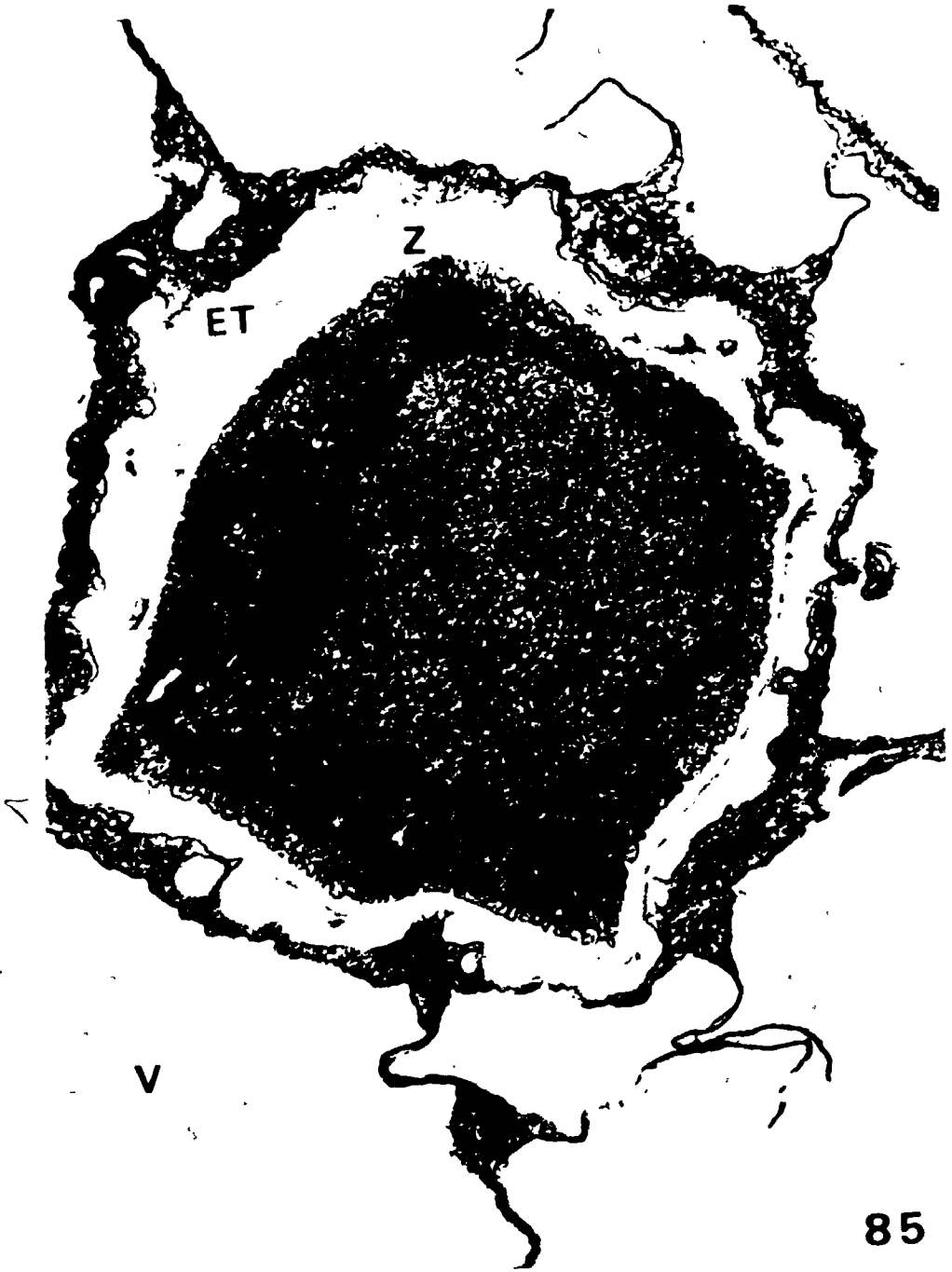


PLATE 34

Figure 86. A section through a branching haustorium. The adjacent intercellular hypha (H) is highly vacuolated while the haustorium contains dense cytoplasm. The hyphal fungal wall (FW) is continuous with the haustorium wall. x18,200

Figure 87. A thin section of a haustorium inside a lower epidermal cell (E). The haustorium and adjoining hypha are vacuolated. Observe the thicker host-wall (HW) on the lower portion of the epidermal cell. The epidermal cell contains a very small amount of cytoplasm and no chloroplasts. x8,900

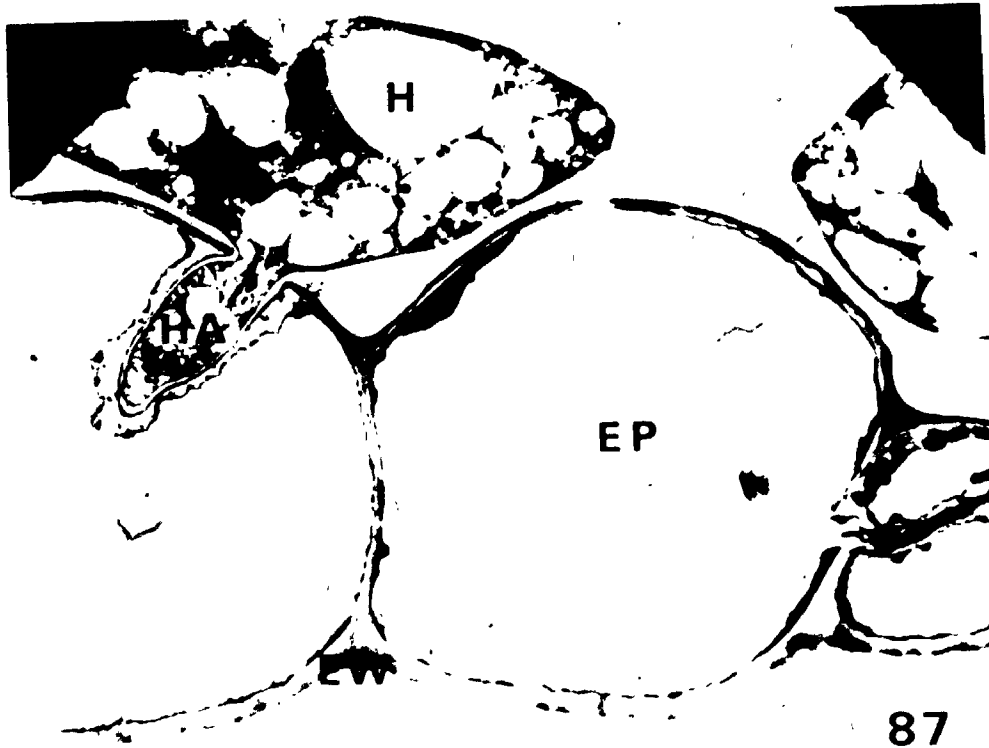


PLATE 35

Figure 88. A longitudinal section of an intercellular hypha (H) and a haustorium. Observe the close contact between the intercellular hypha and the adjacent palisade cell (PA).
x6,800

Figure 89. A cross section of a highly vacuolated intercellular hypha (H). x15,800

Figure 90. A longitudinal section of intercellular hypha. The haustorium and hypha (H) are almost devoid of cytoplasm. x8,000

Figure 91. A young haustorium and adjoining hypha (H). The atypical mitochondria (M) in both hypha and haustorium are irregular in shape.
x22,900

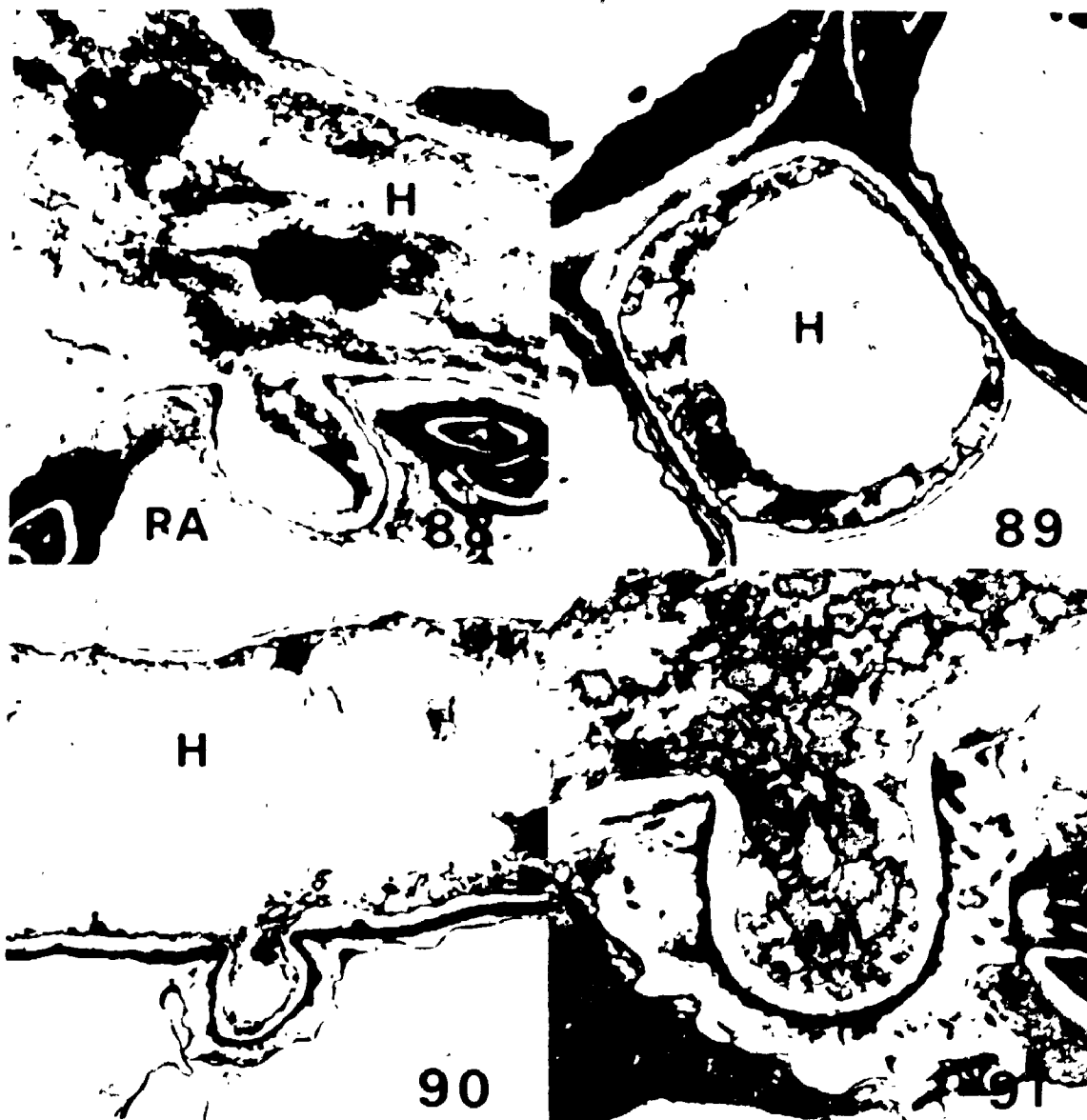


PLATE 36

Figure 92. A longitudinal section through a collapsed haustorium that is surrounded by a thick electron-opaque layer (Z) and an electron-transparent layer (ET) that form the extra-haustorial matrix (EHM). x18,500

Figure 93. A cross section of a collapsed haustorium. The haustorial wall is greatly indented. The extrahaustorial matrix is composed of an electron-opaque layer (Z) and an electron-transparent layer (ET). x15,800

Figure 94. A cross section of collapsed haustorium with a thick electron-opaque layer (Z) and a less developed electron-transparent layer. The adjacent intercellular hypha and host cytoplasm appear normal with no structural disorientation and degradation. x12,400

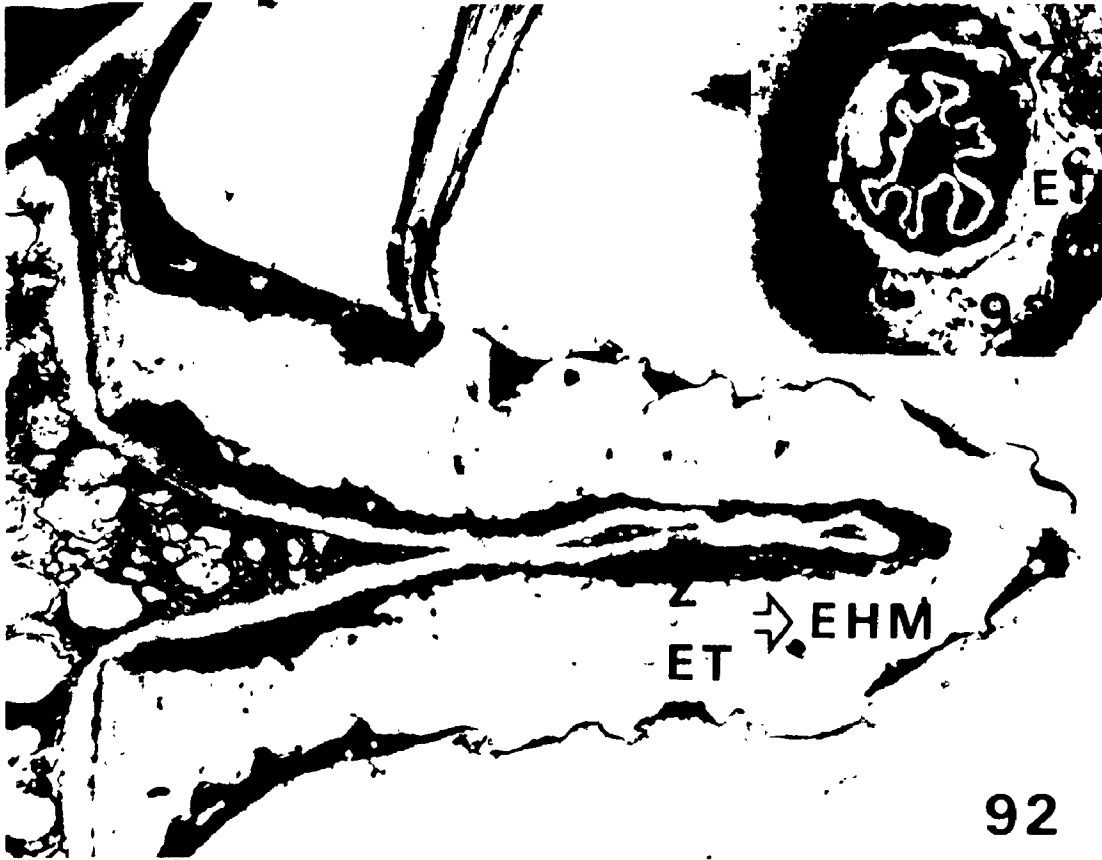


Figure 95A-C. A schematic diagram depicting the developmental stages of haustorium in susceptible host N. tabacum. Young bulb-shaped haustorium (A), cane-shaped haustorium (B) and coil-shaped haustorium (C).

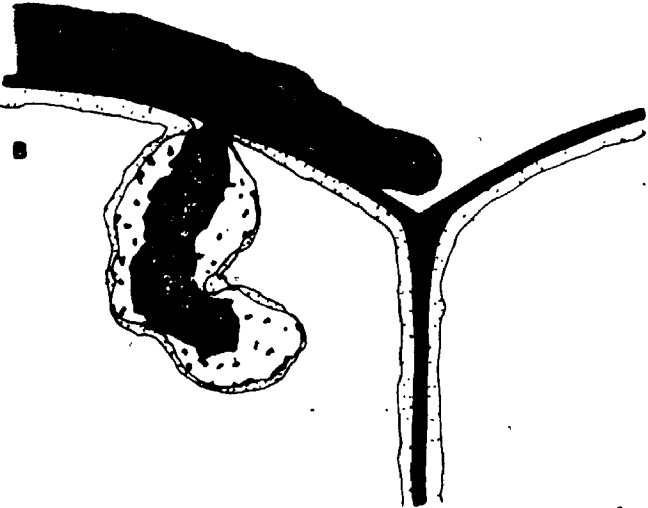


PLATE 38

Figure 96. The quantitative relationship between iodine (IKI) test and total starch assay (TSA) measurements. The iodine test gives semi-quantitative measurements over the lower portion of the total starch range.

Figure 97. Leaves cleared in alcohol and stained in IKI solution. The leaf on the left (IKI +++) contains starch while the leaf on the right (IKI -) does not contain starch. xl

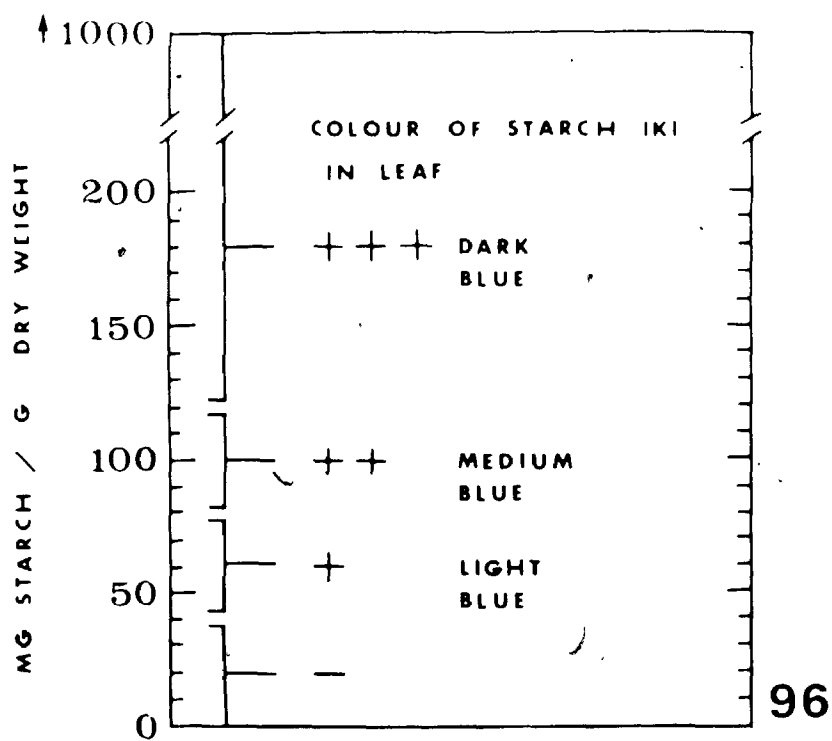


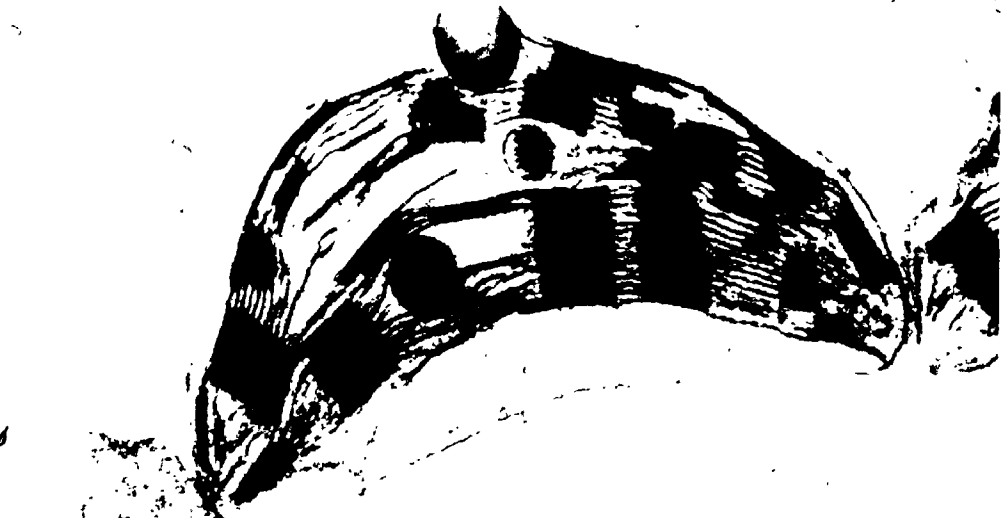
PLATE 39

Figure 98. A section of a chloroplast in a healthy leaf which was fixed after 12 h of darkness. The chloroplast contained no starch granules.

x26,600

Figure 99. A section of chloroplast in a healthy leaf which was fixed after 8 h of light. Observe the presence of the large starch granule (SG).

x26,600



98



99

PLATE 40

Figure 100. A section of 2 chloroplasts after 12 h of darkness. The tissue was infected 2 days prior to fixation. Observe the starch (SG) in the plastids in the host cell adjacent to the fungal hypha (H). x18,000

Figure 101. A section of a chloroplast in infected tissue after 14 h of darkness and 4 days post-inoculation. Observe the presence of starch granules in the chloroplast. x24,200



101

PLATE 41

Figure 102. A section of infected tissue at 6 days post-inoculation. The section was obtained after the plants were exposed to 8 h of darkness. The fungal development in leaf tissue was extensive. Chloroplasts in the infected host cell show normal thylakoid stacking and no starch granules. Observe the presence of the intercellular hypha (H) and haustorial body (HA) in the adjoining host cell. x15,300



102

Figure 103. Starch Formation - Amount of starch present in healthy and diseased leaves after they were exposed to light for specific time periods. Twenty four h prior to illumination the diseased leaves were inoculated and all plants were put in darkness. The amount of starch in the infected and healthy leaves was significantly different at the second, fourth and twelfth h ($p < 0.05$).

H - Healthy Plants

I - Infected Plants

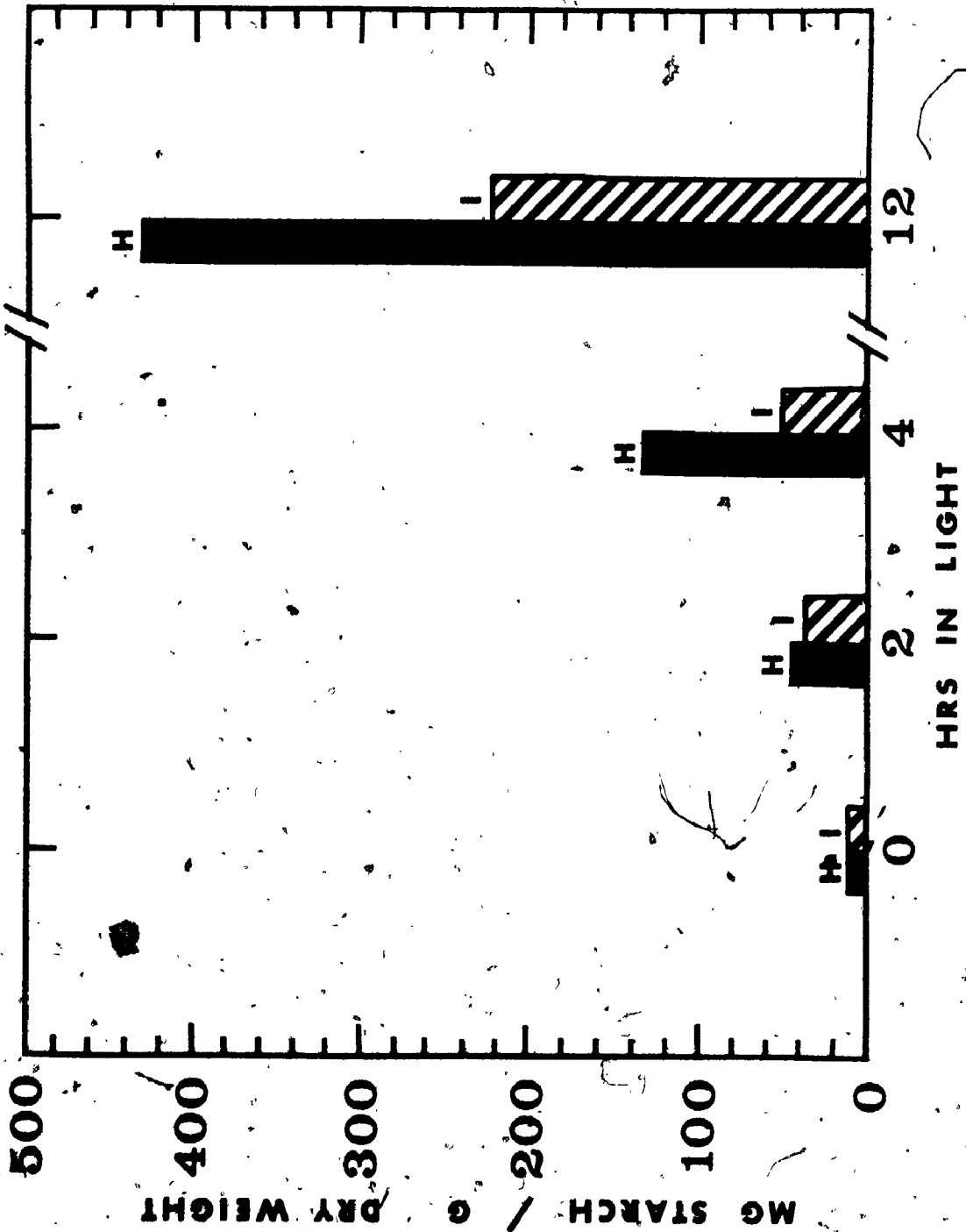


Figure 104. Starch Degradation - Amount of starch present in healthy and diseased leaves after they were put in darkness for specific periods of time. The diseased leaves were inoculated when they entered darkness. Previous to entering darkness all plants were in light, a 12^h light-dark regime. The amount of starch in the infected and healthy leaves was not significantly different at any test time ($p > 0.05$). Arrow indicates the time of inoculation.

H - Healthy Plants

I - Infected Plants

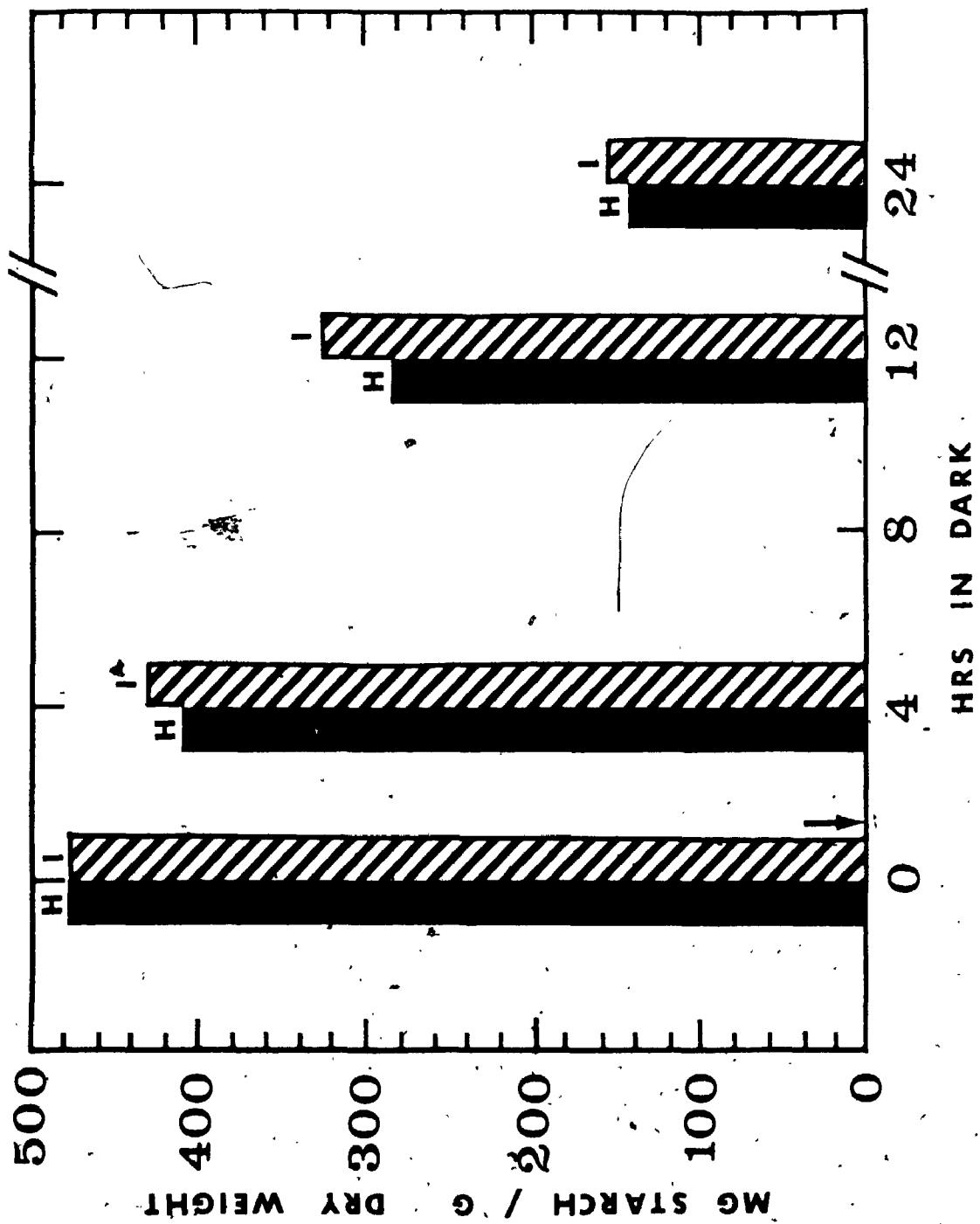


Figure 105. Starch Formation - The bar graph shows the amount of starch present in healthy and diseased leaves after they were exposed to light for specific time periods. Thirty hours prior to illumination all plants were put in darkness. Inoculation of leaves occurred 6 days previously. The amount of starch in the infected and healthy leaves was significantly different at the second, fourth and twelfth h ($p < 0.05$).

H - Healthy Plants

I - Infected Plants

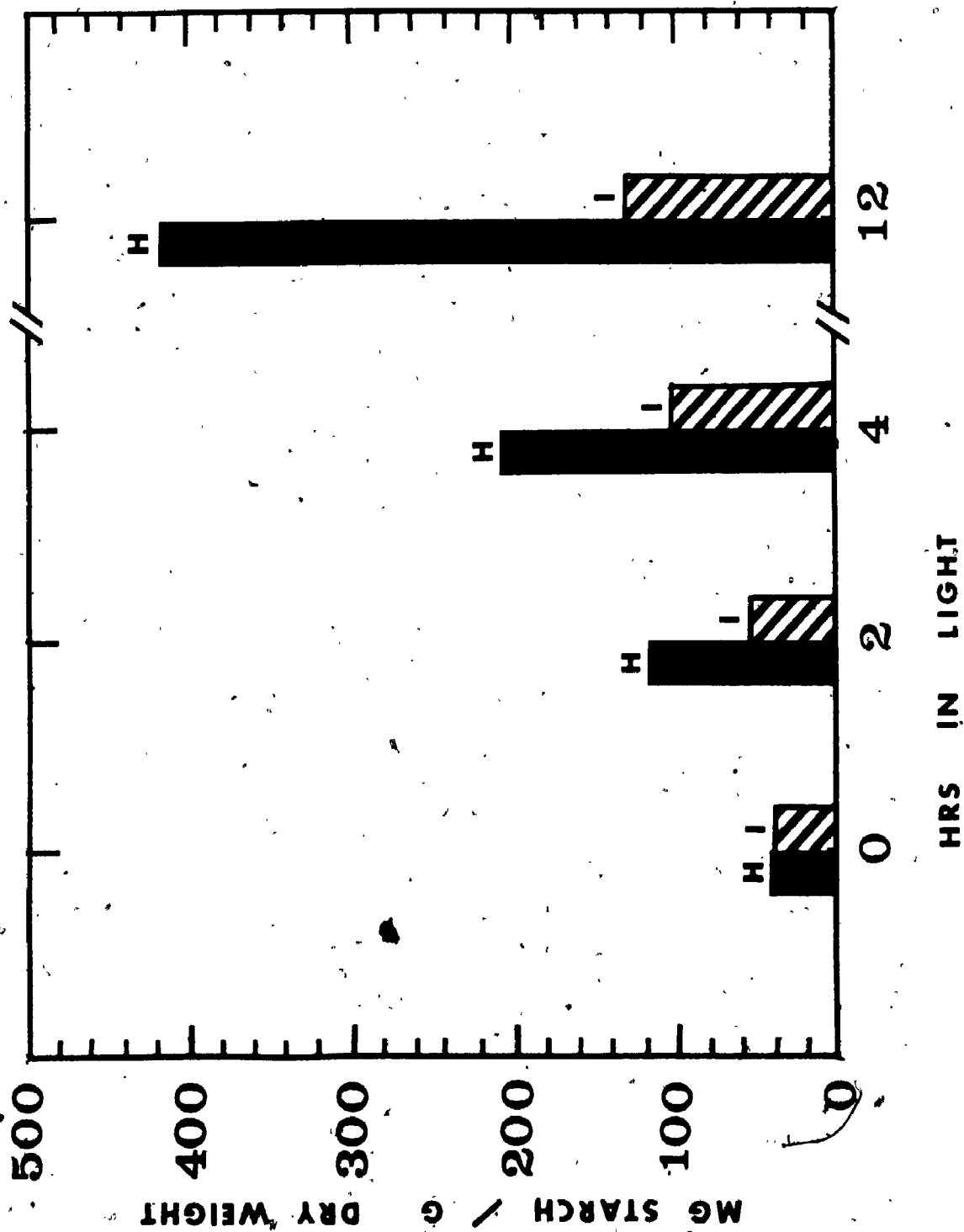


Figure 106. Starch Degradation - The bar graph shows the amount of starch present in healthy and diseased leaves after they were put in darkness for specific periods of time. The diseased leaves were inoculated 6 days previously and plants had a 12 h light-dark regime. The amount of starch in the infected and healthy leaves was significantly different at all test times ($p < 0.05$).

H - Healthy Plants

I - Infected Plants

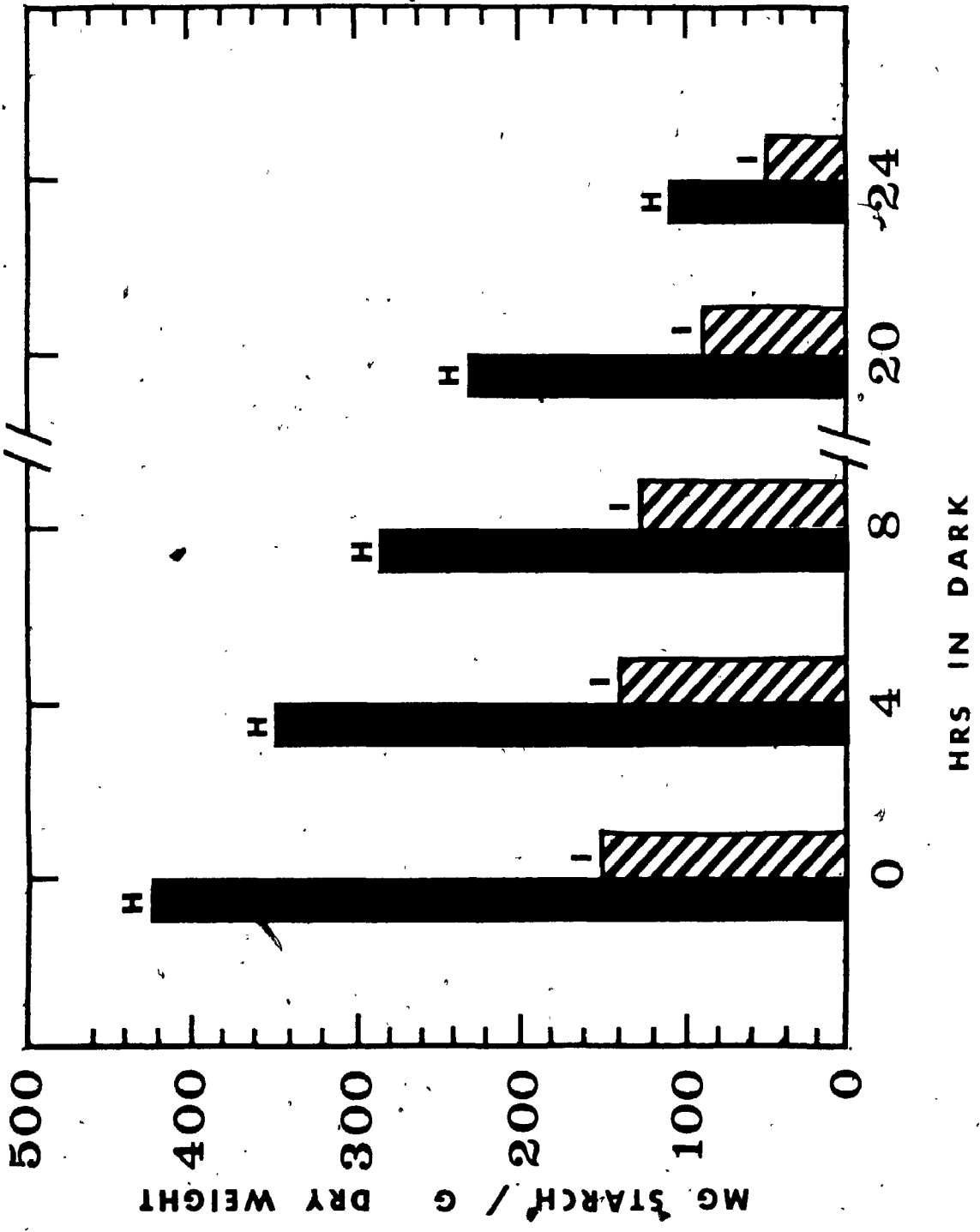


Figure 107. The amount of potato starch remaining after it had been mixed with crude extract from healthy and diseased leaves for 1 h. The extract was taken from diseased leaves after 0-3, 4-5, and 6-7 days. The amount of starch degraded by the crude extract from the diseased leaf was significantly greater than that degraded by the crude extract from the healthy leaf at day 6-7 ($p < 0.01$).

H - Healthy Plants I - Infected Plants

Figure 108. The total protein in healthy and diseased tobacco leaves at 0, 4 and 7 days post-inoculation. There was a significant difference between the diseased and healthy leaves on days 4 and 7 ($p < 0.01$).

H - Healthy Plants I - Infected Plants

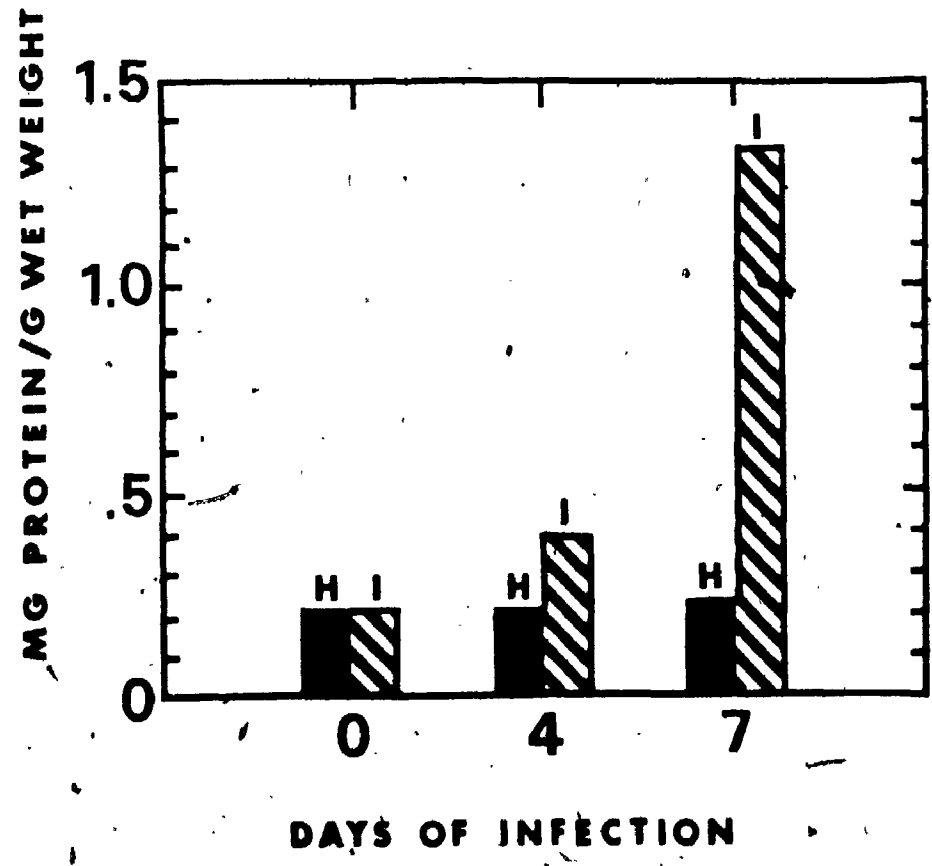
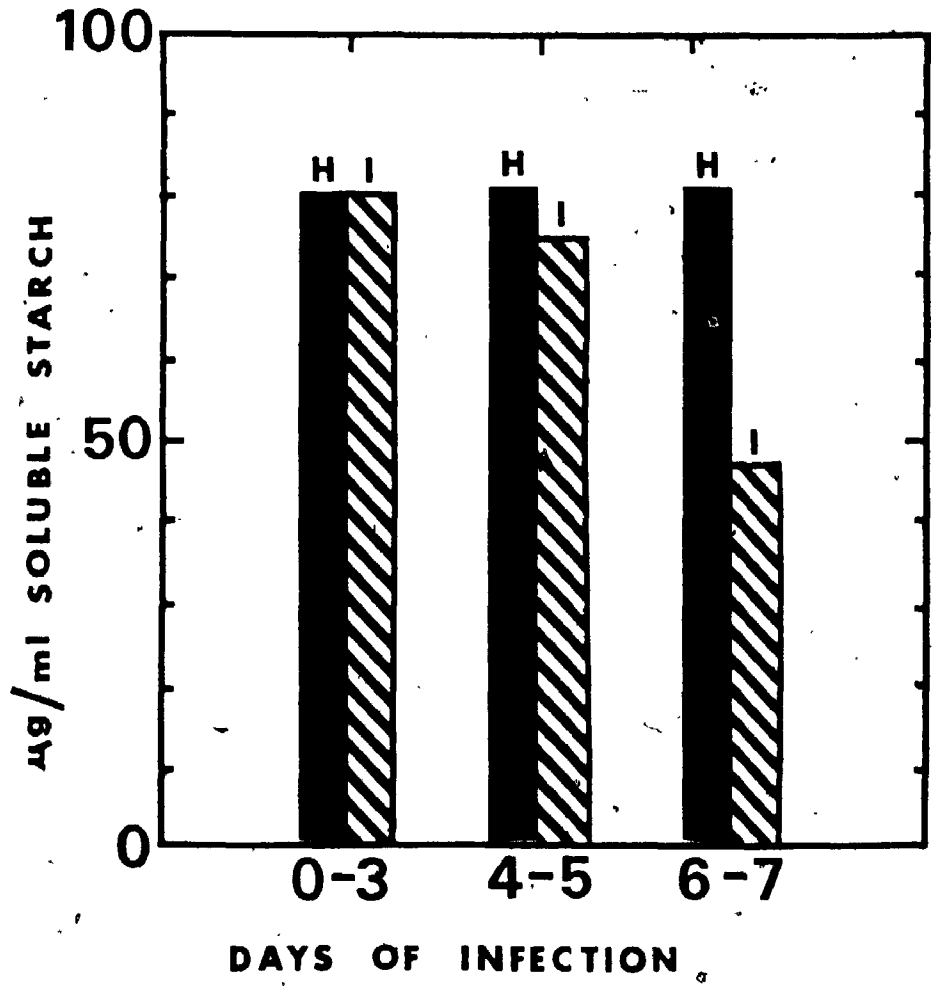


Figure 109. Percent germination of P. hyoscyami f.sp.
tabacina at constant temperatures of 5, 10,
15, 20, 25 and 30°C.

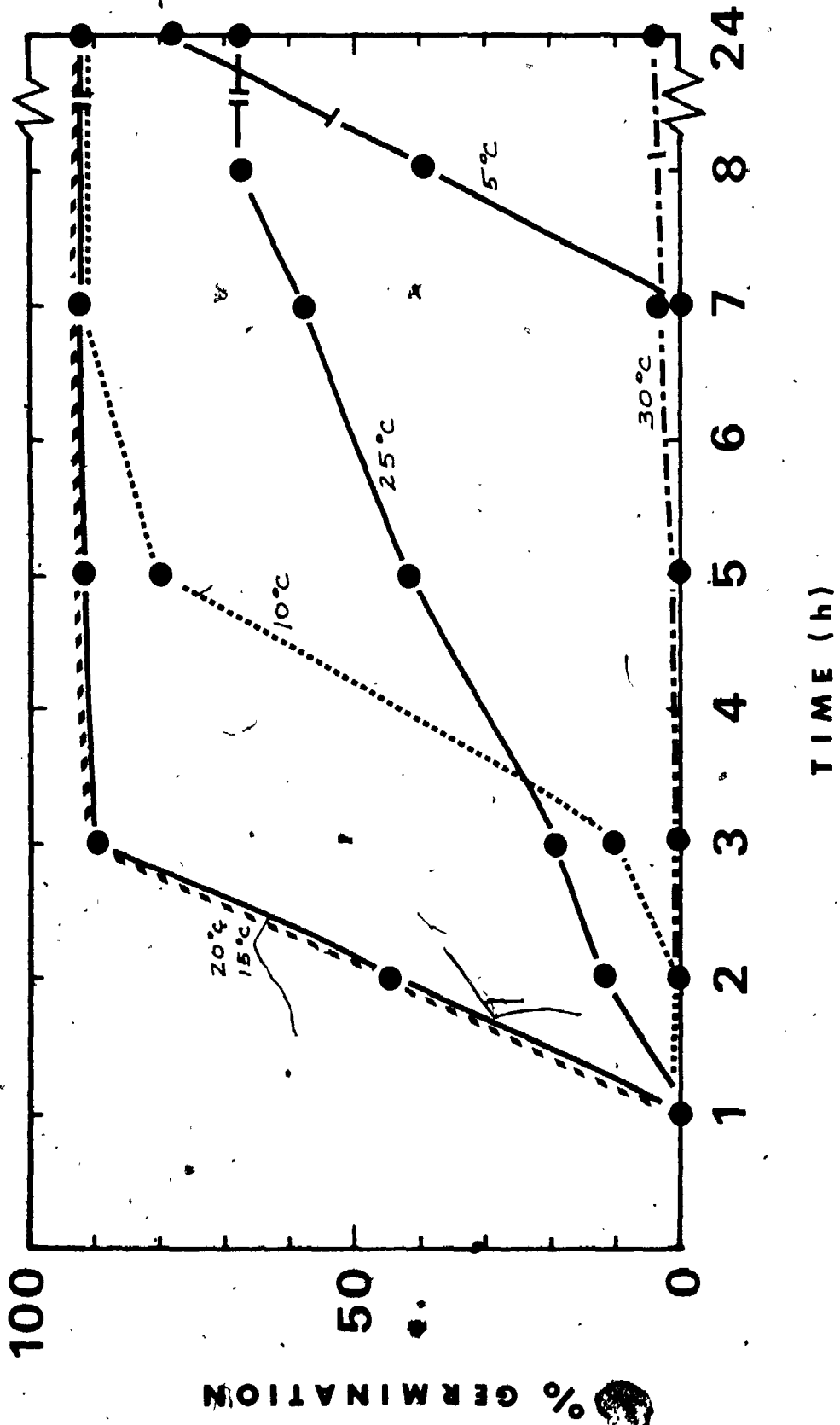


Figure 110. Cumulative percent germination over time
of conidia of P. hyoscyami f.sp. tabacina
on water agar at temperatures of 5, 10, 15,
20, 25 and 30°C.

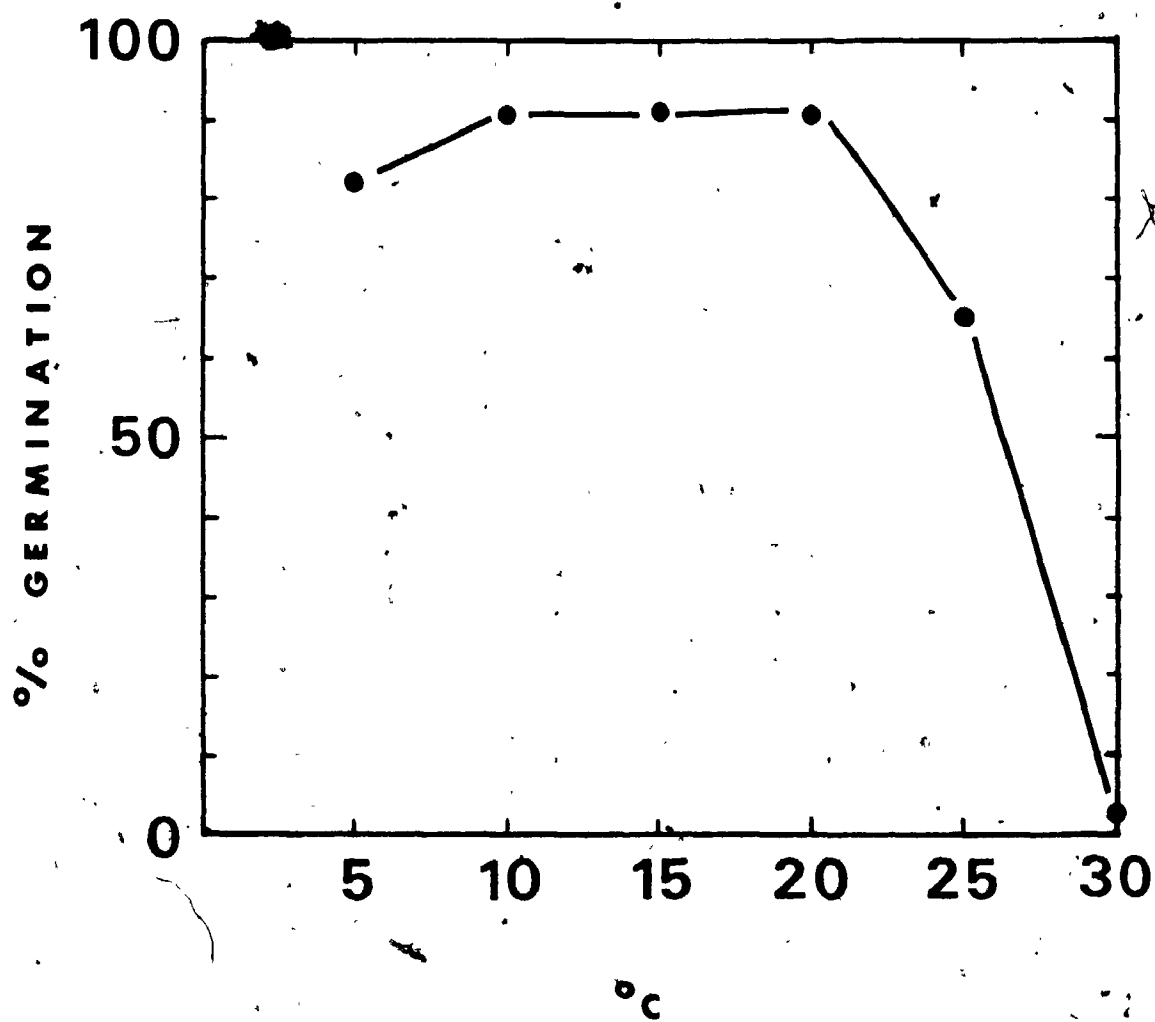
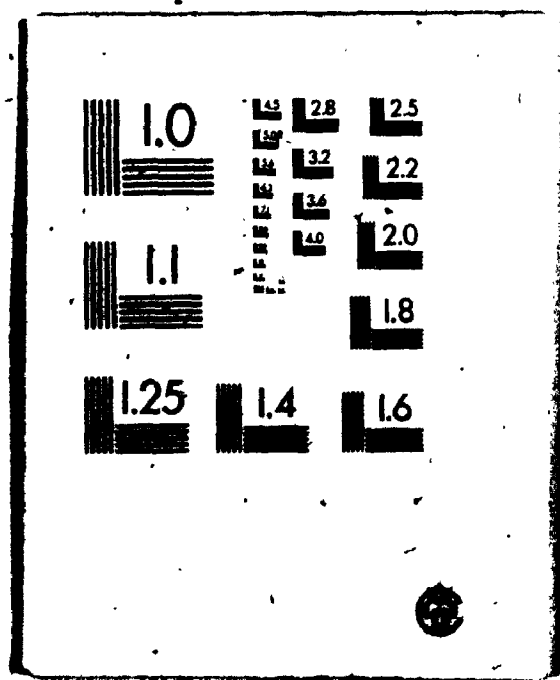


Figure 111. Total percent germination of P. hyoscyami f.sp. tabacina conidia after exposure to 25, 30 and 35°C for periods up to 8 h and then incubation at 20°C for 15 h.

- control at 20°C
- ▲————▲ exposure to 35°C
- exposure to 30°C
- exposure to 25°C

3 3

OF / DE



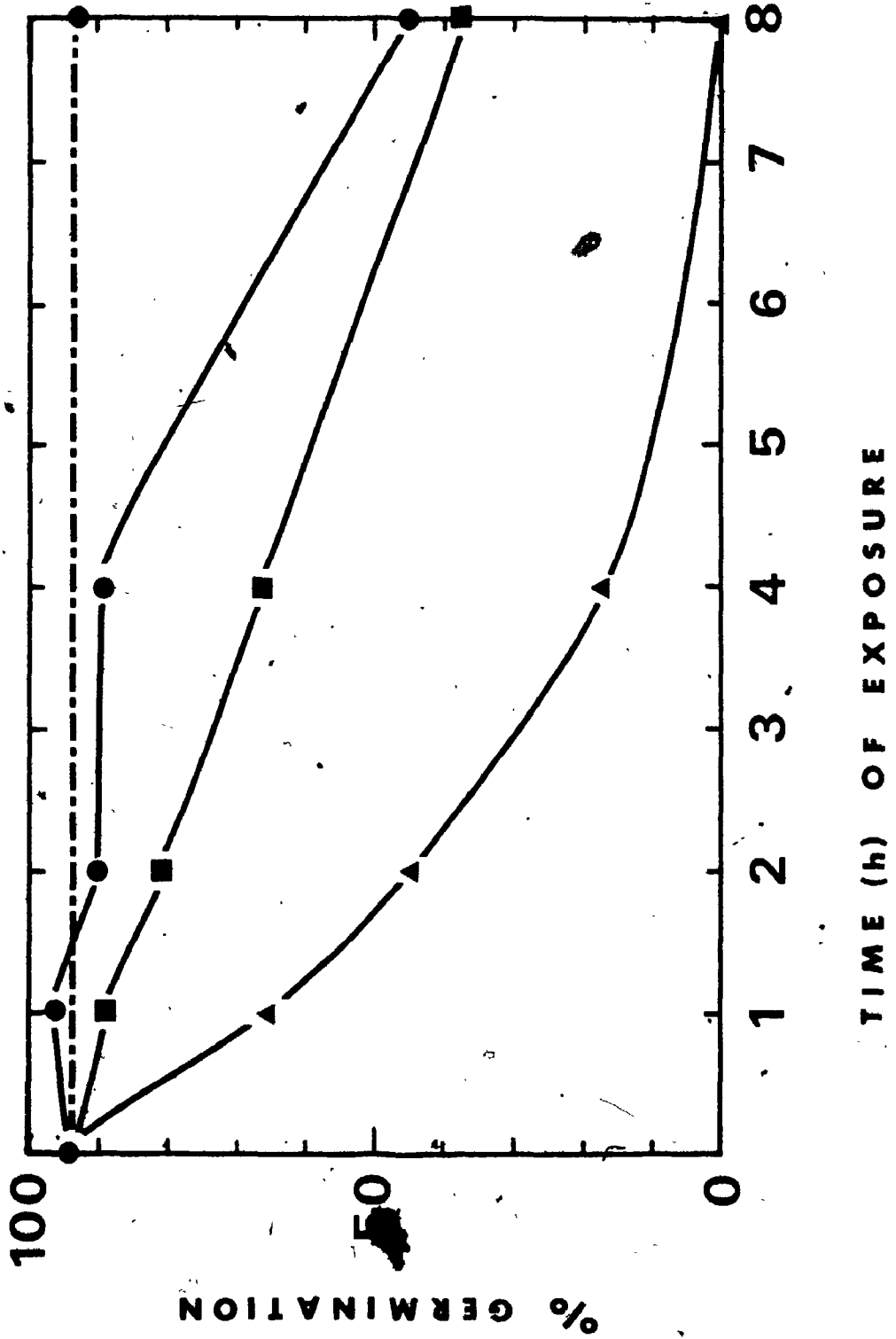


Figure 112. Effect of changing water potential (bars) as controlled by sucrose solutions on turgidity of P. hyoscyami conidia.

Figure 113. Effect of water potential (bars) as controlled by sucrose solutions of varying molalities on conidial germination of P. hyoscyami at 20°C after 15 h incubation.

WATER POTENTIAL (BARS)

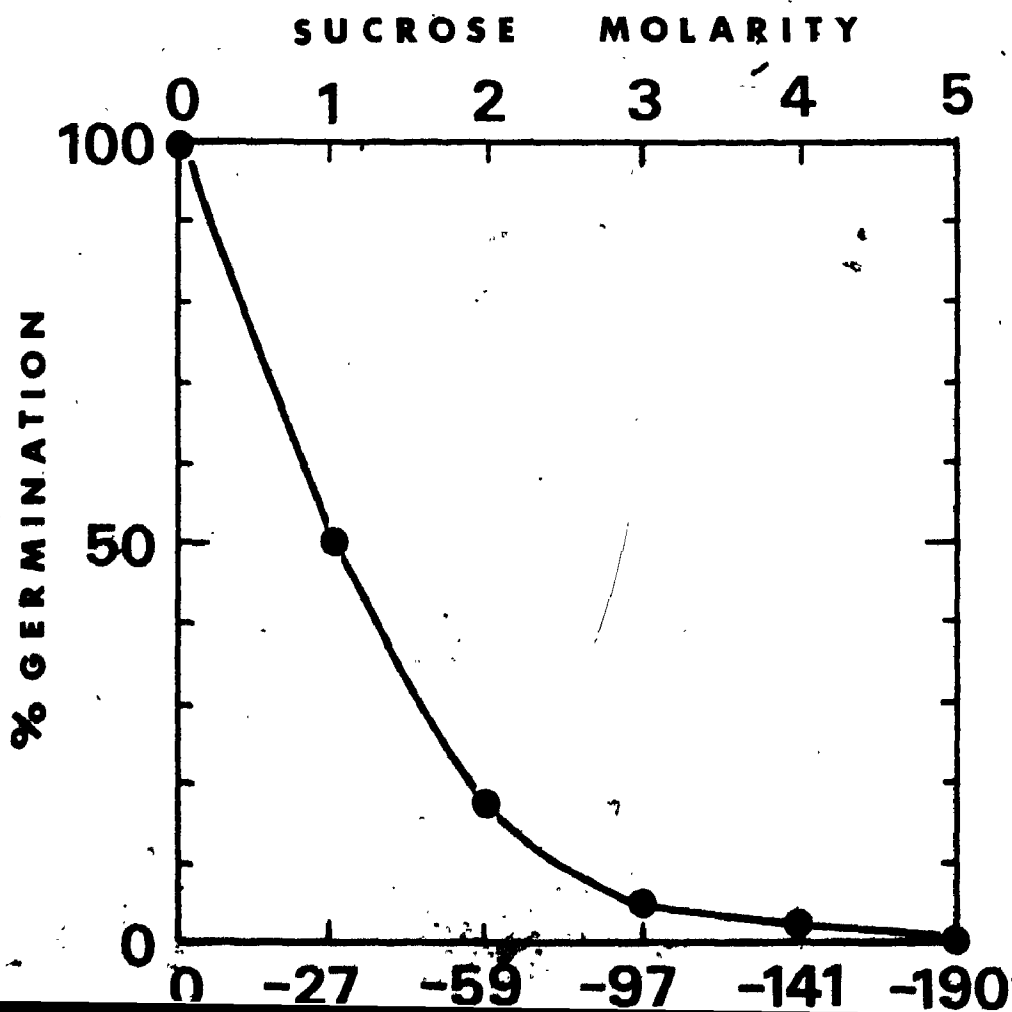
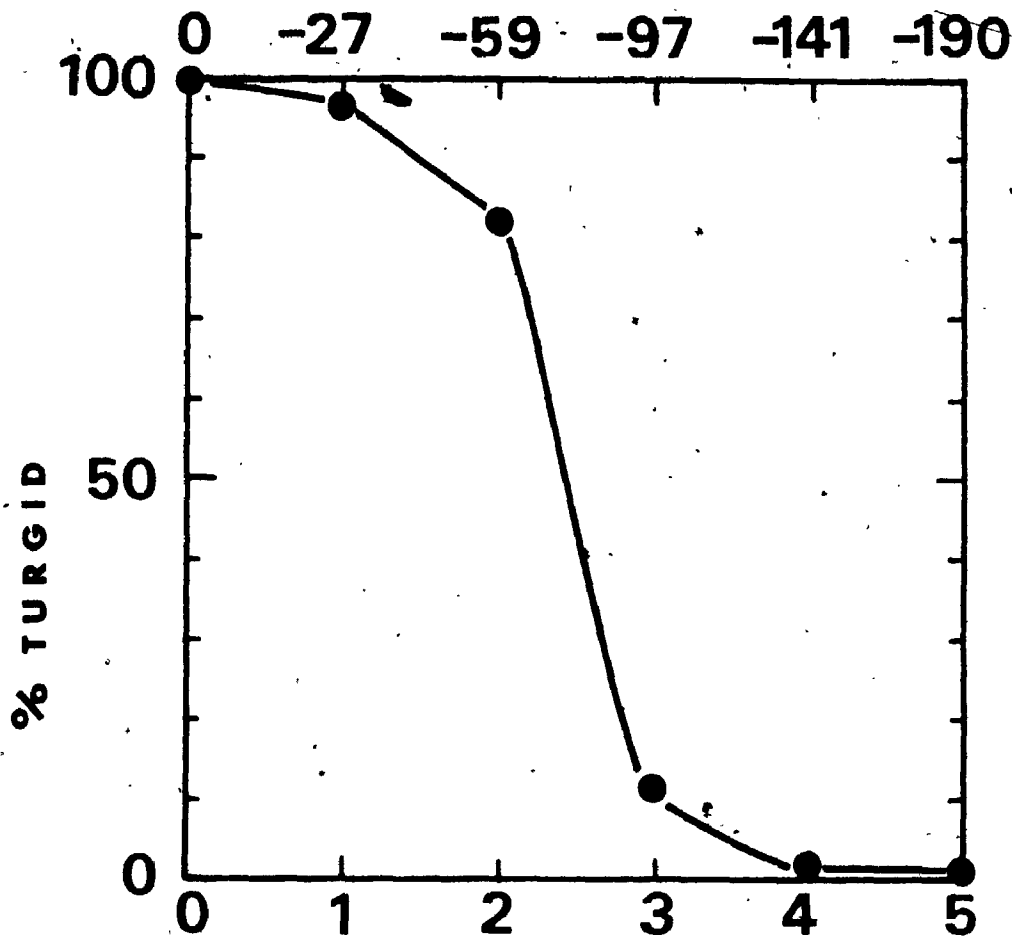


Figure 114. Effect of ultraviolet irradiation (at $120 \mu\text{W cm}^{-2} \text{ sec}^{-1}$) on total percent germination of P. hyoscyami f.sp. tabacina conidia in air (100% RH, 20°C) and conidia suspended in water (20°C).

- ——— ● Control, conidia in air on glass slides
- ▲ ——— ▲ Conidia in air exposed to UV
- - - - ● Control, conidia in water
- ——— ■ Conidia in water exposed to UV

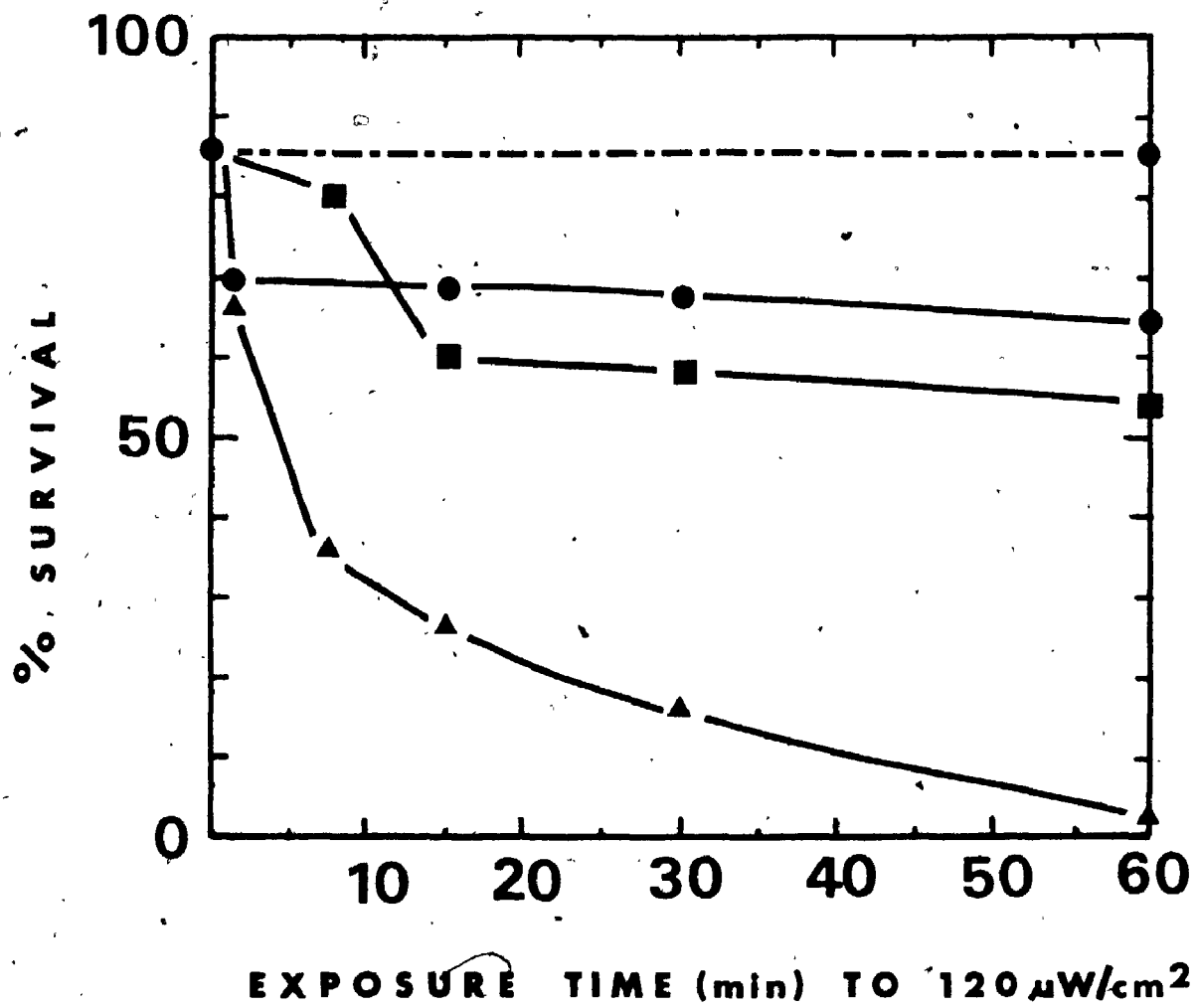


Figure 115. Total percent germination of conidia of P. hyoscyami f.sp. tabacina. The conidia remained attached to one conidiophore during exposure to ultraviolet light (at $120 \mu\text{W cm}^{-2} \text{sec}^{-1}$) for different time durations.

- Control germination of untreated conidia
- Conidial germination following UV treatment

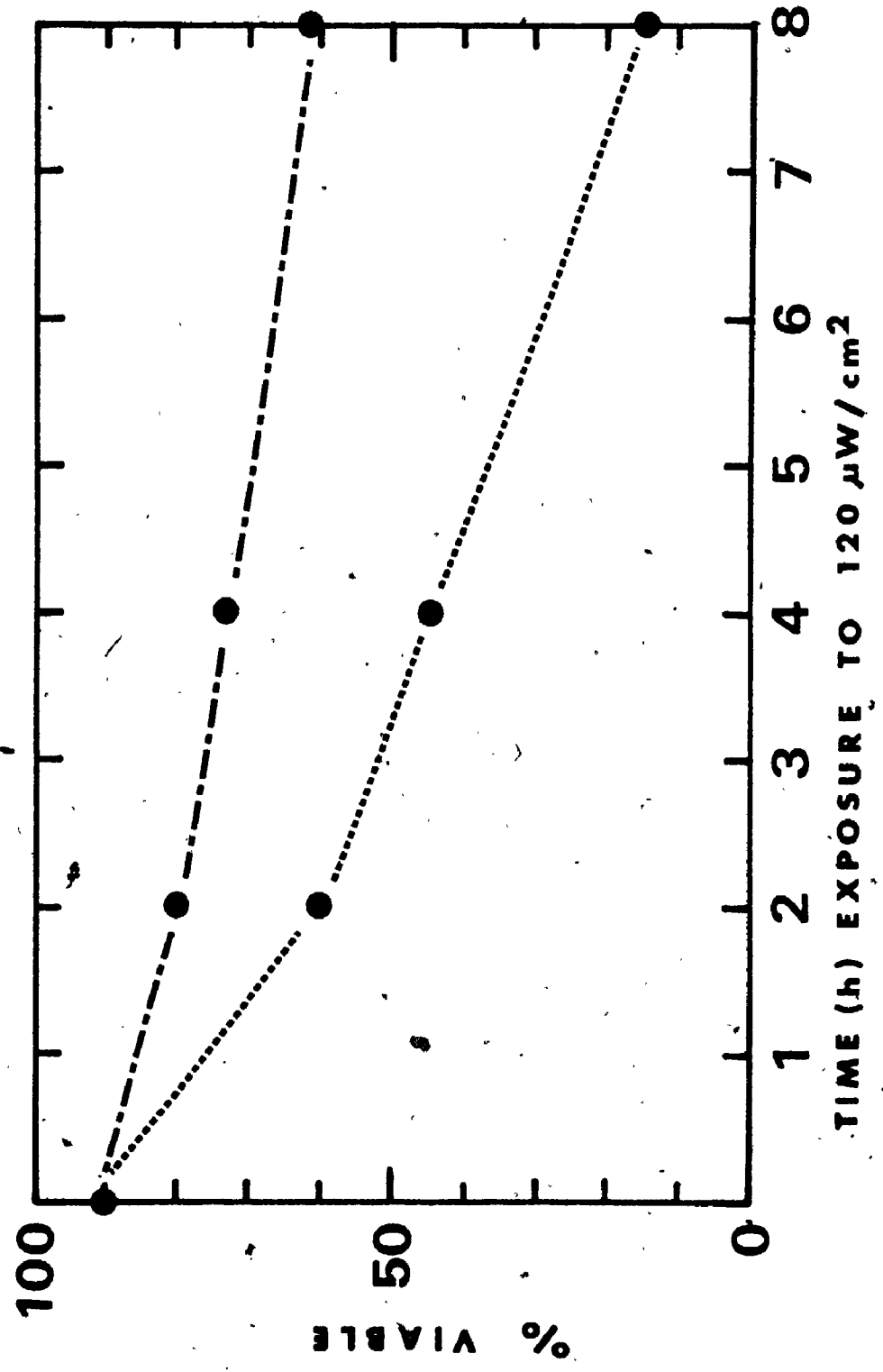


Table 1. The time-course of infection of upper epidermal cells of 6 week old tobacco leaves of one cultivar Virginia 115 by P. hyoscyami f.sp. tabacina.

Time After Inoculation (h)	Stage of Fungal Development
0	inoculation
0.5 - 2	conidial germination
1.0 - 3	appressorial formation
1.5 - 2.5	penetration and formation of vesicle
1.7 - 3	growth beyond vesicle
2.5 - 4	growth to base of epidermal cell
2.6 - 4.1	entrance into intercellular space or palisade cell

Table 2. Time required in light ($150 \mu\text{E m}^{-2}\text{sec}^{-1}$) for starch formation in healthy leaves and leaves heavily infected with P. hyoscyami f.sp. tabacina for 36 h.

Hours in Light	Healthy	Infected
0	-	-
1	a ₊	+
2	++	++
3	+++	+++

a^{*} scale range intensity of IKI

Table 3. Time required in darkness for degradation of starch in healthy tobacco leaves, and leaves heavily inoculated with P. hyoscyami f.sp. tabacina, 2 h after entry into darkness.

Hours in Dark	Healthy	Infected
4	^a +++	+++
6	++	+++
8	++	+++
10	++	+++
12	+	+++
14	-	++
16	-	++
18	-	+
20	-	-

^a scale range intensity of IKI

Table 4. Time required in light ($150 \mu\text{E m}^{-2} \text{sec}^{-1}$) for starch formation in healthy leaves and leaves heavily infected with P. hyoscyami f.sp. tabacina for 6 days.

Hours in Light	Healthy	Infected
0	-	-
.75	a ₊	-
1	++	-
1.5	+++	+
2	+++	++
3	+++	++
5	+++	+++

^a scale range intensity of IKI

Table 5. Time required in darkness for degradation of starch in healthy tobacco leaves, and leaves heavily infected with P. hyoscyami f.sp. tabacina 6 days after infection.

Time in Dark	Healthy	Infected
0	^a +++	+++
2	+++	+++
4	+++	++
6	++	+
8	++	-
10	+	-
12	-	-

^a scale range intensity of IKI

Table 6. Percent viable conidia of P. hyoscyami f.sp. tabacina after storage at various temperatures and relative humidities.^a

Relative Humidity	Days of Storage	Average Percent Viable at			
		5°C	15°C	25°C	35°C
0%	3	14.2	3.0	2.0	0.5
	17	0.0	0.0	0.0	0.0
	28	0.0	0.0	0.0	0.0
	32	0.0	0.0	0.0	0.0
55%	3	49.1	9.4	4.9	0.0
	17	39.5	7.4	0.0	0.0
	28	23.6	5.5	0.0	0.0
	32	24.5	0.0	0.0	0.0
81%	3	95.9	86.2	0.0	0.0
	17	63.8	75.0	0.0	0.0
	28	40.9	0.0	0.0	0.0
	32	14.1	0.0	0.0	0.0

^aStatistical analysis Appendix 2.

Table 7. Percent inhibition of spore germination of P. hyoscyami f.sp. tabacina, Botrytis cinerea and Aspergillus niger caused by carbon dioxide enriched atmospheres at different concentrations.

$$\% \text{ Inhibition in Germination} = 100 - \frac{\text{Test Counts}}{\text{Control Counts}} \times 100$$

Concentration of CO ₂ in air	1%	5%	7.5%	15%
<u>Time</u>	% Inhibition in Germination of <u>P. hyoscyami</u>			
2 h	49	57	90	100
18 h	0	36	70	91
	% Inhibition in Germination of <u>B. cinerea</u>			
2 h	0	60	100	100
18 h	0	0	0	100
	% Inhibition in Germination of <u>A. niger</u>			
2 h	-	-	-	-
18 h	0	0	0	0

h - hours

0 - reading not obtained for conidia, required 15 h to germinate

Statistical analysis in Appendix 3

Table 8. Effect of fluorescent light from 45 to .600 $\mu\text{E m}^{-2} \text{sec}^{-1}$ and darkness on the conidial germination of P. hyoscyami f.sp. tabacina.

Fluorescent Light Intensity ($\mu\text{E m}^{-2} \text{sec}^{-1}$)	Average Percent Germination
45	90
150	88
300	91
600	90
dark (control)	88

APPENDIX I

Composition and concentration of solutions used to provide the stated theoretical relative humidities within sealed glass chambers at 20°C^a.

Material Used	Concentration of Solution	Theoretical Relative Humidity
Water	---	100.00
Sucrose	0.10 Molal	99.85
Sucrose	0.20 Molal	99.62
Sucrose	0.30 Molal	99.43
Sucrose	0.40 Molal	99.24
Sucrose	0.50 Molal	99.04
(NH) ₄ SO ₄	Saturated ^b	81.0
Ca(NO ₃) ₂ ·4H ₂ O	Saturated	55.0
CaCl ₂ (anhydrous)	---	0.0

^a Theoretical relative humidity values vary slightly at different temperatures.

^b An excess of solid phase was maintained in contact with the liquid phase of each saturated solution.

APPENDIX 2

Statistical analysis (Factorial ANOVA) of data presented
in Table 6.

Source of Variation	Sum of Squares	Degrees of Freedom	Mean Square	F
Temperature (T)	2.25500	3	0.751600	553.46*
R. Humidity (R)	1.20509	2	0.602545	443.70*
Time (t)	0.82260	3	0.274200	201.91*
R x T	1.44731	6	0.241210	177.62*
R x t	0.69241	6	0.115400	84.97*
T x t	0.78840	9	0.087600	64.51*
R x T x t	0.95222	18	0.052900	38.95*
Residual	0.13041	96	0.001358	-
Total	8.29344	143	-	-

* Significant at $p < 0.001$

Statistical analysis of data in Table 7.

Time of Exposure to CO ₂	ID ₅₀	\bar{x}	σ^2	t-statistic
<u>P. tabacina</u>				
2 h	0.8, 1.6, 1.0, 1.2	1.15	0.117	5.34 (p<.002)
18 h	2.6, 2.6, 2.6, 3.7	2.88	0.303	
<u>B. cinerea</u>				
2 h	4.5, 4.5, 4.0, 4.0	4.25	0.83	
18 h	0	-	-	
<u>A. niger</u>				
2 h	0	-	-	
18 h	0	-	-	

ID₅₀ - Inhibition dose of 50 percent was determined by randomly choosing pairs of replicates from 1% and 5% CO₂ treatments. The 50% inhibition values were found by interpolations. Means and standard deviations of these values were computed and employed for t-test.

- data not available

0 - ID₅₀ could not be calculated due to 0% inhibition

REFERENCES

- Abbott, I. R. and N. K. Matheson. 1972. Starch depletion in germinating wheat, wrinkled-seeded peas and senescing tobacco leaves. *Phytochem.* 11: 1261-1272.
- Aist, J. R. and P. H. Williams. 1971. The cytology and kinetics of cabbage and root penetration by Plasmodiophora brassicae. *Can. J. Bot.* 49: 2023-2034.
- Allen, P. J. and L. D. Dunkle. 1971. Natural activators and inhibitors of spore germination. pp. 23-49 In Morphological and biochemical events in plant-parasite interaction. S. Akai and S. Ouchi, eds. *Phytopathological Society of Japan*. Tokyo.
- Anonymous. 1938. Blue mold (downy mildew) of tobacco and its control. *Virginia Agr. Exp. St. Bull.* 318: 1-11.
- Asada, Y. and M. Shiraishi. 1976. Discontinuity of the plasma membrane of Raphanus sativus around haustoria of Peronospora parasitica. pp. 32-34 In Biochemistry and cytology of plant parasite interaction. K. Tomiyama, J. M. Daly, I. Uritani, H. Oku, and S. Ouchi, eds. Kadanska Ltd. Tokyo and Elsevier Scientific Pub. Co. Amsterdam, Oxford, New York.
- Beakes, G. W., H. Singh and C. G. Dickinson. 1982. Ultrastructure of host-pathogen interface of Peronospora viciae in cultivars of pea which show different susceptibilities. *Plant Path.* 31: 343-354.
- Berlin, J. D. and C. C. Bowen. 1964. The host parasite interface of Albugo candida on Raphanus sativus. *Am. J. Bot.* 51: 445-452.
- Bracker, C. E. 1967a. Ultrastructure of fungi. *Ann. Rev. Phytopathol.* 5: 343-373.
- Bracker, C. E. 1967b. Ultrastructure of fungi. *Ann. Rev. Phytopathol.* 5: 445-452.
- Bracker, C. E. and L. J. Littlefield. 1973. Structural concepts of host-pathogen interface. pp. 159-318 In Fungal pathogenicity and the plant's response. R. J. W. Byrde and C. V. Cutting, eds. Academic press London, New York.

- Brown, W. 1922. On the germination and growth of fungi at various temperatures and various concentrations of oxygen and carbon dioxide. *Ann. Bot.* 36: 257-283.
- Brown, W. and C. C. Harvey. 1927. Studies in the physiology of parasitism X. On the entrance of parasitic fungi into the host plant. *Ann. Bot.* 41: 643-662.
- Buchanan, B. B., S. W. Hutcheson, A. C. Magyarosy and P. Montalbini. 1981. Photosynthesis in healthy and diseased plants. pp. 13-28 In *Effects of disease on the physiology of the growing plant*. P. G. Ayres, ed. Cambridge Univ. Press, Cambridge.
- Bushnell, W. R. 1971. The haustorium of Erysiphe gramminis: an experimental study by light microscopy. pp. 229-254 In *Morphological and biochemical events in plant-parasite interaction*. S. Akai and S. Ouchi, eds. The Phytopathological Society of Japan. Tokyo.
- Bushnell, W. R. 1972. Physiology of fungal haustoria. *A. Rev. Phytopath.* 10: 151-176.
- Chang, C. W. 1979. Starch and its component ratio in developing cotton leaves. *Plant Physiol.* 63: 973-977.
- Chong, J. and D. E. Harder. 1982. Ultrastructure of haustorium development in Puccinia coronata f.sp. avenae: some host responses. *Phytopath.* 72: 1527-1533.
- Chou, C. H. 1970. An electron-microscope study of host penetration and early stages of haustorium formation of Peronospora parasitica (FR.) Tul. on cabbage cotyledons. *Ann. Bot.* 34: 189-204.
- Clayton, E. E. and J. G. Gaines. 1945. Temperature in relation to development and control of Blue Mold (Peronospora tabacina) of tobacco. *J. Agric. Res.* 71: 171-182.
- Clayton, E. E. and J. A. Stevenson. 1935. Nomenclature of the tobacco downy mildew fungus. *Phytopath.* 25: 516-521.
- Clayton, E. E. and J. A. Stevenson. 1943. Peronospora tabacina Adam, the organism causing blue mold (downy mildew) disease of tobacco. *Phytopath.* 33: 101-108.
- Coffey, M. D. 1976. Flax rust resistance involving the K gene: an ultrastructural survey. *Can. J. Bot.* 54: 1443-1457.

- Coffey, M. D., B. A. Palevitz and P. J. Allen. 1972. Ultra-structural changes in rust-infected tissues of flax and sunflower. Can. J. Bot. 50: 1485-1492.
- Cohen, Y. 1976. Interacting effects of light and temperature on sporulation of Peronospora tabacina on tobacco leaves. Aust. J. Biol. Sci. 29: 281-289.
- Cohen, Y. and J. Kuc. 1980. Infectivity of conidia of Peronospora tabacina after freezing and thawing. Plant Disease 64: 549-550.
- Cruickshank, I. A. M. 1958. Environment and sporulation in phytopathogenic fungi I. Moisture in relation to the production and discharge of conidia of Peronospora tabacina Adam. Aust. J. Biol. Sci. 11: 162-170.
- Cruickshank, I. A. M. 1961a. Germination of Peronospora tabacina Adam: Effect of temperature. Aust. J. Biol. Sci. 14: 58-65.
- Cruickshank, I. A. M. 1961b. Environment and sporulation in phytopathogenic fungi II. Conidial formation in Peronospora tabacina Adam as a function of temperature. Aust. J. Biol. Sci. 14: 198-207.
- Cruickshank, I. A. M. 1963. Environment and sporulation in phytopathogenic fungus IV. The effect of light on the formation of conidia of Peronospora tabacina Adam. Aust. J. Biol. Sci. 16: 88-110.
- Cruickshank, I. A. M. and K. O. Mueller. 1957. Water-relations and sporulation of Peronospora tabacina Adam. Nature. 180: 44-45.
- Cruickshank, I. A. M. and N. E. Rider. 1961. Peronospora tabacina in tobacco: transpiration; growth and related energy considerations. Aust. J. Biol. Sci. 14: 45-57.
- Cummingham, J. L. and D. S. Hagedorn. 1962. Penetration and infection of pea roots by zoospores of Aphanomyces euteiches. Phytopath. 52: 827-834.
- Dixon, L. F., R. A. McLean and F. A. Wolf. 1935. The initiation of downy mildew of tobacco in North Carolina in 1934. Phytopath. 25: 628-639.

- Dixon, L. P., R. A. McLean and F. A. Wolf. 1936. Relationship of climatological conditions to the tobacco downy mildew. *Phytopath.* 26: 735-759.
- Dunn, G. 1974. A model of starch breakdown in higher plants. *Phytochem.* 13: 1341-1346.
- Edreva, A. 1974. A biological study of tobacco blue mold pathogenesis: the activity of certain oxydative enzymes and chloroplast pigment content. *Doklady Sel'skokhozyaistvennoi Akademii.* 7: 73-76.
- Edreva, A. 1975. A biochemical study of tobacco blue mold pathogenesis on some resistance factors. *Doklady Sel'skokhozyaistvennoi Akademii.* 8: 55-58.
- Edreva, A. M. and I. D. Georgieva. 1980. Biochemical and histochemical investigation of α and β -glucosidase activity in a infectious disease, a physiological disorder and in senescence of tobacco leaves. *Physiol. Pl. Path.* 17: 237-243.
- Ehrlich, H. G. and M. A. Ehrlich. 1963a. Electron microscopy of the host-parasite relationships in stem rust of wheat. *Amer. J. Bot.* 50: 123-130.
- Ehrlich, H. G. and M. A. Ehrlich. 1963b. Electron microscopy of the sheath surrounding the haustorium of Erysiphe graminis. *Phytopath.* 53: 1378-1380.
- Fraymouth, J. 1956. Haustoria of the Peronosporales. *Trans. Brit. Mycol. Soc.* 39: 79-107.
- Frey-Wyssling, A. and K. Mühlethaler. 1965. Ultrastructural plant cytology. Elsevier Publ. Co. Amsterdam, London, New York. p. 301.
- Fried, P. M. and D. L. Stuteville. 1977. Peronospora trifoliorum sporangium development and the effects of humidity and light of discharge and germination. *Phytopath.* 67: 890-894.
- Georgieva, I. and A. Edreva. 1974. Cytological and cytochemical changes in blue mold infected leaves. *Doklady Sel'skokhozyastvennoi Akademii.* 1: 25-30.
- Groves, S. N., C. E. Bracker and D. J. Moore. 1970. An ultrastructural basis for hyphal tip growth in Pythium ultimum. *Amer. J. Bot.* 57: 245-266.
- Hanchey, P. 1981. Ultrastructural effects. pp. 449-475 In Toxins in plant diseases R. D. Durbin, ed. Academic Press. New York.
- Harding, H., P. H. Williams and S. S. McNabola. 1968. Chlorophyll changes, photosynthesis and ultrastructure

- of chloroplasts in Albugo candida induced "green islands" on detached Brassica juncea cotyledons. Can. J. Bot. 46: 1229-1234.
- Heath, M. C. 1974. Chloroplast ultrastructure and ethylene production of senescing and rust-infected cowpea leaves. Can. J. Bot. 52: 2591-2597.
- Heath, M. C. and I. B. Heath. 1971. Ultrastructure of an immune and a susceptible reaction of cowpea leaves to rust infection. Physiol. Pl. Path. 1: 277-287.
- Henderson, R. G. 1937. Histological studies of infection and sporulation of Peronospora tabacina in tobacco seedlings. Phytopath. 27: 131 (Abstr.).
- Hickey, E. L. and M. D. Coffey. 1977. A fine structural study of pea downy mildew fungus Peronospora pisi in host Pisum sativum. Can. J. Bot. 55: 2845-2858.
- Hickey, E. L. and M. D. Coffey. 1980. The effect of ridomil on Peronospora pisi parasitizing Pisum sativum: an ultrastructural investigation. Physiol. Pl. Path. 17: 199-204.
- Hill, A. V. 1961. Dissemination of conidia of Peronospora tabacina Adam. Aust. J. Biol. Sci. 14: 208-222.
- Hill, A. V. 1962. Longevity of conidia of Peronospora tabacina Adam. Nature. 195: 827-828.
- Hill, A. V. 1965. The role of temperature in the development of blue mould (Peronospora tabacina Adam) disease in tobacco seedlings II. Effect on plant growth. Aust. J. Agric. Res. 16: 609-615.
- Hill, A. V. 1966. Effect of inoculum spore load, length of infection period and leaf washing on occurrence of Peronospora tabacina Adam (blue mold) of tobacco. Aust. J. Agric. Res. 17: 133-146.
- Hill, A. V. 1969. Factors affecting viability of spore inoculum in Peronospora tabacina Adam and lesion production in tobacco plants: The inoculum. Aust. J. Biol. Sci. 22: 393-398.
- Hill, A. F. and S. Green. 1965. The role of temperature in the development of blue mould (Peronospora tabacina Adam) disease in tobacco seedlings I. In leaves. Aust. J. Agric. Res. 16: 597-667.
- Hirata, K. 1971. Calcium in relation to the susceptibility of primary barley leaves to powdery mildew. pp. 207-208. In Morphological and biochemical events in plant-parasite interaction. S. Akai and S. Ouchi, eds. The Phytopathological Society of Japan. Tokyo.

- Hohl, H. R. and P. Strössel. 1976. Host-parasite interfaces in a resistant and susceptible cultivar of Solanum tuberosum inoculated with Phytophthora infestans: tuber tissue. Can. J. Bot. 54: 900-912.
- Ingram, D. S., J. A. Sargent and I. C. Tommerup. 1976. Structural aspects of infection by biotrophic fungi. pp. 43-78. In Biochemical aspects of plant-parasite relationships. J. Friend and D. R. Thredfall, eds. Academic Press. London, New York.
- Inman, R. E. 1962. Disease development, disease intensity and carbohydrate levels in rusted bean plants. Phytopath. 52: 1207-1211.
- Jensen, A. A. 1962. Botanical histochemistry, principles and practice. W. H. Freeman and Co. San Francisco, London.
- Jones, R. K. and F. J. Dainello. 1982. Occurrence of Race 3 of Peronospora effusa on spinach in Texas and identification of sources of resistance. Plant Disease 66: 1078-1079.
- Kajiwara, T. 1971. Structure and physiology of haustoria of various parasites. pp. 255-277. In Morphological and biochemical events in plant-parasite interaction. S. Akai and S. Ouchi, eds. Phytopathological Society of Japan. Tokyo.
- Kakie, T. and Y. Sagizaki. 1970. Diurnal changes in the starch and sugars of tobacco leaves. Soil Science and Plant Nutrition. 16: 201-203.
- Kluczewski, S. M. and J. A. Lucas. 1982. Development and physiology of infection by the downy mildew fungus Peronospora parasitica (Pers. ex. Fr.) Fr. in susceptible and resistant Brassica species. Plant Pathology 31: 373-379.
- Kohno, M., H. Ishizaki and H. Kunoh. 1970. Cytological studies on rest fungi VI. Fine structures of infection progress of Kuehneola japonica (Diet.) Dietel. Mycopathologia 61: 35-48.
- Kröber, H. 1969. Über das infektionsverhalten der oosporen von Peronospora tabacina Adam an tabak. Phytopathol. Z. 64: 1-6.

- Krober, H. 1981. Germination and longevity of conidia of some Peronosporaceae kept under different conditions. *J. Plant Dis. and Prot.* 88: 510-517.
- Krober, H. and H. Petzold. 1972. Licht-und elektronenmikroskopische untersuchungen über wirt-parasitbeziehungen bei afälligen und gegen Peronospora spp. resistenten gezüchteten sorten von tabak und spinat. *Phytopathol. Z.* 74: 296-313.
- Langcake, P. and P. A. Lovell. 1980. Light and electron microscopical studies of one infection of Vitis spp. by Plasmopara viticola, the downy mildew pathogen. *Vitis* 19: 321-337.
- Littlefield, L. J. and M. C. Heath. 1979. Ultrastructure of rust fungi. Academic Press. New York, San Francisco, London.
- Lowry, O. H. and N. J. Rosebrough, A. L. Farr and R. J. Randall. 1951. Protein measurement with Folin, phenol reagent. *J. Biol. Chem.* 193: 265-275.
- Lucas, G. B. 1980. The war against blue mold. *Science* 210: 147-153.
- McGrath, H. and P. R. Miller. 1958. Blue Mold of tobacco. *Pl. Dis. Report. Supplement* 250. pp. 3-35.
- McKeen, W. E. 1974. The interface between the powdery mildew haustorium and the cytoplasm of one susceptible barley epidermal cell. *Can. J. Microbiol.* 20: 1475-1478.
- McKeen, W. E. 1981. The 1979 tobacco blue mold disaster in Ontario, Canada. *Plant Disease* 65: 8-9.
- McKeen, W. E. and S. R. Rimmer. 1973. Initial penetration process in mildew infection of susceptible barley leaves. *Phytopath.* 63: 1049-1053.
- McKeen, W. E., R. Smith and P. K. Bhattacharya. 1968. Alterations of the host wall surrounding the infection peg of powdery mildew fungi. *Can. J. Bot.* 47: 701-705.
- McKeen, W. E., R. Smith and N. Mitchell. 1966. The haustorium of Erysiphe cichoracearum and the host-parasite interface on Helianthus annuus. *Can. J. Bot.* 44: 1299-1307.

- McMeekin, D. 1981. The response of Peronospora parasitica to a liver medium. Mycologia 73: 551-554.
- Michelmore, R. W. 1981. Sexual and asexual sporulation in the downy mildews. pp. 165-180. In The Downy Mildews. D. M. Spencer, ed. Academic Press. New York, London, San Francisco.
- Mihailová, P. T. 1972. Dynamics of conidia dispersal of Peronospora tabacina Adam. Doklady Sel'skokhozyaistvennoi Akademii. 5: 217-224.
- Milholland, R. D., J. Papadopoulou and M. Daykin. 1980. Histopathology of Peronospora tabacina in systemically infected Burley tobacco. Phytopath. 71: 73-76.
- Misra, A. N. and U. C. Biswal. 1981. Changes in chlorophylls and carotenoids during aging of attached and detached leaves and isolated chloroplasts of wheat seedlings. Photosynthetica 15: 75-79.
- Mollenhauer, H. H. and D. J. Moore. 1966. Golgi apparatus and plant secretion. Ann. Rev. Plant Physiol. 17: 27-46.
- Moore, R. T. and J. H. McLearn. 1963. Fine structure of mycota 4. The occurrence of Golgi dictyosome in the fungus Neobulgaria pura (Fr.) Petrak. J. Cell Biol. 16: 131-141.
- Ohguchi, T. and Y. Asada. 1981. Oospore formation of Japanese radish downy mildew fungus. Ann. Phytopath. Soc. Japan 47: 75-77.
- Okita, T. W. and J. Preiss. 1980. Starch degradation in spinach leaves - isolation and characterization of the amylases and R-enzymes of spinach leaves. Plant Physiol. 66: 870-876.
- Peyton, G. A. and C. C. Bowen. 1963. The host-parasite interface of Peronospora manshurica on Glycine max. Amer. J. Bot. 50: 787-797.
- Pierre, R. E. and R. L. Millar. 1965. Histology of pathogen relationship of Stemphylium botryosum and alfalfa. Phytopath. 55: 909-914.
- Pinckard, J. A. and L. Shaw. 1943. Downy mildew infection of flue cured tobacco in the field. Phytopath. 29: 79-113.
- Powell, M. J. and C. E. Bracker. 1977. Isolation of zoospore organelles from Phytophthora palmiyora. Proc. 2nd Int. Mycol. Congr. Tampa, Florida. p. 533.

- Preiss, J. 1982. Regulation of the biosynthesis and degradation of starch. *Ann. Rev. Plant Physiol.* 33: 431-454.
- Rice, M. A. 1927. The haustoria of certain rusts and the relation between host and pathogen. *Bull. Torrey Bot. Club* 54: 63-153.
- Sargent, J. A. 1981. The fine structure of downy mildews. D. M. Spencer, ed. Academic Press. New York, San Francisco, London.
- Sargent, J. A., I. C. Tommerup and D. S. Ingram. 1973. The penetration of susceptible lettuce variety by the downy mildew fungus Bremia lactucea Regel. *Physiol. Pl. Path.* 3: 231-239.
- Schaus, B. L. 1980. The blue mould epidemic: its pattern and causes. *Geography* 490. Department of Geography. The University of Western Ontario, London, Ontario Canada.
- Shaw, C. G. 1981. Taxonomy and evolution. pp. 17-24. In *The downy mildews*. D. M. Spencer, ed. Academic Press. New York, San Francisco, London.
- Sheperd, C. J. 1962. Germination of conidia of Peronospora tabacina Adam I Germination in vitro. *Aust. J. Biol. Sci.* 15: 483-509.
- Sheperd, C. J. and M. Mandryk. 1963. Germination of conidia of Peronospora tabacina Adam II Germination in vitro. *Aust. J. Biol. Sci.* 16: 77-88.
- Sheperd, C. J., P. Simpson and A. Smith 1971. Effects of variation in water potential on the viability and behaviour of conidia of Peronospora tabacina Adam. *Aust. J. Biol. Sci.* 24: 219-229.
- Smith, G. 1900. The haustoria of the Erysipheae. *Bot. Gaz.* 29: 153-184.
- Spurr, A. R. 1969. A low-viscosity epoxy resin embedding medium for electron microscopy. *J. Ultrastr. Res.* 26: 31-43.

- Stevens, N. E. and J. C. Ayres. 1940. History of tobacco downy mildew in the United States in relations to weather conditions. *Phytopath.* 30: 684-688.
- Stover, R. H. and L. W. Koch. 1951. The epidemiology of blue mold of tobacco and its relation to the incidence of disease in Ontario. *Sci. Agr.* 31: 225-252.
- Strössel, P., G. Lazarovits and E. W. B. Ward. 1982. Light and electron microscopy of *Phytophthora* rot in soybeans treated with metalaxyl. *Phytopath.* 72: 106-111.
- Thornton, J. D. and R. C. Cooke. 1974. Changes in respiration, chlorophyll content and soluble carbohydrates of detached cabbage cotyledons following infection with *Peronospora parasitica* (Pers. ex. Fr.) Fr. *Physiol. Pl. Path.* 4: 117-125.
- Thorpe, T. A. and D. D. Meier. 1974. Enzymes of starch metabolism in *Nicotiana tabacum* callus. *Phytochem.* 13: 1329-1334.
- Todd, F. A. 1961. Occurrence of blue mould on tobacco in West Germany, Switzerland, France and other European countries. *Pl. Drs. Reporter.* 45: 319-326.
- Tomlinson, J. A. and M. J. W. Webb. 1978. Ultrastructural changes in chloroplasts of lettuce infected with beet western yellows virus. *Physiol. Pl. Path.* 12: 13-18.
- Tommerup, I. C. 1981. Cytology and genetics of downy mildews. pp. 121-140. *In* The downy mildews. D. M. Spencer, ed. Academic Press. New York, San Francisco, London.
- Tu, J. C. 1979. Alterations in chloroplast and cell membranes associated with cAMP - induced dissociation of starch grains in clover yellow mosaic virus infected clover. *Can. J. Bot.* 57: 360-369.
- Valleau, W. D. 1955. Tobacco blue mold control through plant bed management. *Plant. Dis. Reporter.* 39: 231-232.
- Viennot-Bourgin, G. 1981. History and importance of downy mildews. pp. 1-14. *In* The downy mildews. D. M. Spencer, ed. Academic Press. New York, San Francisco, London.
- Voliva, C., G. W. Moessen and A. G. Matthyse. 1982. Starch-enhanced synthesis and release of amylolytic enzymes from normal and crown gall tumor tobacco tissue culture cells. *Can. J. Bot.* 60: 1474-1478.
- Wang, M. C. and S. Bartnicki-Garcia. 1980. Distribution of mycolaminarans and cell wall β -glucans in the life cycle of *Phytophthora*. *Exp. Mycol.* 4: 269-280.

- Whipps, J. M. and D. H. Lewis. 1981. Patterns of translocation, storage and interconversion of carbohydrates. pp. 47-83. In Effects of disease on the physiology of the growing plant. P. G. Ayres, ed. Cambridge Univ. Press. Cambridge.
- Wolf, F. A. 1939. Status of investigation of tobacco downy mildew. Phytopath. 29: 194-200.
- Wolf, F. A. 1947. Tobacco downy mildew, endemic to Texas and Mexico. Phytopath. 37: 721-729.
- Wolf, F. A., L. F. Dixon, R. McLean and F. R. Darkis. 1934. Downy mildew of tobacco. Phytopath. 24: 337-363.
- Wolf, F. A., R. A. McLean and L. F. Dixon. 1936. Further studies on downy mildew of tobacco. Phytopath. 26: 760-777.
- Wood, R. K. S. 1967. Physiological plant pathology. Blackwell. Oxford. p. 30.
- Wuest, P. J. and C. G. Schmitt. 1965. Greenhouse tests to compare European and Beltsville isolates of Peronospora tabacina. Plant Dis. Reporter. 49: 367-370.
- Young, P. A. 1926. Penetration phenomena of facultative parasitism in Alternaria, Diplodia and other fungi. Bot. Gaz. 81: 258-279.

END

1 1 1 0 9 1 8 4

FIN